Development of a permanent vacuum prism air refractometer for accurate compensation of the refractive index of air as used in dimensional metrology

Oelof Abraham Kruger

Student number: 215081719

January 2025

Supervisor:

Professor Naven Chetty

Submitted in partial fulfilment of the requirements for the degree of PhD in Physics in the

School of Chemistry and Physics, Discipline of Physics

College of Agriculture, Engineering, and Science

University of KwaZulu-Natal (PMB), Private Bag X01, Scottsville, 3209, South Africa

Abstract

The refractive index has a wide range of applications, and it is used in many different areas of measurement, such as in thin films, sugar contents in beverages and wine, and the medical industry. Compensation of the refractive index of air has been required since the speed of light was measured accurately enough to require a correction for the medium in which it travels. There have been various research advances to measure the refractive index of numerous mediums more accurately, to keep up with technological advances and the increase in accuracy required.

Metrology requires accurate refractive index measurements since it is critical in the definition of the SI units of the metre. Even more so since 2019 with the new definitions of the SI, which is based on physical constants, the kilogram and the Kelvin and the derived unit for pressure, the pascal. This research focussed on length and dimensional metrology where the SI unit, the metre is defined in terms of the speed of light in a vacuum. While the definition of the metre is in terms of the speed of light in a vacuum, most dimensional measurements are performed in the air. The refractive index requires to be measured and correctly applied to the velocity of the light during the measurements compared to the speed of light in a vacuum for more accurate computation of the metre.

This research was motivated by technical limitations observed in existing refractometers. Previous studies where the author researched, designed, and built a low-cost tube refractometer with adequate accuracy to perform the required compensation to the velocity of the laser light during dimensional measurements. However, there were drawbacks to this design; mainly the use of a vacuum pump every time a refractive index measurement needs to be made. This led to unwanted heat generation around the measuring area and drawing a vacuum each time a measurement was made increased the likelihood of dust particles entering the vacuum tube, which may cause the refraction of the laser beams through these particles and thereby reducing the accuracy of the measurement. Adding another notable drawback is the deformation of side windows under vacuum conditions, which alters their thickness and, consequently, the optical path length. Such variations can significantly influence the accuracy of refractive index measurements. These limitations highlighted the need for improved refractometer designs, ultimately leading to the development of more stable and accurate measurement techniques researched in this study.

This research work focused on the design, building, and testing of a refractometer for the compensation of the velocity of the light compensations that does not require the use of a vacuum pump every time a measurement has to be made. The custom-designed and built refractometer uses a permanent vacuum as the reference etalon. In the first design an additional laser beam was incorporated to improve the zero-measurement stability, while the second design introduces an innovative method for the refractive index measurement based on a Fizeau interferometer configuration. The system is simple, cost-effective and highly accurate for use in everyday dimensional measurements. The results showed that although simple in design, the refractometer is accurate to approximately 2,7 x 10^{-8}, which meets the initial conditions for the design and compares favourably with published values obtained through the use of more expensive and specialised techniques.

Preface

This thesis describes the work undertaken by Oelof Kruger at the University of KwaZulu-Natal under the supervision of Prof Naven Chetty between September 2018 and December 2024.

I declare the work reported herein to be my own research unless specifically indicated to the contrary in the text or bibliography.

Signed: [redacted]

Student: O A Kruger

On this May 2025

I hereby certify that this statement is correct.

Signed:……..

Supervisor: Prof Naven Chetty

On this …….day of ……..2025

Signed:……..

Co-Supervisor: Dr Abiola Ilori

On this …….day of ……..2025

Declaration: Plagiarism

I, Oelof Kruger, declare that:

i) The research results in this thesis except where otherwise stated, are my original work.

ii) This thesis has not been submitted in full or in part for any degree to any other university.

iii) This thesis does not contain data, pictures, or graphs from any other work unless cited as originating from others.

iv) This thesis does not contain other persons' writing unless acknowledged as being sourced from others. Where written sources have been quoted:

   a. Their words have been rewritten, but the general information attributed to them has been referenced.

   b. Where their exact words have been used, their writing has been placed inside quotation marks and referenced.

v) Where I have reproduced a publication was contributed by me and I have acknowledged other author's contributions.

Declaration: Publications

I, Oelof Kruger, declare the details of the contribution to the publication that forms part of the research presented as chapters in this thesis.

i. Kruger O A and Chetty N 2021 "A permanent vacuum refractometer for everyday use in dimensional metrology" *Nature/articles* **11** 9290

Ready to submit:

ii. Kruger O A and Chetty N Comparison between a permanent vacuum Fizeau refractometer, a cylinder refractometer, and the weather station method to measure the refractive index of air

Signatory of student:……. …….. Date:……

Acknowledgments

A deepest thank you to my family for coping with all the time I spent away from home and for enduring my temperament when I was home and working on the project.

I also wish to thank my supervisor Prof Naven Chetty, who played a vital role in the original motivation to commence with the projects and to further my studies. My utmost admiration is extended.

Last, but certainly not least, I express my gratitude to NMISA, for providing the environment and funding to undertake this project and further my studies.

Structure of Thesis

Chapter 1 discusses the history of measuring the speed of light. From the early years where the refractive index became relevant and was required in measuring the speed of light until the International Committee for Weights and Measures (CIPM) fixed the speed of light in 1975. The chapter ends with the use of the speed of light as the basis of dimensional metrology.

Chapter 2 focuses on the origin and impact of refractive index measurements in several applications. The chapter moves onto metrology applications with their importance in the SI units, the kilogram and the Kelvin and the derived unit the pascal. Further onto dimensional metrology, which is the area that requires accurate values of refractive index and which this research focuses on, is discussed.

Chapter 3 discusses the literature that was investigated in the refractive index for dimensional metrology and the measurements thereof. The limitations of the weather station method and the advantages and disadvantages of the current designs of refractometers are discussed and the chapter concludes with demonstrating the design of a new refractometer.

Chapter 4 explains the design of a new refractometer and builds on what was learned from the literature review and previous work on the design of a low-cost robust refractometer performed by the author. The full refractometer design and usage are provided.

Chapter 5 investigates a new method to measure the vacuum-air ratio in the refractometer into the final designs with measurements to verify the system by comparing against the weather station method which although not as accurate as the current benchmark has the potential for further developments.

Chapter 6 is a detailed analysis of the error analyses of the new refractometer for the two different measurement methods. Taking into account the equipment used and the uncertainty of each in this setup. In this chapter, the uncertainty budget and equipment used for the weather station, which was used for the verification of the refractometers are also discussed. The chapter concludes with a detailed uncertainty budget for the two methods.

Chapter 7 directs the future work that can potentially lead from this research. The chapter discusses future research to measure refractive index advances to be: i) better uncertainty, and ii) a low-cost stand-alone refractometer.

Chapter 8 is the published paper that discusses the refractometer with a translation stage. This work improves on previous published work with improved stability drastically. The second paper to be submitted discusses a different approach and although still uses a prism as the vacuum etalon, it does not use a translation stage. It uses a Fizeau interferometer setup which improves the time required to perform measurements and with modifications, theoretically the overall accuracy.

Chapter 9 concludes the research, by discussing the literature research, investigations, results, verification, and potential future research.

Ce qui est admirable, ce n'est pas que le champ des étoiles soit si vaste, c'est que l'homme l'ait mesuré.
The wonder is, not that the field of the stars is so vast, but that man has measured it.

Anatole France

Table of Contents

Abstract i

Acknowledgments vi

Table of Contents ix

List of Abbreviations xii

List of Figures xiii

List of Tables xv

List of Graphs xvi

Chapter 1: Introduction to Measurements Using the Speed of Light and Dimensional Measurements 17

1.1 Speed of light 17

1.2 The use of light and the speed of light as the bases of dimensional metrology and measurements 18

1.2.1 First definition of the metre (1799) 18

1.2.2 The International Bureau of Weights and Measures (BIPM) 19

1.2.3 The wavelength definition: A great step forward (1927) 20

1.2.4 The spectral line of Krypton (1960) 20

1.2.5 The metre is defined as the speed of light (1983) 21

Chapter 1 Bibliography 24

Chapter 2: Refractive Index Measurements, Origin, and Impact 27

2.1 Origin and wide-ranging applications of refractive index 27

2.2 Refractive index in metrology 27

2.3 Refractive index in dimensional and length metrology 30

Chapter 2 Bibliography 32

Chapter 3: Literature Research using the Weather station method, Wavelength Trackers and Absolute Refractometers 35

Chapter 3 Bibliography 43

Chapter 4: Design of the Permanent Vacuum Refractometry 46

4.1 Principles of length measurements using distance laser interferometers 46

4.2 Refractometer design 48

4.3 Experimental refractometer using a permanent vacuum prism as vacuum etalon 50

4.4 Uncertainty calculations with a commercial prism in the translation stage 55

4.5 Improvement in the optical layout of the refractometer and the use of the commercial prism. 58

Chapter 4 Bibliography 64

Chapter 5: Final Design of the Permanent Vacuum Refractometer 66

5.1 Newly designed prism 66

5.2 Use of a Fizeau interferometer to measure the vacuum-air ratio. 71

5.3 Results of the Refractive index as measured with the Fizeau interferometer. 75

5.4 Refractive index results from the Fizeau interferometer but using the angle measuring capability of the flatness interferometer. 80

Chapter 5 Bibliography 83

Chapter 6: Equipment Used and Uncertainty Calculations 85

6.1 Equipment used. 85

Chapter 6.1 Bibliography 90

6.2 Uncertainty of the Refractive index using the Edlén weather station method 92

6.3 Uncertainty of Refractive Index using the Translation Stage Setup 92

6.4 Uncertainty in the Refractive index using the Fizeau interferometer setup 93

6.5 Conclusions and Recommendations from Uncertainty Calculations. 94

Chapter 6.2 Bibliography 96

Chapter 7: Concluding remarks and opportunities for future research and application 97

Chapter 8: Journal Papers 102

8.1 A permanent vacuum refractometer for everyday use in dimensional metrology. Nature Scientific Reports. 2021; articles 11, 9290. 102

8.2 Fizeau interferometer to measure the refractive index of air with permanent vacuum prism etalon. 111

Chapter 9: Conclusion 120

Chapter 9 Bibliography 122

Appendix I 123

List of Abbreviations

CMM	Coordinate Measuring Machine
HP	Hewlett-Packard company, now known as Keysight
ISO	International Organisation for Standardisation
GUM	Guide to the Expression of Uncertainty in Measurement
ppm	Parts per million
SI	International System of Units
V.O.L.	Velocity of Light
CGPM	General Conference on Weights and Measures
ITS-90	International Temperature Scale
VIM	Vocabulary in metrology
DIMVIM	Dimensional vocabulary in metrology

List of Figures

Figure 1 Measuring the length of the meridian passing through Dunkirk and Barcelona during the years 1792 to 1798 19

Figure 2 The metre was originally defined by a length marked on a similar bar 20

Figure 3 A typical Krypton lamp was used to define the metre between 1960 and 1983 21

Figure 4 The natural constants realising the SI units after 2019. 22

Figure 5 The SI system of units after 2019 with the metre (m) highlighted. 22

Figure 6 The refractometer to measure the refractive index in the determination of the pressure in chamber.....27

Figure 7 The refractometer to measure the refractive index to determine the pressure in the chamber.....28

Figure 8 The refractometer designed by Terrien.....34

Figure 9 Patented Hewlett-Packard designed wavelength tracker.....35

Figure 10 Zygo wavelength compensator.....35

Figure 11 Zygo measurement of the refractive index of a gas.....36

Figure 12 Patented refractometer by Tsai displaying the vacuum etalon with two flat and parallel windows.....37

Figure 13 Schematic diagram of the Tsai permanent vacuum refractometer.....39

Figure 14 Tsai's U.S. patent US5394244A. 1992 of permanent vacuum prism design.....39

Figure 15 Operation of a heterodyne laser system.....43

Figure 16 Operation of a homodyne laser system.....43

Figure 17 A homodyne laser interferometer with quadrature detection.....44

Figure 18 Schematic diagram of the Kruger and Chetty's Refractometer 48

Figure 19 Hollow prism from 3B Scientific [13].....50

Figure 20 Schematic diagram of the prism refractometer using a laser displacement interferometer and translation stage. 51

Figure 21 Prism refractometer..... 52

Figure 22 Profile of prism side window under atmospheric conditions……54

Figure 23 Profile of prism side window in a vacuum……..54

Figure 24 Vacuum tube the vacuum pump to one inlet and the vacuum gauge to another……56

Figure 25 Setup with extra laser beams to continue measuring the zero position……..59

Figure 26 The newly designed second prism……..65

Figure 27 The second prism setup on the transfer table……67

Figure 28 Profile of prism side window under atmospheric conditions……70

Figure 29 Profile of prism side window under vacuum……69

Figure 30 The second design prism setup in the Zygo flatness interferometer to measure the air-vacuum ratio……72

Figure 31 Fringes are generated with air under normal atmospheric conditions inside and outside the prism……..70

Figure 32 Fringe map with air inside the vacuum chamber of the prism……..71

Figure 33 Fringe map with a vacuum inside the vacuum chamber of the prism……71

Figure 34 Oblique plot air in the vacuum chamber under normal atmospheric conditions……71

Figure 35 Oblique plot under vacuum used to measure the vacuum-air ratio……72

Figure 36 Two horisontal profiles were chosen to measure the vacuum-air ratio. Figure with air inside and outside the prism……72

Figure 37 The two horisontal profiles with vacuum were drawn inside the bottom chamber……72

Figure 38 Experimental setup of the tube refractometer and the newly designed permanent vacuum prism……77

Figure 39 Two horizontal areas were selected to measure the differences between the vacuum and air……79

Figure 40 Two horizontal areas were selected to measure the differences between the vacuum and air……..79

Figure 41 Gold coating setup in flatness interferometer……85

Figure 42 Measurement of gold coating using flatness interferometer……..86

Figure 43 Measurement of gold coating using Taylor Hobson profilometer……..86

Figure 44 Side A, optical flatness……96

Figure 45 Side B, optical flatness……96

Figure 46 Third prism assembled; optical flatness measured……97

Figure 471 Third prism assembly, underscoring the improvements in optical flatness……97

Figure 482 A simple Michelson interferometer setup with the third prism……..98

Figure 49 Fringes from the Michelson interferometer setup with the third prism……99

List of Tables

Table 1 Advantages and disadvantages of a tube refractometer……..42

Table 2 Results for the prism refractometer data compared to the modified Edlin equation using weather station measurement calculation……55

Table 3 Results for the prism refractometer with extra laser added to improve the long-term stability compared to the modified Edlin equation using weather station measurement calculations…… 61

Table 4 Uncertainty budget for prism refractometer at the 25 mm position only……..63

Table 5 Results for the new prism refractometer compared to the modified Edlin equation using weather station measurement calculations……70

Table 6 Results for the Fizeau prism refractometer data compared to the modified Edlén equation using the weather station method……..77

Table 7 Results for the tube refractometer data compared to the modified Edlén equation using the weather station method……..78

Table 8 Results for the prism refractometer data compared to the previously used tube refractometer…….81

Table 9 Results for the angles of the prism as measured with the flatness interferometer……..83

Table 10 Results for the prism refractometer using the angle measuring method compared to the modified Edlén equation using weather station measurement calculations……83

Table 11 Uncertainty budget for Fizeau prism refractometer at the 25 mm position only……..95

List of Graphs

Graph 1 The laser reading was measured relative to the different levels of vacuum 57

Chapter 1: Introduction to Measurements Using the Speed of Light and Dimensional Measurements

1.1 Speed of light

In 1638, Galileo Galilei [1] first attempted to measure the speed of light without using explosions as he experimented to measure the speed of light where he and his assistant each took a shuttered lantern and stood on hilltops one mile apart. Galileo flashed his lantern, and as soon as the assistant saw Galileo's light, would open his shutter. Galileo would then time how long it took before he saw the light from the other hilltop and divide the distance between them by the time it took to calculate the speed of light. However, he could not measure the speed and could only conclude that it was fast. He did however suggest that the orbits of the planets and moons were so regular and could be used to measure the speed of light. This led to many speculating but ultimately to Roemer's discovery.

Only in 1676 did astronomer Ole Roemer [2] manage to measure the speed of light with his observations that Jupiter's moon "Io", takes 1,76 days to orbit Jupiter, the time it takes is always the same. However, he discovered that the moon didn't always appear where he predicted it would be. At certain times of the year, it seemed to be behind and at other times of the year, ahead of the predicted time. Roemer hypothesised that when the earth was closer to Jupiter, the moon was ahead in time and when it was farther away, it was behind the time. When the Earth was farther away from Jupiter, the light would take longer to get to Earth, and the opposite was true when the Earth was closer to Jupiter. So, the moon did not change places but appeared to be doing so depending on how long the light took to travel to the Earth. He based his observations on the movement of the planets and managed to measure the speed of light at about 220 000 kilometres per second (km/s). Although this is approximately 27% off from today's value, it was still fairly accurate for that time and the first recorded measurement of the speed of light. Many other scientists also measured the speed of light; James Bradley in 1728 used the stars to calculate the value of the speed of light to be 301 000 km/s [3].

In 1949, Armand Fizeau conducted non-stellar measurements of the speed of light by employing a reflector placed 8 km away, aimed at the teeth of a spinning rotor. Léon Foucault later enhanced this method [3,4], achieving an accurate measurement of the speed of light of 298 000 km/s [4]. Foucault's findings confirmed that light travelled more slowly in water than in air, emphasising the critical role of the medium in which the light travels. Subsequently, the definition of the speed of light became pivotal, fixed in a vacuum, with the refractive index serving as a correction factor for its velocity in various mediums. The most important date occurred in

1975 when the General Conference on Weights and Measures, CGPM fixed the speed of light at precisely 299 792 459 m/s [5,6]. Equation 1 expresses the refractive index (n),

$$n = \frac{c}{v'} \tag{1}$$

where *n* is the refractive index, *c* is the velocity of light in a vacuum, and v' Is the velocity of light in a particular medium.

1.2 The use of light and the speed of light as the bases of dimensional metrology and measurements

Metrology is the scientific study of measurement, and constitutes a fundamental pillar in various domains, with manufacturing standing out as a pivotal area. As fittingly expressed by Seth Godin, "Measurement is fabulous unless you are busy measuring what is easy to measure as opposed to what is important" [6]. This assertion underscores the essence of meaningful measurement, emphasising the need to focus on parameters of significance.

The subsequent narrative provides a concise yet comprehensive summary and timeline describing the evolution of dimensional metrology. It elucidates how the speed of light has emerged as the definitive standard, shaping the landscape of dimensional and length measurements.

1.2.1 First definition of the metre (1799)

In 1791, the French National Assembly adopted a measurement standard, defining the metre as one-tenth millionth of a meridian quadrant. From this the provisional standard was from 1793, a metre bar was made and later replaced by a definitive metre standard in 1799, the metre standard made from platinum due to its superior stability, density and resistance to corrosion, was placed in the National Archives in Paris.

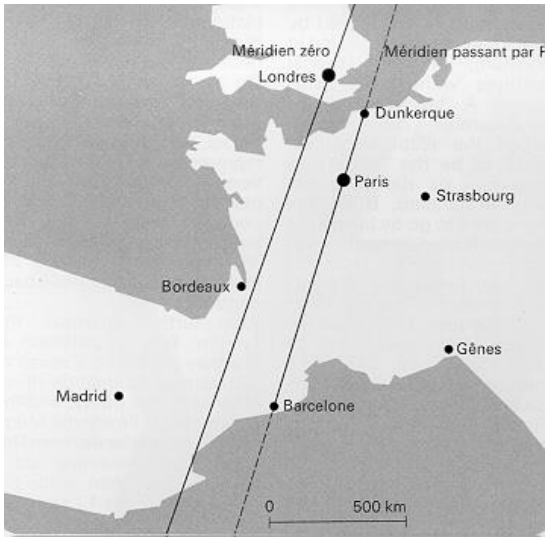

Figure 3 Measuring the length of the meridian passing through Dunkirk and Barcelona during the years 1792 to 1798 [2]

1.2.2 The International Bureau of Weights and Measures (BIPM)

These platinum bars were difficult to reproduce, and in 1889 a number of new platinum-iridium metre bars were produced, and one of these, no 6, replaced the International Prototype Metre and became the new standard [8–10]. This new international prototype was used as a line standard instead of an end standard, which means that instead of the end-to-end distance being the standard, it was between two lines engraved on the bar. The bar was an x-shaped cross-section of 20 mm x 20 mm overall, giving maximum rigidity with minimum mass (Figure 2). The first session of the General Conference in October 1889 confirmed the prototype definition of the metre and granted it legal validity. The uncertainty value for the prototype metre was high at approximating 0,2 µm.

Figure 4 The metre was originally defined by a length marked on a similar bar [8]

1.2.3 The wavelength definition: A great step forward (1927)

In 1927, at the 7th General Conference on Weights and Measures, the metre was defined as 1 552 164,13 times the wavelength of the red spectral line of cadmium in the atmosphere at a pressure of 1 013 mbar and a temperature of 15°C. It was from this definition that wavelength was used to define the metre, and hence, the accurate measurement of the refractive index of air became critical [8,9].

1.2.4 The spectral line of Krypton (1960)

The technical difficulties for spectral measurements were not universally accessible at the time, and therefore, it was decided to continue using the international prototype as the primary reference for as long as necessary [11]. On 14 October 1960, the 11th General Conference on Weights and Measures agreed that the definition of the metre represented by the 85-year-old line standard should be replaced with a new definition. The new definition was "the metre is the length equal to 1 650 763,73 wavelengths in vacuum of the radiation corresponding to the transition between the levels $2p_{10}$–$5d_5$ of the Krypton-86 atom" [11]. This new definition allowed lengths to be defined with a measurement uncertainty of only 4 nm per metre (4×10^{-9}). Figure 3 shows a typical Krypton lamp.

Figure 3 illustrates a typical Krypton lamp, offering a more accurate defining the metre through the wavelength-based on the characteristics of the Krypton-86 atom.

Figure 5 A typical Krypton lamp was used to define the metre between 1960 and 1983 [11]

1.2.5 The metre is defined as the speed of light (1983)

In 1960, the world was presented with a new type of optical technology that was referred to as "the solution in search of a problem" [8,9]. This device was the laser, an acronym for 'light amplification by stimulation emission of radiation'. The 1960 definition for the metre lasted only 23 years. On 20 October 1983, at the 17th General Conference on Weights and Measures the new definition for the metre as "the length of the path travelled by light in vacuum during a time interval of (1/299 792 458) of a second" was adopted [13,14,15].

In essence, there is no longer a physical standard for length. This strange definition defines the metre more accurately because the time interval can be measured with an accuracy of better than 1×10^{-13}. Wilke [12] explains that once the physicists could measure the speed of light more accurately than they could measure the metre itself, the days of the metre were numbered.

In 2019 the definition was changed to be more consistent with the other definitions of the SI units, with the change of the SI for Mass, the kilogram the last standard which still used an artefact as the standard for the SI, together with three other SI units were changed so that all the SI units will be defined in terms of natural constants, namely Cs frequency, speed of light, Planck constant, elementary change *e*, Boltzmann constant, Avogadro constant, and the monochromatic radiation of frequency 540 × 1012 hertz, K_{cd}. Figure 4 shows the relation between these natural constants and the SI units [16, 17, 18, 19]

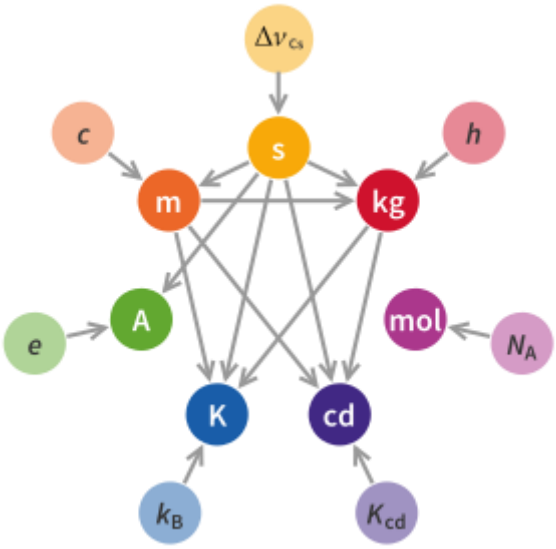

Figure 6 The natural constants realising the SI units after 2019.

The value of the metre did not change, but the definition from the 1983 definition changed and since 2019 it is the following: "The metre, symbol m, is the SI unit of length. It is defined by taking the fixed numerical value of the speed of light in vacuum *c* to be 299 792 458 when expressed in the unit ms^{-1}, where the second is defined in terms of the caesium frequency $\Delta\nu_{Cs}$" [20]. This allows each country to realise the metre through a reproduction of the SI definition of the metre. Figure 5 illustrates the SI system of units after 2019.

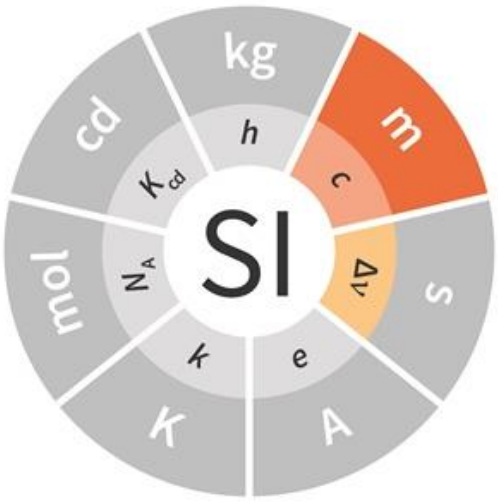

Figure 7 The SI system of units after 2019 with the metre (m) highlighted.

In national metrology institutes, the metre can be realised using one of the following two methods:

- By direct measurement of the light travel time; or
- By indirect measurements of the light travel time

The second method finds its application in dimensional metrology within the manufacturing sector, as detailed in the strategy document of the Consultative Committee for Length, overseeing the definition of the metre [21]. In dimensional metrology, the metre is defined through the concept termed the "practical realisation of the metre" [21].

Historically, since the 1980s, national metrology institutes primarily employed iodine-stabilized HeNe lasers to realise the metre. These systems provided accurate and effective means of ensuring traceability from the SI unit, the metre, to length and dimensional measurements. However, a transformative milestone occurred in 2006 with the development of the frequency comb, for which R. Glauber, J. Hall, and T. Hänsch were awarded the Nobel Prize in Physics in 2005 [22]. The frequency comb offered an accuracy that surpassed iodine-stabilized HeNe lasers by a factor of 1 000 [23–26].

Accurate length and dimensional measurements, coupled with a precise definition of the metre, are to support the manufacturing industry through the precise determination of positions and dimensions. The global market highlights the significance of accurate measurements, as parts manufactured in one country must fit with those produced in another, necessitating the importance of measuring uncertainty. The importance is highlighted by Savio and De Chiffre in the Manufacturing Industry [27]. In South Africa, this importance is further emphasised by McKinsey & Company, highlighting manufacturing as the largest potential income generator with a market size exceeding R500 billion [28].

These measurements are largely performed using optical techniques that require standardisation to the international unit of length, the SI unit, and the metre. Optical measurements cover a large range, from kilometres for long distances down to the nanometre range with a target uncertainty as low as 10 picometers. The significance of dimensional metrology and its intersection with the refractive index of air is well-documented by various researchers, including Gao et al., Ranusawud et al., Lazar et al., Pisani et al., Voigt et al., Schwenke et al., and Estler et al. [29–36]. The refractive index of air emerges as a critical factor not only in dimensional metrology but also in various other metrological fields, as expanded upon in the subsequent chapter.

Chapter 1 Bibliography

1. Bobis L, Lequeux J. Cassini, Rømer and the velocity of light. Journal of Astronomical History and Heritage. 2008;11(2):97–105. https://ui.adsabs.harvard.edu/abs/2008JAHH...11...97B/abstract
2. Raynaud L. Determining the speed of light (1976–1983): an internalist study in the sociology of science. L'Anee Sociolgique. 2013:63(2):359–98. https://doi.org/10.3917/anso.132.0359
3. Walker BH. (Ed.). Speed of light. In: Optical engineering fundamentals. 2nd ed. Bellingham: SPIE Press; 2009. https://spie.org/publications/tt82_25_speed_of_light
4. Adkins J, Orzel J, Vandemark K. PHY 335 Modern Physics Lab Experiment 1A: Speed of Light Measurement (Foucault Method) https://sciences.csuohio.edu/sites/csuohio.edu.sciences/files/media/physics/documents/Speed%20of%20Light_0.pdf
5. News from the BIPM. Metrologia. 1975;11(25):179–83. https://www.bipm.org/en/history-si/metre
6. Relicsworld. Seth Godin Quotes.[cited 2021 Dec 8]. https://www.relicsworld.com/seth-godin
7. Kruger OA. Robust air refractometer for accurate compensation of the refractive index of air every day. Master Thesis. 2016.
8. Cardarelli F. Encyclopaedia of Scientific Units, Weights and Measures. Springer; 2003.
9. NPL. Skills and learning. 2010. http://www.npl.co.uk/educate-explore/posters/history-of-length-measurement/
10. Bruce CF, Hill RM. Wavenumber reproducibility of the radiation 2p10–5d5 of Krypton 86. Australian Journal of Physics. 1962; 15.
11. Directed Light Inc. Laser flash lamp. 2016. http://directedlight.com/laser-components/catalog/laser-lamps/
12. Wilke T. Time to remeasure the metre. New Scientist. 1983;27:258–63.
13. Resolution 1. Metrologia. 1984; 25.
14. Practical realization of the definition of the metre. Metrologia. 1997.
15. Mise en practique of the definition of the metre. Metrologia. 2006.
16. Zong Y. From candle to candela. Nature Physics. 2016; 12:614. https://www.nature.com/articles/nphys3787.pdf?proof=t%253B
17. NPL. The redefinition of the SI units. [cited 2021 Dec 8]. https://www.npl.co.uk/si-units/the-redefinition-of-the-si-units

18. BIMP. The international system of units. 9th ed. 2019. https://www.bipm.org/en/publications/si-brochure/
19. NIST. Home. [cited 2021 Dec 8]. https://www.nist.gov/pml/weights-and-measures
20. BIMP. SI base unit: metre (m). [cited 2021 Dec 8]. https://www.bipm.org/en/si-base-units/metre
21. BIMP. Practical realization of the definition of some important units. [cited 2021 Dec 8]. https://www.bipm.org/en/publications/mises-en-pratique
22. The Nobel Prize. The Nobel Prize in Physics 2005. 2021. https://www.nobelprize.org/prizes/physics/2005/summary/
23. Ecole Polytechnique Federale de Lausanne. Optical frequency combs with a new dimension. Phys.org. 2021, Feb 22. https://phys.org/news/2021-02-optical-frequency-dimension.html
24. Stone JA, Egan P. An optical frequency comb tied to GPS for laser frequency/wavelength calibration. J Res Natl Inst Stand Technol. 2010;115(10):413–31. https://tsapps.nist.gov/publication/get_pdf.cfm?pub_id=904835
25. Kim S-W. Combs rule. Nature Photonics. 2009;3:313–4. https://doi.org/10.1038/nphoton.2009.86
26. NIST. Frequency combs. 2021, Jun 10. https://www.nist.gov/noac/technology/quantum-optics-and-radiometry/frequency-combs
27. Savio E, De Chiffre L, Carmignato S, Meinertz J. Economic benefits of metrology in manufacturing. CIP Annals—Manufacturing Technology. 2016;65(1). http://dx.doi.org/10.1016/j.cirp.2016.04.020
28. Mckinsey & Company. South Africa's big five: Bold priorities for inclusive growth. 2015.
29. Gao W, Kim SW, Bosse H, Haitjema H, Chena L, Lu D. Measurement technologies for precision positioning. CIRP Annals—Manufacturing Technology. 2015;64:773–96. https://doi.org/10.1016/j.cirp.2015.05.009
30. Ranusawud M, Limsuwanb P, Somthonga T, Vacharanukul K. Effects of the environment on the refractive index of air in long gauge blocks interferometry. Precision Engineering. 2013;37:782–6. https://doi.org/10.1016/j.precisioneng.2013.02.002
31. Lazar J, Holá M, Číp O, Čížek M, Hrabina J, Buchta Z. Refractive index compensation in over-determined interferometric systems. Sensors. 2012 Oct 19;12(10):14084–94. https://doi.org/10.3390/s121014084
32. Pisani M, Yacoot A, Balling P, Bancone N, Birlikseven C, Çelik M. Comparison of the performance of the next generation of optical interferometers. Metrologia. 2012; 49:499. https://doi.org/10.1088/0026-1394%2F49%2F4%2F455
33. Voigt D, Ellis JD, Verlaan AL, Bergmans RH, Spronck JW, Schmidt RHM. Towards interferometry for dimensional drift measurements with nanometer uncertainty. Measurement Science and Technology. 2011;22(9). https://doi.org/10.1088/0957-0233/22/9/094029

34. Schwenke H, Neuschaefer-Rubea U, Pfeifer T, Kunzmann H. Optical methods for dimensional metrology in production engineering. CIRP Annals. 2007;51:685–99. https://doi.org/10.1016/S0007-8506(07)61707-7
35. Estler WT, Edmundson KL, Pegg GN, Parker DH. Large-scale metrology—An update. CIRP Annals. 2002;51:587–609. https://doi.org/10.1016/S0007-8506(07)61702-8
36. Birch KP, Reinboth F, Ward RE, Wilkening G. The effect of variations in the refractive index of industrial air upon the uncertainty of precision length measurements. Metrologia. 1993;30(1):7–14.

Chapter 2: Refractive Index Measurements, Origin, and Impact

2.1 Origin and wide-ranging applications of refractive index

Thomas Young was most possibly the person who created the name refractive index with his double slit experiment in 1807 [1–4]. Since then, research into the refractive index has taken off and has been used widely in various fields. It is used in the measurement of thin films using optical methods [5]. In the medical industry, the refractive index is used to measure, for example, the specific gravity of human urine to determine whether a kidney is working [6–9]. In veterinary medicine, it is used to measure plasma protein and also in cell measurements of biological tissues [9,10]. Furthermore, the refractive index is critical in the design of optical eye lenses [11] and has been researched for use in human tears [12]. The refractive index is also used to determine the sugar content in various beverages, including wine [13], and the OIML TC17/SC/N2 published a directive for the "Methods and Means of Verification of Automated Refractometers" [14].

Singh [15] captured the application and impact of refractive index measurements well.

The examples above clearly illustrate the significates of refractive index on overall analysis.

2.2 Refractive index in metrology

Refractive index of air plays a critical role not only in dimensional metrology, but also in other areas of metrology. The 2019 revision of the International System of Units (SI) has emphasised the importance of natural constants [16], marking a significant conversion detailed by Foster in 2010 [17]. Three areas outside of metrology where the refractive index undertakes a vital role are:

i) the kilogram
ii) the kelvin; and
iii) pressure metrology, the pascal

i) The kilogram was till 2019 the only SI unit that was still defined as a physical artefact, but due to the instability in using an artefact, it was decided to change to a natural constant. The new definition of the SI unit the kilogram reads as follows: The kilogram, symbol kg is defined by the fixed numerical value of the Planck constant, h, which is 6 626 070 15 x 10^{-34} when expressed in the unit J s, which is equal to kg m^2. s^{-1} [18,19].

As is the case in many other SI units, the practical realisation and dissemination of the SI unit add uncertainties to the measurements. In the case of mass, there are buoyancy corrections of the air and are a major component to the overall uncertainty in the calibrations of mass standards as described by Pendrill [20]. The reason is that in the previous artefact, the kilogram and calibrations were made between similar artefacts, shapes, and material which led to no or extremely small buoyancy corrections required, but with the new definition this is not the case. In studies by Picard and Fang, the refractive index of air was in the calculation of the density of air required for buoyancy correction [21,22]. Picard and Fang demonstrated that air buoyancy can be determined based on the correlation between the air density, the buoyancy force is directly proportional to the density of the air, and the refractive index of the air. Formula 2, the density of the air, p can be calculated from *n* the refractive index and ratio R', the specific refraction.

$$p = \frac{2}{3R'}(n\text{-}1) \tag{2}$$

ii) The revised definition of the kelvin, also introduced in 2019, replaced the previously used International Temperature Scale (ITS-90) which was in use since 1990. The ITS-90 is based on fixed points, including the triple point of water at 0,01°C and the melting point of Gallium at 29,76460°C, which for temperature calibration as used in dimensional metrology. The new definition aligned the kelvin with physical constants as the other SI units. As expressed in the 2019 definition; "The kelvin, symbol K, is the SI unit of thermodynamic temperature. It is defined by taking the fixed numerical value of the Boltzmann constant k to be 1,380 649 x 10^{-23} when expressed in the unit $J.K^{-1}$, which is equal to kg m^2. s^{-2}. K^{-1}, where the kilogram, metre, and second are defined in terms of h, c and ΔvCs" [23].

The revised definition has several methods for temperature determination, with one approach by means of a Refractive index gas thermometer as described by Fischer and Zandt [24]. Formula 3 is used to calculate the temperature (T), using parameters the pressure (*p)*, the Boltzmann constant (k), the temperature (T), the refractive index (*n)*, the dielectric constant ($\mathcal{E}$) and the static electric polarisation (α).

$$p = kT\frac{(n^2-1)\mathcal{E}}{\alpha} \tag{3}$$

iii) The realisation of the unit pascal, although not a base unit, has research in realising more accurate measurements of the pascal which led to one advanced method containing measurement of the refractive index for pressure determination, as detailed by Mari et al [25] and figure 6 illustrates the application of a Michelson interferometer in this context. The measuring arm of the interferometer uses a double mirror multiplication setup, where the laser beam has multiple reflections between mirrors A and B, while the reference beam is directly focused on the mirror M_R.

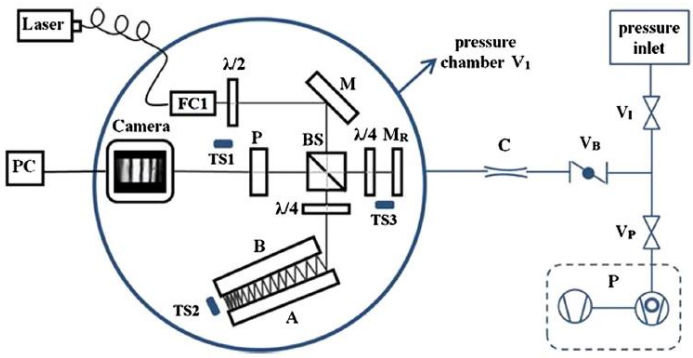

Figure 6 The refractometer to measure the refractive index in the determination of the pressure in chamber V_1[25]

Extensive research has been done to refining gas-modulated refractometers for the pascal realisation, as highlighted by Silander et al. and Egan et al. [26, 27]. Egan's study, shown in Figure 7, compares two laser refractometers and a validated manometer in the low-pressure range below 100 Pa. The manometer, positioned to the left in Figure 7, determines pressure by measuring the height difference (h) in the mercury columns of the reference (ref) and measure (meas) columns.

In this setup, two laser refractometers are employed, positioned at the top and bottom to the right in the figure. Following the standard configuration, these refractometers compare the measured (meas) cavity with a reference (ref) cavity in a vacuum. The principles of this refractive index measurement are explained in Chapters 3 and 4. Additional validations, including leak assessments, are conducted using two capacitance diaphragm gauges (PCDG) showcased in the centre of the figure.

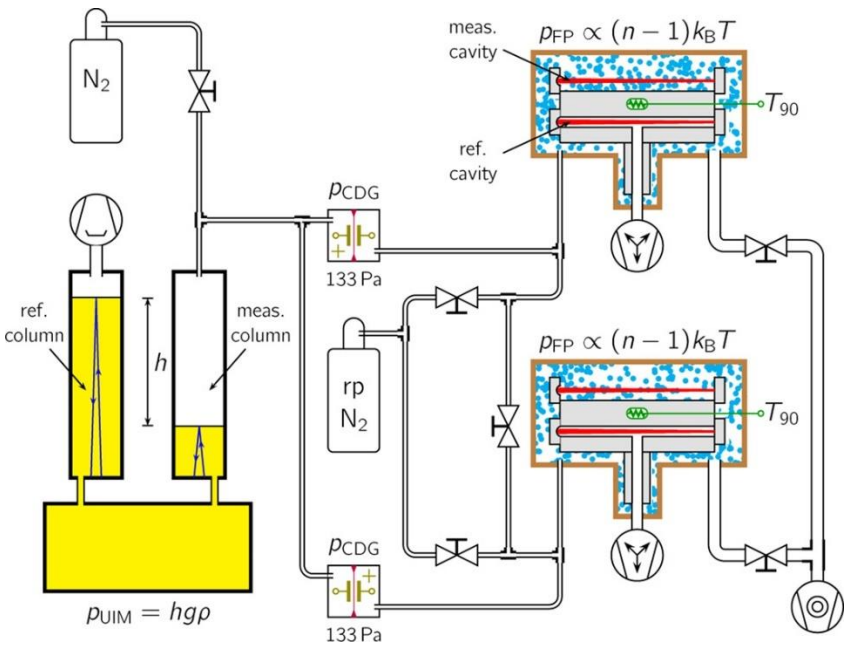

Figure 7 The refractometer to measure the refractive index to determine the pressure in the chamber V_1[26]

This research demonstrates the viability of refractometers in achieving highly reproducible and linear measurements of pressures below 1 kPa, with a precision better than 10^{-6} p. Egan et al contends that this system offers superior accuracy for pressure realisation, especially at lower pressures, and facilitates the mercury-free realization of the pascal.

2.3 Refractive index in dimensional and length metrology

In the area of dimensional and length metrology, the impact of highly accurate refractive index measurements is evident as discussed in previous chapters and form the topic of this research. The redefinition of the SI unit, the metre, in 2019 brought about a new definition: "The metre, symbol m, is the SI unit of length. It is defined by taking the fixed numerical value of the speed of light in a vacuum c to be 299 792 458 when expressed in the unit $m.s^{-1}$, where the second is defined in terms of the caesium frequency ΔvCs" [28]. This replaced the 1983 definition: "the metre is the length of the path travelled by light in a vacuum during a time interval of 1/299 792 458 of a second" [29]. However, the numerical value of the metre remained the same.

Precision dimensional and length measurements, particularly over the past three decades, largely use light specifically laser light. The accuracy of these measurements depends on an accurate knowledge of the refractive index, requiring a correction due to the fact that most measurements are conducted in air, as articulated by Haitjema [30].

While the metre is defined in terms of light and measurement using mainly laser systems, industrial measurements are mainly of mechanical components, especially metal parts. Gauge block standards bridge the gap between optical and mechanical measurements. Gauge blocks, made of materials for example steel, ceramic, tungsten carbide, or chrome carbide, is used as the standard between the optical to mechanical measurements. Calibration of gauge blocks is performed using a gauge block interferometer, initially with a light source of Krypton or Cadmium lamps and later laser systems since the 1980s. This method for gauge block measuring is well-documented by Doiron and Beers [31]. The uncertainty in gauge block measurements, as per Decker and Pekelski [32] and Zivkovic et al [33], is expressed as (19 + 0,28L) nm and (23 + 0,18L) nm, where L is the nominal length of the gauge block in millimetres and is the length dependant portion of the total uncertainty. The refractive index measurements contribute almost 0,2L nm in the Decker setup and 0,1L nm in the Zivkovic setup for the length-dependent part of the uncertainty. Accounting for uncertainties, it is evident that the refractive index holds the most substantial effect in the length-dependent uncertainty budget in gauge block interferometry, as explained by Coddington et al. and Meiners-Hagen [34,35].

Furthermore, in angle metrology, a subsection of dimensional measurement, the influence of refractive index on angle measurements is often overlooked in most practises and setups and is well described and documented by Geckeler and Kren [36].

Given the impact of the refractive index of air in dimensional metrology, applying corrections becomes critical. To achieve an accurate correction, the refractive index of air under specific environmental conditions must be accurately measured and calculated. The refractive index is calculated by dividing the speed (velocity) of light in a vacuum, c, by v', the velocity of light in air at the time of the measurements.

Equation 3 articulates the refractive index (*n)* as a measure of the speed of light in a vacuum (c) and the velocity of light in a specific medium (v''), particularly in this context, air:

$$n = \frac{c}{v''}, \tag{3}$$

Here, *n* signifies the refractive index*, c* represents the speed of light in a vacuum, and *v''* denotes the velocity in the specified medium, which, in this case, is air.

Chapter 2 Bibliography

1. Walker BH. (Ed.). Speed of light. In: Optical engineering fundamentals. 2nd ed. Bellingham: Spie Press; 2009. https://spie.org/publications/tt82_25_speed_of_light
2. Hecht E, Zajac A. Optics. Addison-Wesley; 2002.
3. Tretkoff E. This month in physics history: May 1801: Thomas Young and the nature of light. APS. 2008; 17(5). https://www.aps.org/publications/apsnews/200805/physicshistory.cfm
4. Young T. The Bakerian lecture. Experiments and calculation relative to physical optics. Philosophical Transactions of the Royal Society of London. 1803; 94:1–16. https://doi.org/10.1098/rstl.1804.0001
5. Joo H-Y, Kim SJ, Kim SJ, Kim SY. Spectrophotometric analysis of aluminium nitride thin films. J. Vac. Sci. Technol. A. 2016;17:862–70. https://doi.org/10.1116/1.582035
6. Putnam DF. Composition and concentration properties of human urine. *NASA.* 1971. https://ntrs.nasa.gov/archive/nasa/casi.ntrs.nasa.gov/19710023044.pdf
7. Anton Paar. Refractometric analysis of urine. [cited 2021 Dec 9]. https://www.anton-paar.com/corp-en/products/applications/refractometric-analysis-of-urine
8. Osborne CA, Nwaokorie E. Urine specific gravity measurement and interpretation in veterinary medicine. DVM360. 2013, May 1. https://www.dvm360.com/view/urine-specific-gravity-measurement-and-interpretation-veterinary-medicine
9. Carpignano F, Rigamonti G, Mazzini G, Merlo S. Low coherence reflectometry for refractive index measurements of cells in microcapillaries. Sensors. 2016;16:1670. https://dx.doi.org/10.3390%2Fs16101670
10. Zhou Y, Chan KKH, Lai T, Tang S. Characterizing refractive index and thickness of biological tissues using combined multiphoton microscopy and optical coherence tomography. Biomed. Opt. Express. 2013;4: 38–50.
11. Pierscionek BK, Augousti, AT. The refractive index in the eye lens—implications for clinical practice and optical design. Eyenews. 20016;23(2). https://www.eyenews.uk.com/features/ophthalmology/post/the-refractive-index-in-the-eye-lens-implications-for-clinical-practice-and-optical-design
12. Craig JP, Simmons PA, Patel S, Tomlinson A. Refractive index and osmolality of human tears. Optom. Vis. Sci. 1995 Oct;72(10):718–24. https://doi.org/10.1097/00006324-199510000-00004
13. Robinson J. The Oxford Companion to Wine. Vol. 3. Oxford University Press; 2006.

14. Organisation Internationale de Métrologie Légale. Automated refractometers: methods and means of verification. OIML TC17/SC/N2. 2006. https://www.oiml.org/en/tc-sc-pg/committee-drafts/files/tc17-sc2-2cd-refractometers.pdf
15. Singh S. Refractive index measurements and its applications. Phys Scripta. 2006;65(2):167.
16. BIPM. Resolution 1 of the 26th CGPM (2018); On the revision of the International System of Units (SI). Proceedings of the 26th CGPM (2018). 2019:472. https://www.bipm.org/en/committees/cg/cgpm/26-2018/resolution-1
17. Foster M. The next 50 years of the SI: a review of the opportunities for the e-Science age. Metrologia. 2010;47(6).
18. BIPM. SI base unit: kilogram (kg). [cited 2021 Dec 9]. https://www.bipm.org/en/si-base-units/kilogram
19. Kuramoto N, Mizushima S, Zhang L, Fujita K, Ota F, Okubo S, Inaba H. Realization of the new kilogram using 28Si-enriched spheres and dissemination of mass standards at NMIJ. JAPAN. 2020;35:491–8. https://doi.org/10.1007/s12647-020-00393-2
20. Pendrill LR. Density of moist air monitored by laser refractometry. Metrologia. 1988;25(2):87. http://dx.doi.org/10.1088/0026-1394/25/2/005
21. Picard A, Fang H. Three methods to determine the density of moist air during mass comparisons. Metrologia. 2002;39:31–40.
22. Picard A, Fang H. Methods to determine the density of moist air. EEE Transactions on Instrumentation and Measurement. 2003 Apr;52:504–7. http://dx.doi.org/10.1109/TIM.2003.810460
23. BIMP. SI base unit: kelvin (K). [cited 2021 Dec 9]. https://www.bipm.org/en/si-base-units/kelvin
24. Fischer J, Zandt T. New definition of the kelvin and the dertermination of the Boltzmann constant. 56th Internation Sceintific colloquium. 2011.
25. Mari D, Pisani M, Zucco M. Towards the realisation of an optical pressure standard. Measurement. 2019;132:402–7. https://doi.org/10.1016/j.measurement.2018.09.069
26. Silander I, Hausmaninger T, Forssen C, Zelan M, Axner O. Gas equilibration gas modulation refractometry for the assessment of pressure with sub-ppm precision. J Vac Sci Technol B. 2019;37:042901. https://doi.org/10.1116/1.5090860
27. Egan P, Stone J, Schereshligt J, Harvey A. Measured relationship between thermodynamic pressure and the refractivity for six candidate gases in laser barometry. J Vac Sci Technol A. 2019;37. https://doi.org/10.1116/1.5092185
28. BIMP. SI base unit: metre (m). [cited 2021 Dec 8]. https://www.bipm.org/en/si-base-units/metre
29. BIMP. Resolution 1 of the 17th CGPM (1983). Definition of the metre. Proceedings of the 17th CGPM (1983). 1984:97. https://www.bipm.org/en/committees/cg/cgpm/17-1983/resolution-1

30. Haitjema H. Achieving traceability and sub-nanometer uncertainty using interferometric techniques, Meas. Sci. Techno. 2008;19:084002.
31. Doiron T, Beers J. The Gauge Block Handbook, https://emtoolbox.nist.gov/publications/nistmonograph180.pdf
32. Decker, J. E.; Pekelsky, J. R. Uncertainty evaluation of Gauge block by optical interferometry, Metrologia, Volume 34, Number 6. 1997
33. Zivkovic V, Zelenika S, and Stefanovic G. Uncertainty evaluation for the gauge blocks calibration using the modified DMDM gauge block interferometer. Int. J. Metrol. Qual. Eng. 3, 19–27 (2012)
34. Meiners-Hagen K, Bošnjakovic A, Köchert P, Pollinger F. Air index compensated interferometer as a prospective novel primary standard for baseline calibrations. Meas. Sci. Technology. 2015;26:084002.
35. Coddington I, Swann WC, Nenadovic L, Newbury NR. Rapid and precise absolute measurements at long range. Nature Photonics. 2009;3. https://tsapps.nist.gov/publication/get_pdf.cfm?pub_id=901111
36. Geckeler RD, Kren P, Just A, Schumann M, Krause M. Influence of the air's refractive index on precision angle metrology with autocollimators, Meas. Sci. Technology. 2018;29:075002.

Chapter 3: Literature Research using the Weather station method, Wavelength Trackers and Absolute Refractometers

As described in the previous chapter, the metre was first defined by the speed of light in 1983 as "the length of the path travelled by light in vacuum during a time interval of 1/299 792 458 of a second" and in May 2019, the definition changed but not the value of the SI unit the metre [1]. In the previous chapters, we looked at the history of the metre to how and why the metre came to be defined as the speed of light in a vacuum despite most dimensional and length measurements being performed in air [2].

The refractive index in air fluctuates according to different environmental conditions, such as a change in air pressure, air temperature, relative humidity, and CO_2, so the refractive index of air at specific conditions must be calculated to make corrections to the speed of light in air compared to the speed of light in a vacuum [3].

Two methods exist for determining the refractive index. The first method, known informally as the weather station method, requires measuring the environmental parameters of the air; the temperature, pressure, humidity, and occasionally CO_2 levels depending on the contents of CO_2 in the air, followed by calculating the refractive index employing equations initiated by Edlén [3] and subsequently refined by Muijilwijk and Downs [4,5]. Ciddor and others have further investigated this method, particularly concerning its application to electronic distance meters operating in the visible and near-infrared spectrum [4-6]. However, the weather station method is affected by numerous limitations, described in many studies, and captured well by Bonsch and Potulski [7], and Chetty and Kruger [8].

The second method comprises using a refractometer to measure the refractive index by comparing the optical path of a light beam in air against the same path length in a vacuum. Given the limitations associated with the weather station method, prior research by Bonsch and Potulski [7], and by the author Chetty and Kruger [8], previous research by the author focused on the use of refractometers to measure the refractive index of air for use in dimensional metrology. This method is a simple calculation of the path differences in the air and vacuum.

Since the metre was defined by light waves in 1960, refractometers have been subject to frequent research and development. Terrien documented the construction of an air refractometer for interference-length metrology in 1965 [9], shown in Figure 8.

Detailing the development of a refractometer for length metrology shortly after the redefinition of the metre in 1960, which designated the Krypton wavelength to realise the SI unit the metre. This refractometer, designed to measure the refractive index of air, utilises two paths of interference fringes, one in air and the other in vacuum. The achieved uncertainty of this design was 1×10^{-8}, limited by the vacuum wavelength of the Krypton.

Despite its simplistic design, this refractometer achieved remarkable accuracy, paving the way for subsequent research.

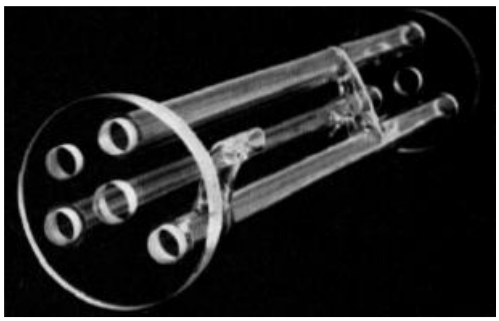

Figure 8 The refractometer designed by Terrien [9]

The effort to develop commercial refractometers for everyday use was led by Zygo and Keysight (formerly Hewlett-Packard Company, HP, and Agilent), resulting in designs that are both inexpensive to manufacture and commercially viable. However, it is crucial to note that these instruments function as optical wavelength compensators, only tracking wavelength changes rather than directly measuring the absolute value of the refractive index [11,12].

Figure 9 illustrates the design of the Hewlett-Packard (Agilent) system, while Figure 10 displays the Zygo wavelength compensator, both bearing a striking resemblance to the Terrien refractometer. These wavelength-tracking compensators form parts of laser displacement interferometers and feature a stable vacuum cavity fixed to a baseplate. An interferometer is employed to measure changes between the vacuum cavity and its ambient air environment.

It is however important to emphasise that these instruments solely measure the relative change between the vacuum cell and the surrounding air, requiring the input of the initial refractive index at the start of measurements. Typically, this is conducted through the utilisation of modified Edlén's equations in the weather station method. In both systems, measurement and reference beams traverse identical optical paths, with the reference beam traversing through vacuum tubes and the measurement beam traversing through air.

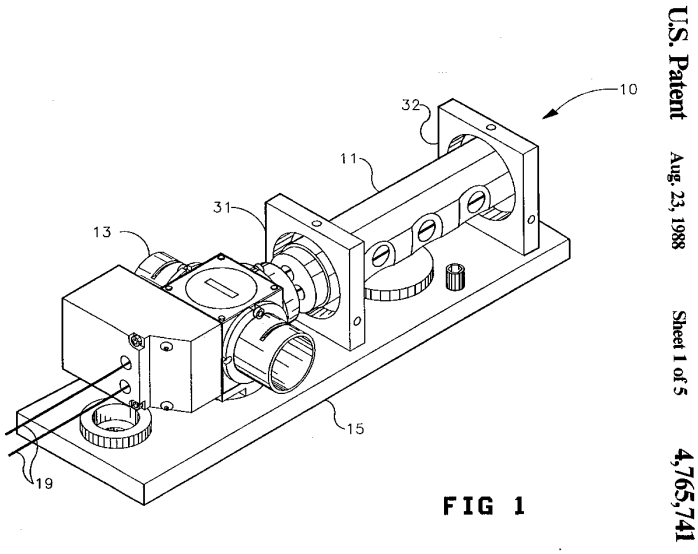

Figure 9 Patented Hewlett-Packard designed wavelength tracker [10]

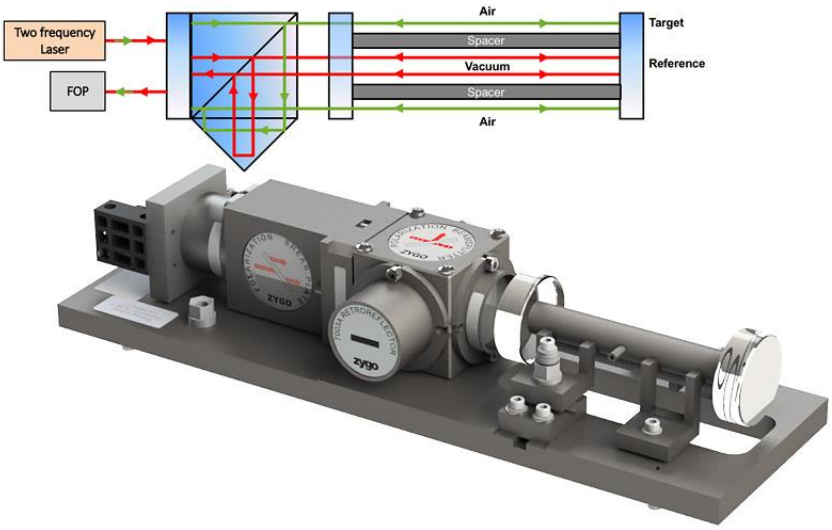

Figure 10 Zygo wavelength compensator [11]

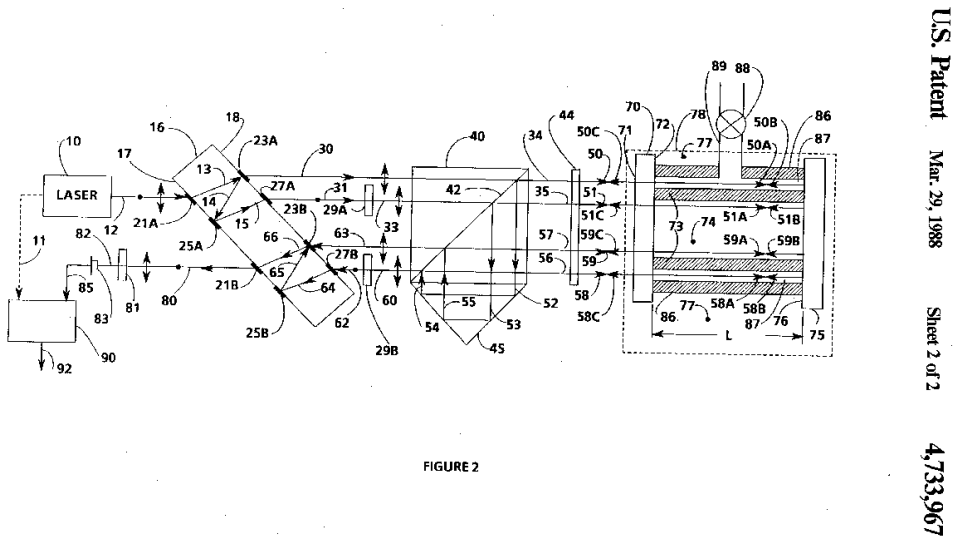

Figure 11 Zygo measurement of the refractive index of a gas [12]

Zygo has continued the development with two patents authored by Sommargren, which not only track wavelength changes compared to a vacuum cell but also measure the absolute refractive index [13, 14], as depicted in Figure 11. This second system by Zygo employs a vacuum pump to set up a vacuum, enabling absolute measurements of the refractive index of air [12, 13]. These were studied in the development of an absolute refractometer in previous research by the author, as outlined by Kruger and Chetty [8].

Significant research has been conducted and continues to be undertaken using refractometers to measure the refractive index of air for correcting the velocity of light (V.O.L) in displacement lasers utilised in dimensional metrology. These refractometers also contribute to the improvement of the original Edlén equation. Kruger and Chetty have extensively documented much of this research [8,14].

In 1992, Tsai filed a patent (US Patent 5394244) [6], as discussed earlier, proposing a laser refractometer incorporating an interferometer as the optical measuring element, alongside an object mirror and an etalon, illustrated in Figure 12.

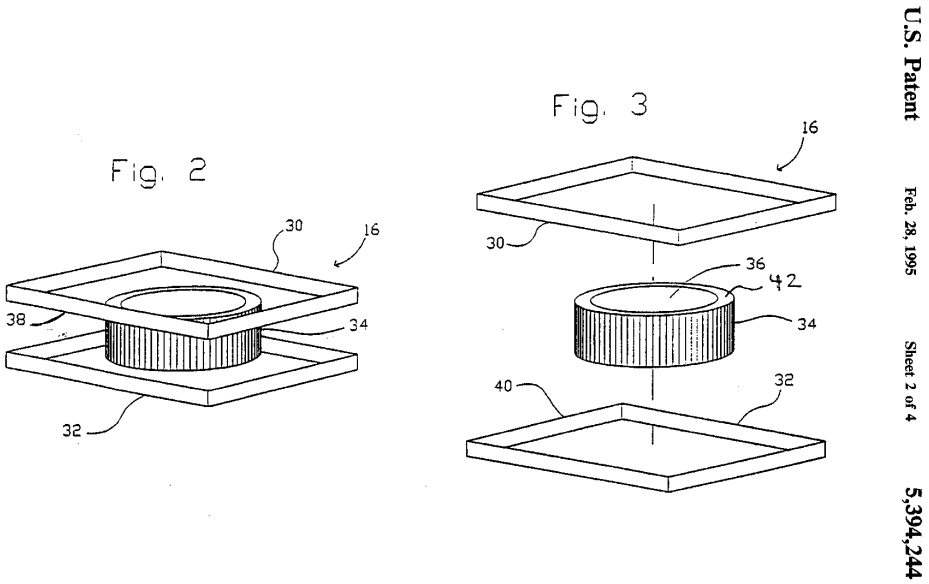

Figure 12 Patented refractometer by Tsai displaying the vacuum etalon with two flat and parallel windows [6]

In the search for a refractometer design, numerous studies have applied different approaches. Lazar, Číp et al., and Lazar, Holá et al. [15,16] describe a method using two counter-measuring interferometers, combining tracking and displacement interferometry, a referencing laser wavelength to a mechanical standard with ultra-low thermal expansion, achieving high accuracy of 5×10^{-8}.

The use of two-colour interferometry presents a promising avenue for research, offering advantages over single-beam refractometers in measuring the refractive index. Zhu et al., Meiners-Hagen and Abou-Zeid, and Matsumoto and Honda have researched this method [17, 18, 19]. However, Meiners-Hagen and Abou-Zeid note its suitability only for dry air, and its requirement of using two-colour interferometers will make production more costly.

Wu et al. further research into two-colour interferometry, employing a frequency comb to measure the refractive index, a method also researched by Balling et al. and Zhang et al. [20, 21, 22, 23]. While offering high repeatability, the cost of a frequency comb is also extremely expensive to be used in everyday measurements of the refractive index, one of the criteria of the original target for this research.

Additionally, there are studies indirectly employing refractometers to measure the refractive index, contributing valuable insights to the design of a permanent vacuum refractometer. Notable among these are the works of Lewis and Ellis, who extensively utilised interferometry techniques in their measurement designs.

The development of refractometers has been driven by companies supplying laser measurement systems, such as Keysight and Zygo. Primarily, wavelength trackers have been commercialised mainly due to the technical challenges associated with vacuum pumps and their cumbersome nature, impacting the practicality and accuracy of refractometers in daily use.

Several other studies use refractometers to measure the refractive index, but this was not the main focus of their research but was very valuable for the design of a permanent vacuum refractometer. Lewis and Ellis [26,27] used interferometry techniques extensively in their measurement designs, where Lewis's research was into an accurate system to measure gauge blocks using a two-laser measurement method and Ellis used optical measurements to determine the dimensional stability of various materials. As both used optical measurements to a high accuracy, they required a high accurate measurement of the refractive index of air.

Research continued into the more accurate measurements of the refractive index of air with investigation by 1988, Bonsch and Potulski [7] into the change of the optics during the air and vacuum stages. Their study investigated the complexities of refractive index measurements using the Edlin equation and the challenges inherent in refractometry. Their research significantly influenced the design of the refractometer in the current study.

Later research by, Renkens and Schellekens [29] and Tsai's [30] appeared promising, with the use of a permanent vacuum etalon in the form of a prism. Tsai founded Exel Precision, a company specialising in laser measurement systems, including refractometers compatible with their developed laser systems.

In the Tsai patent, a refractometer is described where a vacuum etalon is transferred across the paths of two laser beams, a reference and a measurement beam. This setup is that the reference beam traverses in a vacuum within the etalon while the measurement beam travels the same distance in ambient air around the vacuum etalon. Renkens and Schellekens did research with the same optical setup as Tsai, also using a permanent vacuum etalon traverse across the laser beams to measure the refractive index. However, the findings of both Renkens and Schellekens and Tsai were inconclusive owing to doubts about whether this approach had a clear advantage over the cylinder refractometers. The Tsai second patent is illustrated in Figures 13 and 14.

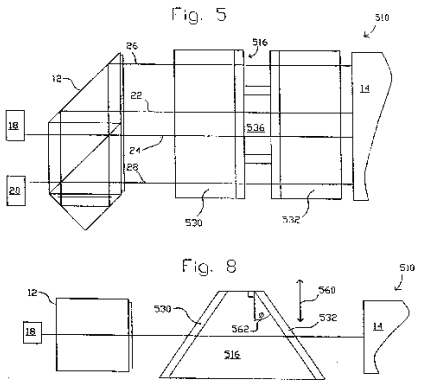

Figure 13 Schematic diagram of the Tsai permanent vacuum refractometer [31]

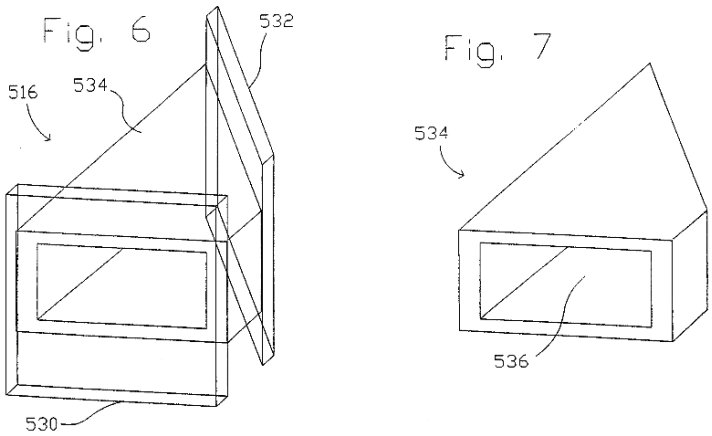

Figure 14 Tsai's U.S. patent US5394244A. 1992 of permanent vacuum prism design [31]

After a detailed study of the literature mentioned above, it was decided that the design of a new permanent vacuum refractometer should be based on the approaches initiated by Renkens, Schellekens, and Tsai. Although other research by Wu and Takahashi, who used of a frequency comb for high refractive index measurements, with high resolution the final accuracy of such systems was comparable to other designs due to factors such as

optical layout and optical changes from air to vacuum. Additionally, concerns were raised regarding the stability of the distance between mirrors in these systems. These are summarised in table 1 below.

Table 1 Advantages and disadvantages of a tube refractometer.

Advantages of tube refractometer	Disadvantages of tube refractometer
Very high resolution	The use of vacuum pump generating unwanted heat
Simple construction	Change of optics under vacuum
Straightforward calculation of refractive index	Stability between mirrors/windows of tube
High accurate refractive measurements	

Therefore, the decision to adopt the methods proposed by Renkens, Schellekens, and Tsai was made for this research effort.

Therefore, the decision to adopt the methods proposed by Renkens, Schellekens, and Tsai was made for this research effort.

Chapter 3 Bibliography

1. BIMP. SI base unit: metre (m). [cited 2021 Dec 8]. https://www.bipm.org/en/si-base-units/metre
2. Haitjema H. Achieving traceability and sub-nanometer uncertainty using interferometric techniques. Meas. Sci. Techno. 2008;19:084002.
3. Edlén B. The refractive index of air. Metrologia. 1965;2:71–80.
4. Birch KP, Downs MJ. An updated Edlén equation for the refractive index of air. Metrologia. 1993;30:155–62.
5. Muijilwijk R. Update of the Edlén formulae for the refractive index of air. Metrologia. 1988;25:189.
6. Ciddor PE. Refractive index of air: new equations for the visible and near-infrared. Appl. Opt. 1996;35: 1566–73.
7. Bonsch G, Potulski E. Measurement of the refractive index of air and comparison with the modified Edlén's formulae. Metrologia. 1998;35:133–9.
8. Kruger O, Chetty N. Robust air refractometer for accurate compensation of the refractive index of air in everyday use. OSA. 2016;55:9118–22.
9. Terrien J. An air refractometer for interference length metrology. Metrologia. 1965;1(3):80.
10. Hewlett-Packard Journal 1983, https://www.hpl.hp.com/hpjournal/pdfs/IssuePDFs/1983-04.pdf
11. Zygo. Interferometers. ZMI™ Series—Displacement Measuring Interferometers. [cited 2021 Dec 9]. https://www.zygo.com/products/nano-position-sensors/displacement-measuring-interferometers/interferometers
12. Scott M, Filed A. Wavelength tracking compensator for an interferometer. US patent: US4765741A. 1987.
13. Sommargren G. Apparatus for the measurement of the refractive index of a gas. US patent: US4685803A. 1986.
14. Sommargren G. Apparatus for the measurement of the refractive index of a gas. US patent: US4733967A. 1987.
15. Kruger OA. Robust air refractometer for accurate compensation of the refractive index of air in every day. Master Thesis. 2016.
16. Lazar J, Číp O, Čížek M, Hrabina J, Buchta Z. Suppression of air refractive index variations in high-resolution interferometry. Sensors. 2011;11: 7644–55. https://doi.org/10.3390/s110807644

17. Lazar J, Holá M, Číp O, Čížek M, Hrabina J, Buchta Z. Refractive index compensation in over-determined interferometric systems. Sensors. 2012 Oct 19;12(10):14084–94. https://doi.org/10.3390/s121014084
18. Zhu Y, Matsumoto H, Oishi T. Long-arm two-color interferometer for measuring the change of air refractive index. Proceedings 1319, Optics in Complex Systems. 1990. https://doi.org/10.1117/12.34845
19. Meiners-Hagen K, Abou-Zeid A. Refractive index determination in length measurement by two-colour interferometry. Meas. Sci. Techno. 2008;19:084004.
20. Matsumoto H, Honda T. High-accuracy length-measuring interferometer insing two-colour method of compensating for the refractive index of air. Meas. Sci Techno. 1992;3.
21. Wu G, Arai K, Takahashi M, Inaba H, Minoshima K. High accuracy correction of air refractive index by using two-color heterodyne interferometry of optical frequency combs. Meas. Sci. Techno. 2013;24:015203.
22. Wu G, Arai K, Takahashi M, Inaba H, Minoshima K. Extremely high-accurate correction of air refractive index using two-colour optical frequency combs. Scientific Reports. 2013;3:1894.
23. Balling P, Masika P, Kren P, Dolezal M. Length and refractive index measurements by Fourier transform interferometry and frequency comb spectroscopy. Meas. Sci. Techno. 2012;23.
24. Zhang J, Lu ZH, Wang LJ. Precision measurements of the refractive index of air with frequency combs. Optics Letters. 2005;30:3314–6. https://doi.org/10.1364/OL.30.003314
25. Schellekens P, Spronck J, van de Pasch E. Design and results of a new interference refractometer based on a commercially available laser interferometer. Annals of the CIRP. 1986;35.
26. Schellekens P, Wilkening G, Reinboth F, Downs MJ, Brirch KP, Spronck J. Measurements of the refractive index of air using interference refractometers. Metrologia. 1986;22:249–87.
27. Lewis A. Absolute length measurement using multiple wavelength phase setting interferometry. PhD thesis. 1993.
28. Ellis D. Optical metrology techniques for dimensional stability measurements. PhD dissertation. Delf: Technische Universiteit; 2010.
29. Renkens M, Schellekens P. An accurate interference refractometer based on a permanent vacuum chamber. CIRP Annals: Manufacturing Technology. 1993;42:581–3. https://doi.org/10.1016/S0007-8506(07)62514-1
30. Tsai JC. Ambient air refracture index device. US Patent: US5394244A. 1992, https://excelprecision.com/

31. Wu, G., Takahashi, M., Arai, K., Inaba, H. & Minoshima, K. Extremely high-accurate correction of air refractive index using two-colour optical frequency combs. *Sci. Rep.* **3,** 1894 (2013).

Chapter 4: Design of the Permanent Vacuum Refractometry

4.1 Principles of length measurements using distance laser interferometers

Since the discovery of the laser in 1960, it has been used in dimensional metrology to achieve the highest accuracy of measurement. In most laboratories, including at NMISA, the predominant displacement lasers are manufactured by Renishaw, Zygo, SIOS, and Agilent. Among the laser interferometers used, two main types are utilised: heterodyne and homodyne laser systems. Both utilise a helium-neon (HeNe) gas laser tube to generate a coherent light beam within the laser head. Figure 15 illustrates the heterodyne laser system developed by companies such as Keysight, Renishaw, and Zygo [1,4].

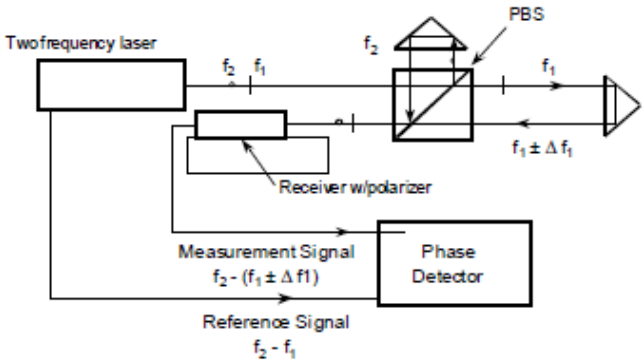

Figure 15 Operation of a heterodyne laser system [1]

In recent years, the homodyne laser system developed by SIOS has gained increasing popularity. Figure 16 illustrates the configuration of the homodyne laser measuring system [2]. In this setup, a HeNe laser is employed, mirroring the HeNe laser used in the heterodyne interferometer of Zygo laser systems.

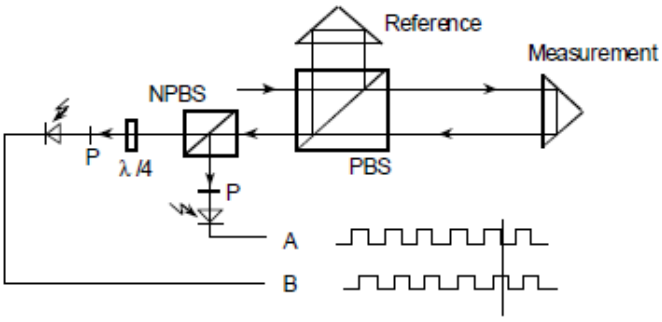

Figure 16 Operation of a homodyne laser system [1]

The setup features a simple Michelson interferometer, allowing the determination of the relative displacement of the moving mirror by calculating the sinusoidal pulses [3]. This configuration is illustrated in Figure 17.

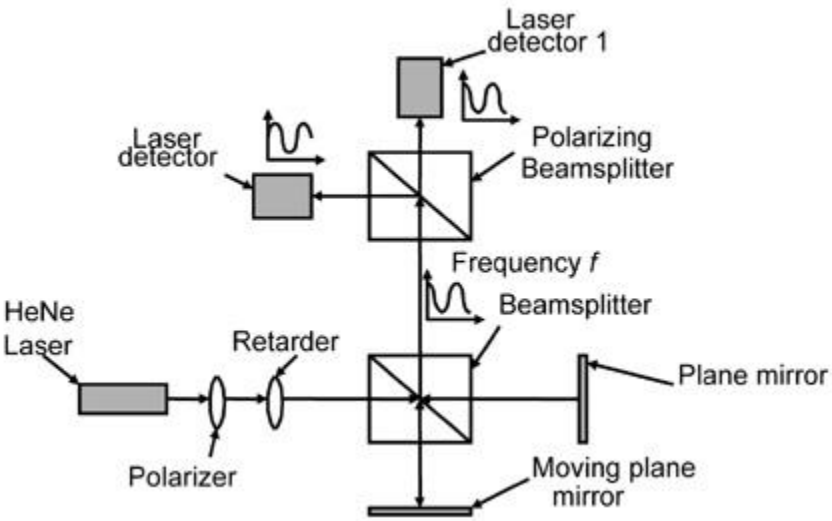

Figure 17 A homodyne laser interferometer with quadrature detection [3]

While theoretically any of these laser systems could be used, this study used a commercial dual-frequency heterodyne laser, specifically the Zygo ZMI 2000 interferometer, and in certain experiments, an additional Keysight laser interferometer was employed. The frequency split of the two laser beams for the Zygo system is approximately 20 MHz [1], whereas the Keysight laser exhibits a 2 MHz frequency difference [1,4]. Although theoretically feasible, the homodyne SIOS laser for this research has not been used and was not verified.

4.2 Refractometer design

The work by Kruger and Chetty on a low-cost, robust refractometer [8,9] played a pivotal role in deciding on the refractometer design. Their research involved developing refractive index measurements through a robust refractometer, which utilised a commercial laser displacement interferometer alongside a vacuum cylinder/tube and vacuum pump to achieve refractive index measurements accurate to parts in the 10^{-8} range. Figure 18 illustrates the optical layout of their refractometer. Notably, this refractometer was designed to measure the velocity of light by directly comparing the optical path of a laser beam in air to that in a vacuum. Its simplicity in design and measurement model (Equation 1) enabled its daily use, although it necessitated a vacuum pump during each refractive index measurement. The proximity of the vacuum pump to the refractometer introduced heat from the pump, affecting the air temperature during laser measurements. Furthermore, the repeated vacuum cycles could lead to the introduction of dust particles into the vacuum cylinder, consequently influencing measurements through laser beam diffraction.

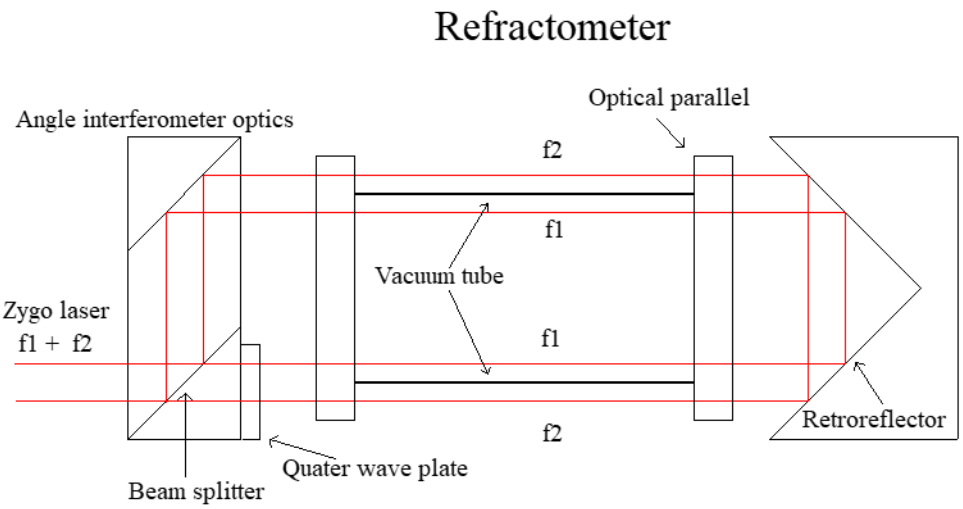

Figure 18 Schematic diagram of the Kruger and Chetty's Refractometer [8]

Traditional cylinder refractometers face several challenges with these identified as problems areas which must be eliminated or reduced in the design of a new refractometer:

i) **Change in Optical Thickness:** Bonsch and Potulski [8] detected a variation in the optical thickness of the side windows in tube refractometers during the transition from air to a vacuum, measuring it to be 8 nm. Although very small, this change contributes to the overall uncertainty of tube refractometers.

ii) **Change in Cylinder Length**: Stone and Stejskal [10] reported a change in the length of the cylinder under vacuum, resulting in uncertainties up to 4×10^{-8} for their refractometer.

iii) **The use of a vacuum pump**: As described by Kruger and Chetty [8,9] where the vacuum pump generates extra, unwanted heat and can lead to dust particles in the vacuum tube.

Given these challenges, the objective of this research is to design, construct, and evaluate an air refractometer suitable for everyday laser-based measurements, eliminating the need for a vacuum pump. Additionally, an attempt was made to overcome the difficulties identified with tube refractometers named by Bonsch and Potulski [7] and Stone and Stejskal [10].

4.3 Experimental refractometer using a permanent vacuum prism as vacuum etalon.

The initial prototype of the refractometer was developed based on the same principle of the above research where a permanent vacuum etalon is traversing across laser beams to measure the refractive index. Additionally, it was attempted to use commercially available components for both the permanent vacuum etalon and the laser measuring systems to reduce costs. A similar optical arrangement, tested for its stability over extended periods, as confirmed in previous research by Kruger and Chetty, was adopted [8,9], with laser readings demonstrating stability of less than 2 nm over periods exceeding a month.

The Agilent angle interferometer, model 10770A, was used to split the heterodyne laser beams into two frequencies through the use of a polarising beam splitter, aligning the beams, shown as f1 and f2, parallel and a distance of approximating 32 mm [4] apart. Whereafter, the two laser beams were reflected to the laser by using the Agilent angle retroreflectors. The optical paths and the etalon used as the permanent vacuum prism are displayed in Figure 14.

For the first design of the refractometer, a commercially available prism whose intended design was for the measuring of the refractive index of liquids was used [12]. The specific prism from 3B Scientific, shown in Figure 19 did not have detailed specifications regarding the optical flatness and parallelism of the side windows, which were later identified as critical features. Further discussions on this matter are discussed later in this section. To allow for a permanent vacuum etalon, the prism was modified by attaching a vacuum pipe to its opening on top of the prism.

Figure 19 Hollow prism from 3B Scientific [13]

As previously cited, the optical configuration is similar to the previously researched tube refractometer, as displayed in Figure 20 [8,9]. However, in this study, the vacuum tube was replaced with the aforementioned prism. In place of a vacuum pump to generate the required vacuum for comparing the air and vacuum ratios, the permanent vacuum prism was traversed across the laser beams to replace the optical path length from vacuum to air.

In this arrangement, in Figure 14 the commercial heterodyne laser (Zygo ZMI 2000 laser interferometer) is used. The frequency split between the two laser beams is approximately 20 MHz [1]. The Agilent angle interferometer optics (model 10770A) is used to split the frequency laser beams through the polarising beam splitter and to maintain separation between them, similar to the previous tube refractometer as in Figure 9.

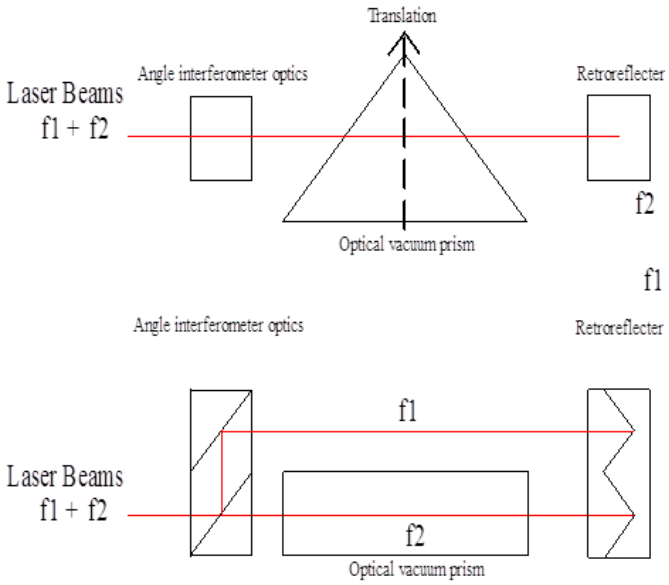

Figure 20 Schematic diagram of the prism refractometer using a laser displacement interferometer and translation stage.

The placement of vacuum prism was positioned in such a way as to have one laser frequency, f2, through the prism, while the other laser frequency, f1, was through the air above the prism. With the use of a translation stage, the prism was moved through the laser beam f2, effectually substituting the air with vacuum. As demonstrated in Figure 21, the prism is securely positioned on the translation stage, with a displacement laser (HP/Agilent Model 5519A) used to accurately measure the displacement of the translation stage.

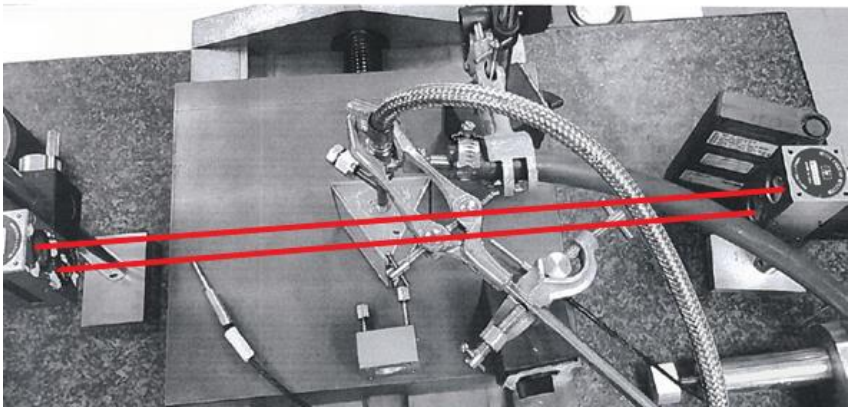

Figure 21 Prism refractometer.

The distance travelled by the translation stage is given as L_t, and the angle, θ, are used to calculate the light path within the vacuum inside the prism, given as L_i, given that a small position for L is already positioned within the vacuum, the calculation for L is expressed as follows:

$$L = 2 * (\tan * L_t) \tag{4}$$

Subsequently, the refractive index can be calculated the same as for the tube refractometer methodology, with l representing the change between the two laser readings:

$$n = \left(\frac{L+l}{L}\right) \tag{5}$$

By substituting Equation 3 into Equation 4, Equation 5 is derived to calculate the refractive index:

$$n = \frac{2*(tan\theta*Lt)+l}{2*(tan\theta*Lt)} \tag{6}$$

The angle of the prism was accurately measured using a Zeiss Prismo Coordinate Measuring Machine (CMM). The accuracy of the CMM measurement is discussed in Chapter 6.

The commercial hollow prism used was not optimal, and while the angle could be measured very accurately, the optical flatness and parallelism of the sides of the prism and the effect of these could not. It was necessary to determine the difference in the wavefront of the optical path through the prism while it is traversed across the laser beams. To determine this, measurements were taken with air inside the prism. The complete

refractometer and all optics were covered with Perspex to equalise the environmental air outside and inside the prism and after hours of stabilisation, it was expected that the air inside and outside the prism was at the same temperature, pressure, and humidity. These readings were used as a baseline measurement and were added to the final measurements when the vacuum inside the prism was drawn.

The results of the prism refractometer were compared to the weather station method, which measures the air temperature, pressure, and humidity and then calculates the refractive index using the updated Edlén equation [14,15,16]. In Table 1, the velocity of light compensation (V.O.L.) was calculated as most of the manufacturers of laser displacement systems use this V.O.L. in their software calculations [1–4]. The relation between the V.O.L. and the refractive index is shown in Equation 6 and is the inverse of the refractive index *n.*

$$\text{V.O.L.} = n^{-1} \tag{7}$$

Table 2 is the velocity of light compensation (V.O.L.), in 5 mm intervals over a 25 mm transverse travel. The differences between the two methods were examined, with the worst difference recorded as $1{,}2 \times 10^{-7}$. These differences inclined to reduce with longer travel in the traverse direction, attributed to the increased air-vacuum distance, resulting in reduced sensitivity of laser readings to the overall uncertainty.

Multiple sets of readings were taken over a two-week period, with the standard deviation between the readings calculated to measure the repeatability of the system. The standard deviation calculated was $5{,}5 \times 10^{-8}$ which will be investigated further in the subsequent section.

Table 2: Results for the prism refractometer data compared to the modified Edlin equation using weather station measurement calculations.

Stage moved		Prism readings								
Transverse laser reading (mm)	Air length replaced (nm)	Laser reading in the air (nm)	Laser reading in vacuum (nm)	Laser reading combined (nm)	Air temp. (°C)	Air pres. (mbar)	Air humd. (%RH)	V.O.L. Edlin Eq.	V.O.L. prism	Diff in V.O.L. between Edlin eq. and prism refract.
					20,47	862,92	62.6	0,999769653		
5	5795372,598	1305	31	1336					0,999769524	1,28619E-07
10	11590745,2	2475	195	2670					0,999769697	-4,38533E-08
15	17386117,79	3248	758	4006					0,999769639	1,36373E-08
20	23181490,39	3564	1778	5342					0,999769611	4,23826E-08
25	28976862,99	3692	2985	6677					0,999769628	2,51354E-08

4.4 Uncertainty calculations with a commercial prism in the translation stage

The estimation of the uncertainty for the Edlén weather station method involved estimating the uncertainties associated with each sensor's measurements, taking in both calibration uncertainties and sensor uncertainties during the measurements. The uncertainty estimates for the air temperature, humidity, and pressure were 0,05°C, 2% RH, and 0,1 mbar, respectively, resulting in refractive index uncertainties of $5{,}1 \times 10^{-8}$, $1{,}7 \times 10^{-8}$, and $2{,}7 \times 10^{-8}$, respectively. Combining these uncertainties using the root sum square (RSS) method resulted In an overall uncertainty of $5{,}9 \times 10^{-8}$ in the refractive index [18]. This is further discussed in Chapter 6.

The uncertainty calculation for the translation stage was calculated only for the maximum travel of 25 mm with a Keysight (HP) laser displacement system, resulting in a conservative uncertainty estimate of 0,5 µm, translating to a refractive index uncertainty of $0{,}5 \times 10^{-9}$.

The uncertainty in the angle of the prism was determined using the uncertainty of the Zeiss CMM, resulting in an uncertainty of 0,004° in the prism's angle. This angle uncertainty was calculated from the Maximum Permissible Error of the Zeiss CMM [19], which in linear distance calculation was calculated to be 0,5 µm over the 25 mm total travel. This uncertainty contributed $0{,}37 \times 10^{-9}$ to the refractive index uncertainty.

The uncertainty in the deviation of the change in the vacuum-air ratio of the Zygo laser interferometer was calculated based on the manufacturer's specifications of the Zygo laser interferometer [1] to be 2 nm, resulting in an uncertainty of $7{,}2 \times 10^{-8}$ in the refractive index.

The imperfections of the optical flatness and parallelism of prism faces were addressed by the baseline measurements taken in air and largely eliminated this uncertainty.

However, the prism deformation under vacuum conditions was considered an uncertainty contributor. Straightness measurements using the Zeiss CMM were performed with air inside the prism at normal atmospheric conditions. Straightness measurements using the Zeiss CMM showed a 1 µm change in straightness between air and vacuum conditions, resulting in a refractive index uncertainty of $0{,}7 \times 10^{-9}$. Figures 22 and 23, show the straightness measurements of a side window of the prism under normal atmospheric and vacuum conditions.

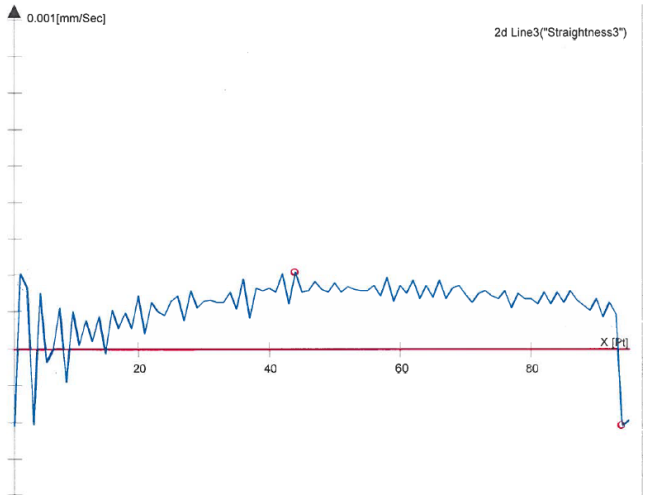

Figure 22 Profile of prism side window under atmospheric conditions

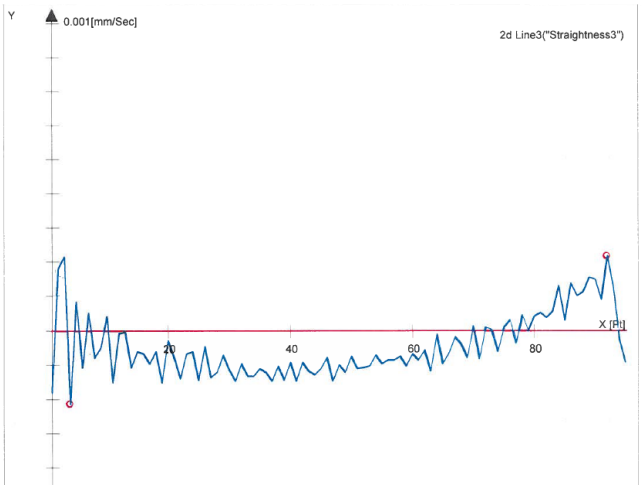

Figure 23 Profile of prism side window in a vacuum.

The combined uncertainties in the measurement of the refractive index, calculated using the root sum square method [18], were $7{,}2 \times 10^{-8}$. Measurements taken with the commercial prism resulted in satisfactory results, as shown in Table 1, with an uncertainty of $7{,}2 \times 10^{-8}$, validated against the updated Edlin weather station to an agreement of $1{,}2 \times 10^{-7}$. These results confirm that the permanent vacuum refractometer, using a commercial prism and commercial laser measuring system with secondary optics, has sufficient uncertainty for refractive index measurements in dimensional metrology.

However, two primary issues were identified with this setup, both related to the use of the commercial prism:

1. **Single Vacuum Entry Limitation**: The commercial prism provides only a single entry point for the vacuum pump attachment, which limits the accuracy of vacuum measurement within the prism. Research by Kruger [9] emphasises that to achieve accurate vacuum measurements within the etalon, a second entry point for a vacuum gauge is required. Kruger's study investigated the required vacuum for accurate refractive index measurements, signifying that a vacuum, as proposed by Bonsch and Potulski [7], is 1×10^{-2} Pa, which converts to 1×10^{-4} mbar in mbar units [17]. Kruger's findings indicate that a vacuum below 1×10^{-3} mbar is adequate for refractometer applications, as shown in graph 1. Although the vacuum pump (described in Chapter 7) was capable of achieving this level, the single-entry limitation prevented confidence in the true vacuum within the prism etalon and changed to two entrees as per previous research and illustrated in figure 24.
2. **Optical Quality of the Side Windows**: The side windows of the commercial prism, through which light passes, are of below-standard optical quality. While baseline measurements were used to mainly illuminate this effect, the windows' deformation under vacuum conditions added through possibly small but important uncertainty. This deformation, illustrated previously in figures 22 and 23, contributed an additional uncertainty. Although not significant, improvement in the quality of these windows could improve the refractometer's overall uncertainty.

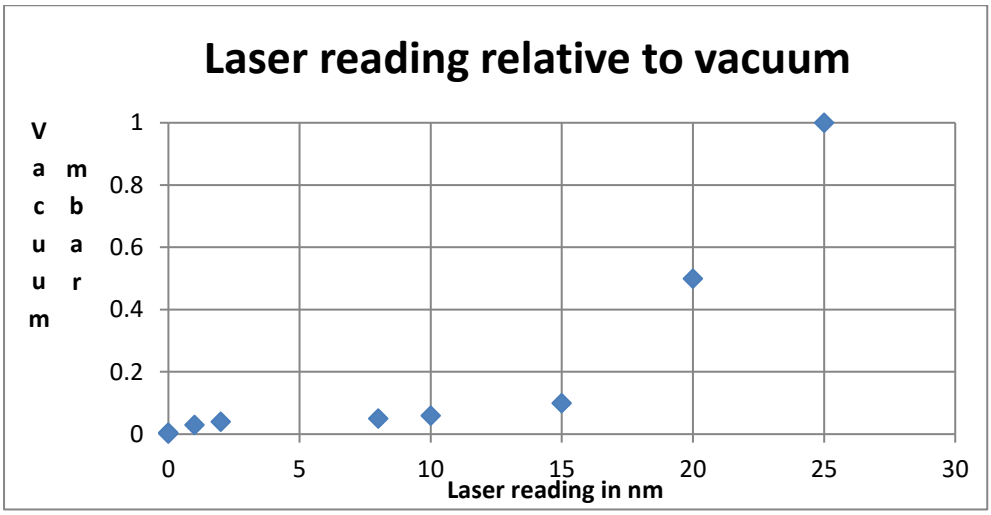

Graph 1 The laser reading was measured relative to the different levels of vacuum [9]

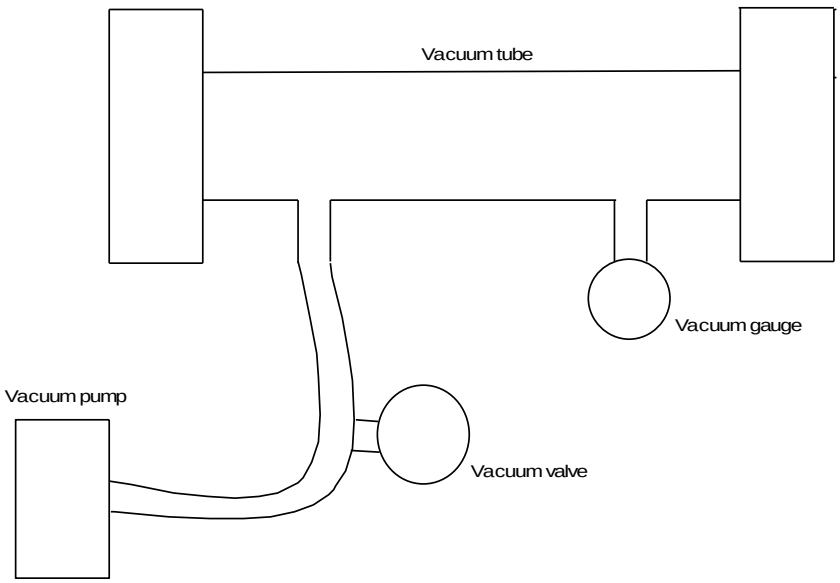

Figure 24 Vacuum tube the vacuum pump to one inlet and the vacuum gauge to another. [9]

4.5 Improvement in the optical layout of the refractometer and the use of the commercial prism.

In addition to the two imperfections noted in the commercial prism, the long-term stability of the system was found to be unsatisfactory due to drift in the zero position of the reference laser beam passing through the vacuum prism. Despite the low vacuum levels applied, the drift in optical alignment, as measured by the laser system, was significant, with deviations of up to 50 nm occurring over several days between the reference, vacuum, and measuring, air laser beams.

To address this issue, a new optical layout was implemented, as illustrated in Figure 25, by incorporating an additional pair of laser beams into the system. This pair of beams served to continuously monitor the zero position. The optics of the second laser were aligned to track movement with the translation stage, thereby maintaining a constant measurement of the zero position within the prism. This second laser reading was used to correct the first laser's measurements for zero-position drift, providing an expected improvement in long-term accuracy.

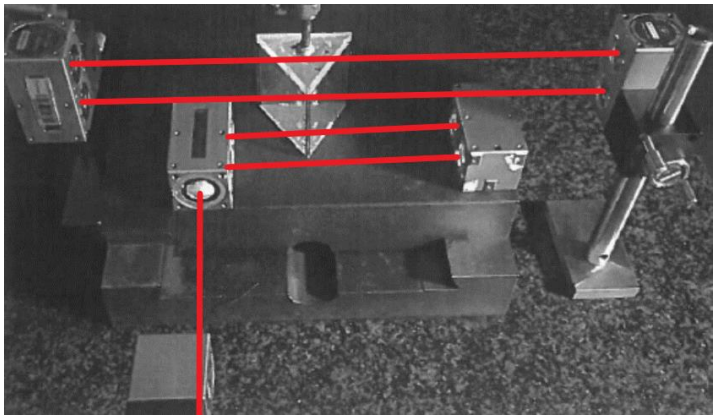

Figure 25 Setup with extra laser beams to continue measuring the zero position.

The new optical layout was tested over several days with both lasers set to the zero position. The readings between the two laser beams remained within the laser system's uncertainty values of 3 nm and demonstrated stability comparable to that of the cylinder refractometer from Kruger and Chetty's previous design [8,9], which had a stability of 2 nm. Table 3 presents the results from the added laser used exclusively for zero-position monitoring.

Table 3 Results for the prism refractometer with extra laser added to improve the long-term stability compared to the modified Edlin equation using weather station measurement calculations.

Distance Stage moved		**Laser on Prism readings**			**Weather station and Prism V.O.L. readings**					
Transverse laser reading, *Lt* (mm)	**Air length replaced, *L* (nm)**	**Laser reading in air (nm)**	**Laser reading in vacuum (nm)**	**Laser reading combined, *l* (nm)**	**Air temp. (°C)**	**Air pres. (mbar)**	**Air humid. (%RH)**	**V.O.L. Edlin Eq.**	**V.O.L. prism**	**Diff. in V.O.L. between Edlin eq. and prism refract.**
Use only for Edlin calculation					20,14	866,53	4,.3	0,999768124		
5	5773503	1305	33	1338	-	-	-	-	0,999768305	-1,82E-07
10	11547006	2475	202	2677	-	-	-	-	0,999768219	-9,50E-08
15	17320509	3248	770	4018	-	-	-	-	0,999768074	4,93E-08
20	23094012	3564	1791	5355	-	-	-	-	0,999768175	-5,17E-08
25	28867514	3692	3003	6695	-	-	-	-	0,999768132	-8,40E-09

The V.O.L was calculated using the Edlin equation, based on environmental conditions of an air temperature of 20,14 °C, an air pressure of 86,53 mbar, and an air humidity of 45,3 %RH, resulting in a value of 0,999768124.

To further the research on uncertainty calculations as described earlier in this chapter, an uncertainty budget for the prism refractometer was developed using Equation (5) and the Guide to the Expression of Uncertainty in Measurement (GUM) method [18]. Sensitivity coefficients were determined for each contributing factor. The laser system, the primary traceable link to the SI unit of the metre, was calibrated against the National Standard for length in South Africa, an iodine-stabilized HeNe laser. Although the CMM was calibrated, the manufacturing specifications were used in the uncertainty calculations [19].

Table 4 is the uncertainty budget for the refractive index, calculated only for the 25 mm position, as it signifies the position of highest uncertainty.

Table 4: Uncertainty budget for prism refractometer at the 25 mm position only

Sym	Description	Value	Uncertainty	Sensitivity Coefficient	Uncertainty Contributor	Significance %
q	The angle of the prism (rad)	0,52359	0,000011	$-530*10^{-6}$	$-6*10^{-9}$	2
Lt	Translation distance (um)	25000	0,5	$-9.3*10^{-9}$	$-3*10^{-9}$	1
l	Difference in laser reading, including repeatability (um)	6,677	0,002	$35*10^{-6}$	$40*10^{-9}$	97
Combined uncertainty					$4*10^{-8}$	
Expanded uncertainty					$8,4*10^{-8}$	

In addition to the uncertainty contributors listed in the table, the imperfections on the prism side windows were estimated by analysing the baseline measurements. The method of using the baseline measurements theoretically eliminates the uncertainty due to surface imperfections, with only the repeatability of laser readings included in the uncertainty budget.

The primary objective of this research was to explore the use of a permanent vacuum hollow prism as the vacuum etalon in an air refractometer, to eliminate the need for a vacuum pump during refractive index measurements. Results from translational measurements demonstrated agreement to within $1{,}82 \times 10^{-7}$ with the Edlin weather station method over short travel distances, and better agreement of $0{,}84 \times 10^{-8}$ over longer travel distances of the transverse stage.

The application of a prism as the vacuum etalon further solved issues associated with the varying optical path length due to changes in the side windows in tube refractometers, as identified by Bonsch and Potulski [7]. Since the optical components remained under consistent conditions throughout the measurement, this represents a significant improvement in the potential accuracy of prism refractometers over traditional tube/cylinder refractometers.

Moreover, the addition of a secondary laser measuring system improved the long-term stability of the refractometer, setting it apart from other prism refractometer designs, such as those reported by Renkens and Schellekens [11] and John Tsai [6]. This configuration allows for an extended period of measurements after positioning the prism at the 25 mm traverse mark, demonstrating a significant improvement over previous designs. Consequently, the refractometer now proves beneficial for both routine refractive index measurements in dimensional metrology and high-precision research applications.

Further research will focus on improving the commercial prism itself. Improved optical materials and improved manufacturing standards for flatness and parallelism of the side windows could further improve the system's overall uncertainty. Additionally, thicker optical side windows should reduce the deformation between the prism's air and vacuum conditions, therefore enhancing the measurement uncertainty.

The results, applicable to both every-day and long-term measurements and high-accurate research, validate the objective of the original research and were published as "A Permanent Vacuum Refractometer for Everyday Use in Dimensional Metrology" in *Nature Scientific Reports* (2021; Article 11, 9290, Chapter 8, Journal Papers).

Chapter 4 Bibliography

1. Zygo. Zygo laser system, ZMI-2000 system manual. 1997 [cited 2020 Sept] https://www.zygo.com/support/reference-library/product-manuals
2. Schott W, Dontsov D, Poshel, W. Developments in homodyne interferometry. tm–Technisches Messen. 2009 Sept 25;76:239–44. https://doi.org/10.1524/teme.2009.0962
3. Saptari V. Fourier-transform spectroscopy instrumentation engineering. Bellingham: SPIE Press; 2003. https://spie.org/publications/tt61_541_laser_interferometer?SSO=1
4. Agilent (HP). 5528A Laser measurement system, user guide. 1988. [cited 202 Sept] https://www.pearl-hifi.com/06_Lit_Archive/15_Mfrs_Publications/20_HP_Agilent/HP_5528_Laser/HP_5528A_Measurement_System/HP_5528A_Users_Manual.pdf
5. Terrien J. An air refractometer for interference length metrology. Metrologia. 1965;1(3):80.
6. Tsai JC. Ambient air refracture index device. US Patent: US5394244A. 1992.
7. Bonsch G, Potulski E. Measurement of the refractive index of air and comparison with the modified Edlén's formulae. Metrologia. 1998;35:133–9.
8. Chetty N, Kruger OA. Robust air refractometer for accurate compensation of the refractive index of air in everyday use. OSA. 2016;55:9118–22.
9. Kruger OA. Robust air refractometer for accurate compensation of the refractive index of air in every day. Master Thesis. 2016.
10. Stone J, Stejskal A. Using Helium as a standard of refractive index: correcting errors in a gas refractometer. Metrolgia. 2004;41:189.
11. Renkens M, Schellekens P. An accurate interference refractometer based on a permanent vacuum chamber. CIRP Annals: Manufacturing Technology. 1993;42:581–3. https://doi.org/10.1016/S0007-8506(07)62514-1
12. Daimon M, Masumura A. Measurement of the refractive index of distilled water from the near-infrared region to the ultraviolet region. *Appl. Opt.* 2007;46:3811–20.
13. 3B Scientific. Prisms. [cited 2020, Sept]. https://www.3bscientific.com/hollow-prism-equal-sided-1014618-u11922,p_639_23222.html
14. Edlén B. The refractive index of air. Metrologia. 1965;2:71–80.
15. Birch KP, Downs MJ. An updated Edlén equation for the refractive index of air. Metrologia. 1993;30:155–62.
16. Muijilwijk R. Update of the Edlén formulae for the refractive index of air. Metrologia. 1988;25:189.
17. BIPM. The International System of Units (SI). 9th ed. 2019.

18. BIPM. Evaluation of measurement data—Guide to the expression of uncertainty in measurement. JCGM 100. 2008 https://www.bipm.org/documents/20126/2071204/JCGM_100_2008_E.pdf/cb0ef43f-baa5-11cf-3f85-4dcd86f77bd6
19. Zeiss. When precision matters the most. ZEISS PRISMO Family. [cited 2021 Des 11]. https://www.zeiss.com/metrology/products/systems/coordinate-measuring-machines/bridge-type-cmms/prismo.html#technicaldata

Chapter 5: Final Design of the Permanent Vacuum Refractometer

5.1 Newly designed prism

The new prism was designed to address the challenges identified with the commercial prism, as detailed in Chapter 4. This new design incorporates the following key considerations:

1. **Dual Ports**: The prism includes two ports—one for vacuum pump attachment and another for a vacuum gauge—addressing the critical need for dual access points as highlighted in the research by Chetty and Kruger [7].
2. **Optimised Side Windows**: The side windows are precisely manufactured to be flat and parallel, ensuring the least optical deflection of the laser beam as it passes through the prism. Additionally, the windows are manufactured to be taller to allow both laser beams to pass through the same optical path, similar to the vacuum cylinder design described by Chetty and Kruger [7].
3. **Material and Refractive Index**: The prism is constructed from thicker quartz, specifically BK7 optical glass, with a refractive index of 1,51, as reported in the Schott data sheet [1–3]. This was to reduce or eliminate the deformation under vacuum.
4. **Optimised Apex Angle**: The angle at the prism's apex has been changed to maximize the vacuum-to-air ratio. However, the maximum angle was limited to prevent total reflection at the side windows where the laser beams pass through. To optimise this, the Brewster angle was chosen, providing the ideal polarisation angle where the laser beam can transmit through the prism windows with no reflection. For a quartz medium with a refractive index n≈1,5, the Brewster angle for each window is approximately 56°, resulting in a 112° angle at the prism's apex. Equation (8) was applied to calculate the Brewster angle:

$$Tan\theta = \frac{n1}{n2} \tag{8}$$

Figure 26 shows the newly designed prism used further in this research which incorporates the above considerations.

Figure 26 The newly designed second prism.

Figure 27 displays the new prism mounted on the translation stage. The HP/Agilent displacement laser is used to measure the movement of the translation stage, ensuring accurate measurement of translational distance. A Zygo displacement laser was used to measure the vacuum-air ratio.

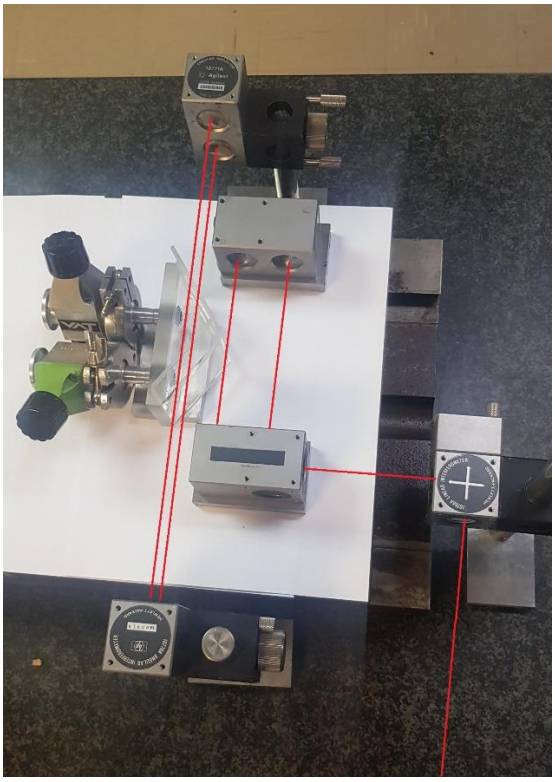

Figure 278 The second prism setup on the transfer table

As discussed in Chapter 4, the refractive index is determined by the distance moved by the translation stage, L_t, along with θ, the prism's half-angle. These parameters are used to calculate the length of the vacuum inside the prism, resulting in the air-to-vacuum ratio required for the refractive index calculation.

$$n = \frac{2*(tan\theta*Lt)+l}{2*(tan\theta*Lt)} \tag{9}$$

Table 5: Results for the new prism refractometer compared to the modified Edlin equation using weather station measurement calculations.

Stage moved		**Prism readings**								
Transverse laser reading, *Lt* (mm)	**Air length replaced, *L* (nm)**	**Laser reading in air (nm)**	**Laser reading in vacuum (nm)**	**Laser reading combined, *l* (nm)**	**Air temp (°C)**	**Air pres. (mbar)**	**Air humid. (%RH)**	**V.O.L. Edlin Eq.**	**V.O.L. prism**	**Diff. in V.O.L. between Edlin eq. and prism refract.**
Use only for Edlin calculation					20,47	86,.92	62,6	0,999769653		
25	74,267	0,00242	0,015411	0,017157	20.5	865	41	0,99976883	0,999768923	9,28E-08

The side windows were inspected to determine whether the deformation under vacuum conditions displayed less deviation compared to the commercial prism. The uncertainties of the measurement of the windows' straightness were also improved by using a Taylor Hobson profilometer over the CMM previously used. Measurements were performed following the same procedure as with the CMM, initially under normal atmospheric conditions with air inside the prism, as shown in Figure 28. Subsequently, a vacuum was drawn, and the straightness of the same side and position was remeasured, as displayed in Figure 29.

It should be noted that the y-axis scales in the two graphs differ, as the profilometer software automatically selects the optimal scale for display. The straightness measurements showed a change of approximately 1 µm between air and vacuum over the area used for refractive index measurements. Unfortunately, this did not result in the expected improvement in deformation. This outcome is attributed to the lack of process control during the manufacturing process, as the prism was measured only after completion, with no intermediary checks throughout production. The thickness of the prisms was much thinner, 5 mm as per the design criteria, which was to be thicker than 10 mm, but unfortunately not manufactured to this specification.

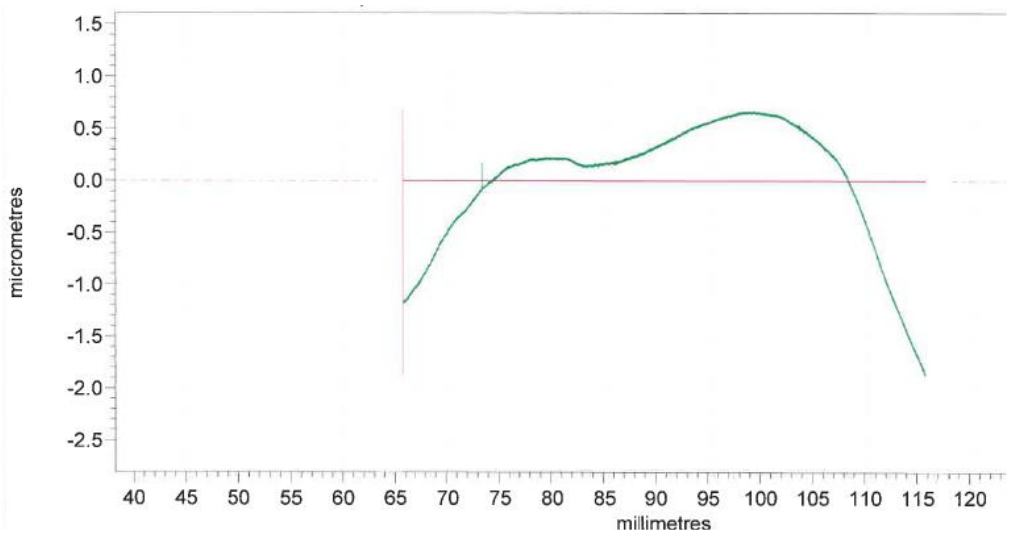

Figure 289 Profile of prism side window under atmospheric conditions.

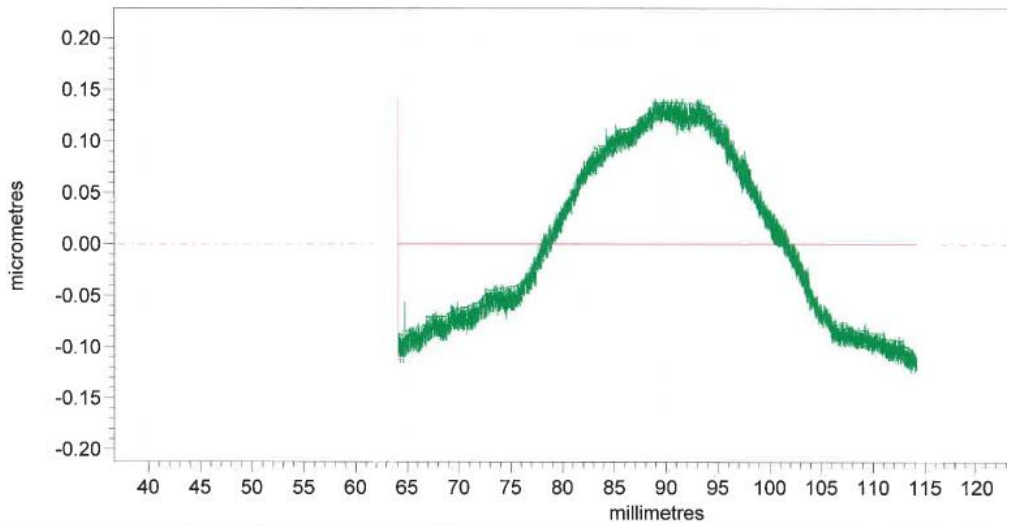

Figure 29 Profile of prism side window under vacuum.

5.2 Use of a Fizeau interferometer to measure the vacuum-air ratio.

During the initial use of the first prism in the refractometer, the optical quality of the side windows was identified as an area of concern. To evaluate this, a Zygo GPI phase-shifting interferometer [6] was used to measure the wavefront quality of the side windows, using interference fringes to attain the measurements. During these evaluations, it became apparent that the fringe shifts could potentially be used as a method to measure changes in the optical path length related to the vacuum-air ratio. Further investigation into this method led to the development of the following setup.

The Zygo interferometer is designed for measuring the optical flatness, parallelism, and wavefront quality of optical components, such as lenses and mirrors, using a Fizeau interferometer arrangement [4]. By measuring the spacing and angle of interference fringes, the Zygo system determines the optical quality [6].

The method comprises taking optical measurements and can be used to perform these measurements simultaneously of both the vacuum chamber and the surrounding air. In this configuration, the Zygo interferometer was used to measure the vacuum-air ratio directly and simultaneously, without the need for an additional laser displacement interferometer and a translation stage. Figure 30 shows the second designed prism positioned within the Zygo interferometer's optical layout for air-vacuum ratio measurements.

Figure 30 The second design prism setup in the Zygo flatness interferometer to measure the air-vacuum ratio.

The interferogram in Figure 31 displays the vacuum chamber at the bottom [B] and the surrounding air at the top [A]. The same method of baseline measurements was performed as previously under normal atmospheric conditions, air in both areas [A] and [B]. Using the Zygo interferometer software [6], two regions were selected for measurement, shown in Figure 32 with air inside the vacuum chamber. Subsequently, a vacuum was drawn in the bottom chamber, resulting in the fringe map in Figure 33, where the differences in fringe spacing and orientation between air and vacuum conditions are evident. These variations in fringe patterns are used to calculate the refractive index of the surrounding air, as per the method of the Zygo interferometer to measure optical flatness.

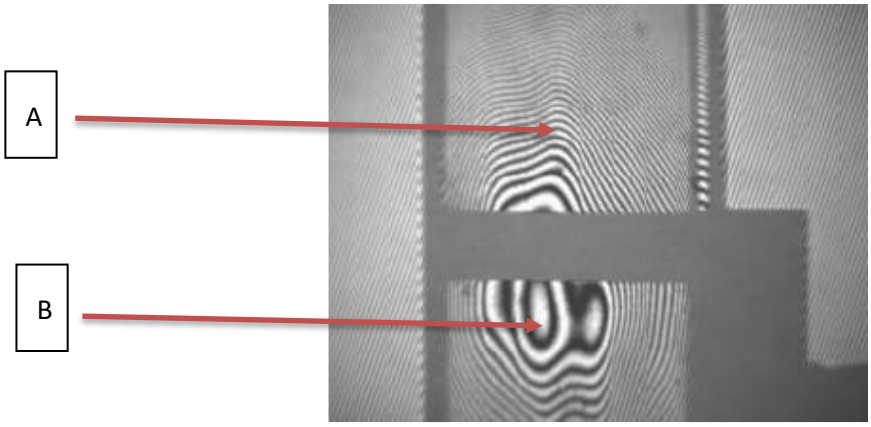

Figure 31 Fringes are generated with air under normal atmospheric conditions inside and outside the prism.

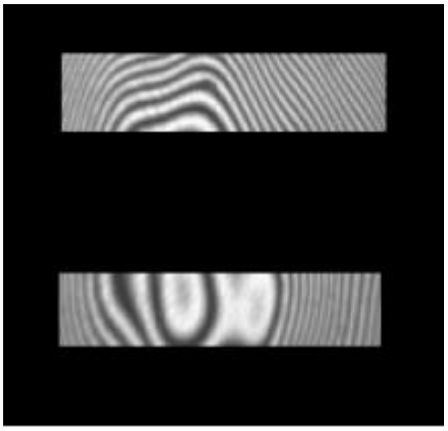

Figure 32 Fringe map with air inside the vacuum chamber of the prism.

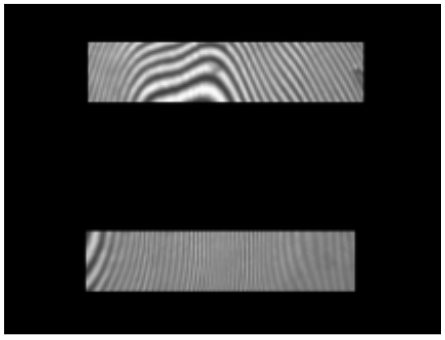

Figure 33 Fringe map with a vacuum inside the vacuum chamber of the prism.

Figures 34 and 35 show oblique plots for both air (Figure 34) and under vacuum (Figure 35).

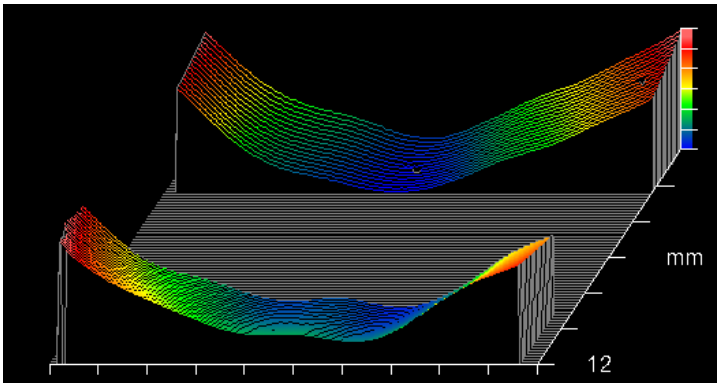

Figure 34 Oblique plot air in the vacuum chamber under normal atmospheric conditions.

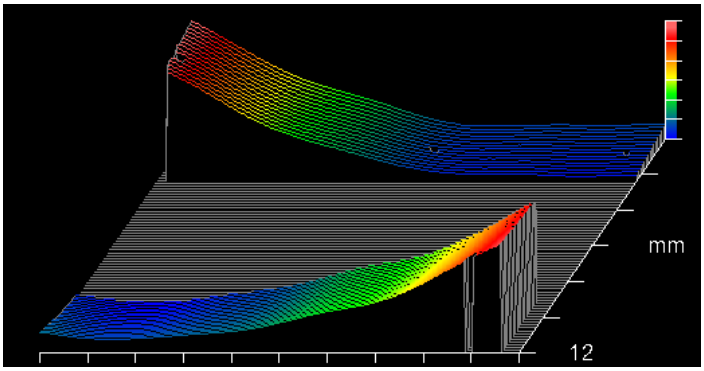

Figure 35 Oblique plot under vacuum used to measure the vacuum-air ratio.

To further assess the differences in the displacement ratio between vacuum and air conditions, two horisontal profiles were selected, illustrated in Figures 36 and 37.

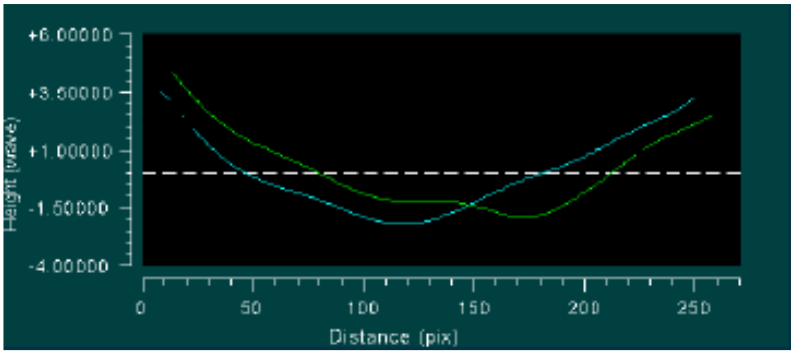

Figure 36 Two horisontal profiles were chosen to measure the vacuum-air ratio. Figure with air inside and outside the prism.

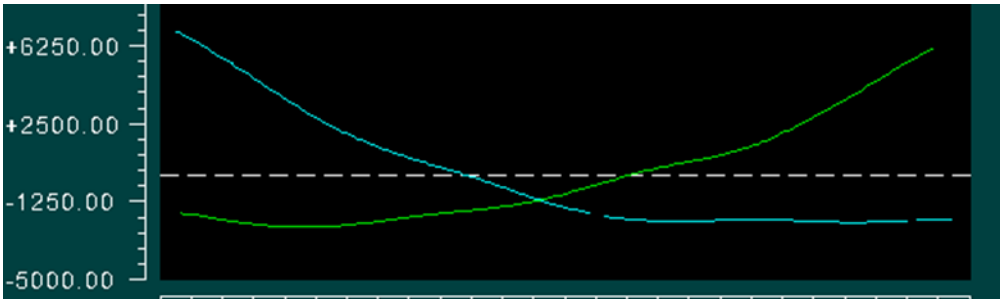

Figure 37 The two horisontal profiles with vacuum were drawn inside the bottom chamber.

The calculations used here replicate those discussed in Chapter 4,3, where two displacement laser measuring systems and the translation stage were used to measure and determine the vacuum-air ratio.

$$n = \left(\frac{L + l}{L}\right) \tag{10}$$

5.3 Results of the Refractive index as measured with the Fizeau interferometer.

This chapter discusses the use of a Fizeau Zygo flatness interferometer with the newly designed second prism. The refractive index measurements obtained using this prism-based refractometer were compared with those derived from two different methods: the weather station method and the cylinder refractometer, the latter previously used in studies by Chetty and Kruger [7] and Kruger [8].

Table 6 presents refractive index measurements recorded over three days. These measurements were calculated using the Edlin equation and compared with those obtained using the Fizeau interferometer. The maximum observed difference between the Fizeau refractometer and the Edlin equation method was $0{,}85\times10^{-7}$, with an average difference of $5{,}5\times10^{-8}$. These results are consistent with previous results, where refractometers—including the prism refractometer with a translation stage and the tube refractometer—showed similar agreement when compared with the Edlin equation-based weather station method.

Table 6: Results for the Fizeau prism refractometer data compared to the modified Edlén equation using the weather station method.

Reading Number	Laser in vacuum (µm)	Air temperature (°C)	Pressure (mbar)	Humidity (%RH)	VOL correction from Fizeau refractometer	Refractive index from Fizeau refractometer	Refractive index (Edlin)	Difference between Fizeau Refrac. and Edlin
1	13,751	20,354	870,185	50,3	0,999767419	1,000232635	1,000232693	5,79385E-08
2	13,757	20,187	870,081	51,3	0,999767318	1,000232737	1,000232794	5,74324E-08
3	13,739	20,451	869,964	55,4	0,999767622	1,000232432	1,00023251	7,79507E-08
4	13,743	20,014	868,923	52,4	0,999767554	1,0002325	1,000232616	1,1628E-07
5	13,767	20,289	871,043	52,5	0,999767148	1,000232906	1,000232957	5,12555E-08
6	13,757	20,932	871,490	53,2	0,999767318	1,000232737	1,000232542	-1,94568E-07
7	13,720	20,224	867,712	50,1	0,999767943	1,000232111	1,000232138	2,73866E-08
8	13,767	20,365	871,814	56,3	0,999767148	1,000232906	1,000233068	1,62256E-07
9	13,769	20,105	870,174	52,6	0,999767115	1,00023294	1,000232875	-6,45798E-08
10	13,737	20,517	869,751	50,5	0,999767656	1,000232398	1,000232441	4,2786E-08

Table 7: Results for the tube refractometer data compared to the modified Edlén equation using the weather station method.

Reading Number	Laser in vacuum (µm)	Air temperature (°C)	Pressure (mbar)	Humidity (%RH)	Refractive index from refractometer, Tube	Refractive index (Edlin)	Difference between Refractometer and Edlin
1	27,875	20,334	867,32	55,3	1,000231845	1,000231896	5,06357E-08
2	27,901	19,825	866,40	54,7	1,000232062	1,000232073	1,13853E-08
3	27,958	19,762	868,42	57,4	1,000232536	1,000232644	1,08298E-07
4	27,979	19.718	868,23	60,4	1,00023271	1,000232605	-1,05366E-07
5	27,907	19,155	865,12	62,5	1,000232112	1,000232217	1,05481E-07
6	27,913	18,772	864,22	61,1	1,000232161	1,000232303	1,41577E-07
7	27,904	19,872	867,16	58,7	1,000232087	1,000232204	1,17433E-07
8	27,967	20,191	869,75	56,3	1,000232611	1,000232657	4,6442E-08
9	27,869	20,342	867,55	59,3	1,000231795	1,000231916	1,2054E-07
10	27,895	20,354	869,97	55,4	1,000232012	1,000232105	9,32892E-08

Although the Fizeau refractometer confirmed favourable comparability with the weather station method, a direct comparison with the cylinder refractometer was deemed necessary. This decision was based on the reported uncertainty of the weather station method and the Edlin equation, which, according to Bonsch and Potulski, is limited to approximately 1×10^{-7} [3].

The tube refractometer had been used in previous research; however, it was thought necessary to first verify the complete tube refractometer system before proceeding with a comparison against the Fizeau refractometer. This verification was performed by taking measurements with the cylinder refractometer and comparing the results to those obtained using the weather station method. The maximum observed difference between the tube refractometer and the Edlin equation method was $0{,}9\times10^{-7}$, with an average difference of 4×10^{-8}, which was considered satisfactory. Results shown in table 7.

The comparison between the Fizeau permanent vacuum refractometer and the tube refractometer was conducted to assess their performance under controlled conditions. In this setup, the vacuum prism was positioned between the two optical flats of the Fizeau interferometer, as described earlier and illustrated in Figure 24. The cylinder refractometer, previously utilised by Chetty and Kruger [7] and validated above, was placed in close proximity to the Fizeau refractometer and aligned at the same height to ensure consistent air pressure conditions.

It is important to note that a height difference of 1 m corresponds to an approximate air pressure variation of 0,11 mbar. Given that a pressure difference of 0,4 mbar introduces a refractive index error of 1 ppm, it was critical to maintaining the height discrepancy between the refractometers below 10 mm to limit the effect on the refractive index to less than 0,01 ppm. Both refractometers were enclosed within a Perspex cover to stabilize the air, primarily to control the air temperature. This setup ensured that the refractometers had similar air pressure and temperature conditions, thereby improving the comparison of their refractive index measurements. The experimental layout is displayed in Figure 38.

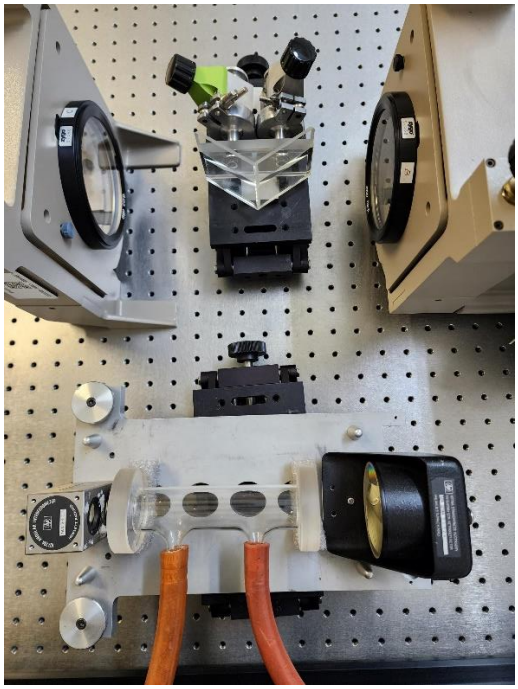

Figure 38 Experimental setup of the tube refractometer and the newly designed permanent vacuum prism.

The results of the comparison are presented in Table 8. As expected, the agreement between the Fizeau and cylinder refractometers was closer than the agreement between either refractometer to the Edlin weather station method. The maximum observed difference between the tube refractometer and the Edlin equation method was $0{,}5\times10^{-7}$, with an average difference of $2{,}3\times10^{-8}$, which was considered satisfactory.

Table 8: Results for the prism refractometer data compared to the previously used tube refractometer.

Reading Number	Laser in Fizeau refract. (µm)	Laser in Tube refract. (µm)	Refractive index from Fizeau from refractometer	Refractive index from Tube from refractometer	Difference between Fizeau and Tube refractometers
1	13,764	28,002	1,000232855	1,000232902	4,66729E-08
2	13,677	27,811	1,000231383	1,000231313	-7,00973E-08
3	13,728	27,921	1,000232246	1,000232228	-1,79937E-08
4	13,698	27,869	1,000231738	1,000231795	5,70361E-08
5	13,703	27,879	1,000231823	1,000231879	5,56209E-08
6	13,655	27,784	1,000231011	1,000231088	7,7524E-08
7	13,615	27,703	1,000230334	1,000230415	8,05282E-08
8	13,696	27,856	1,000231705	1,000231687	-1,72538E-08
9	13,737	27,945	1,000232398	1,000232428	2,93629E-08
10	13,701	27,875	1,000231789	1,000231845	5,6187E-08

This method is documented in the second paper, prepared for submission, in Chapter 8.2. The results obtained through this approach demonstrate strong agreement between the two refractometer methods, namely, the tube and the Fizeau refractometers. A more detailed discussion of these findings is presented in Chapter 7, Future Work.

5.4 Refractive index results from the Fizeau interferometer but using the angle measuring capability of the flatness interferometer.

The Zygo flatness interferometer also has an angle measurement capability, primarily utilised for assessing optical wedges [9]. This angle-measurement functionality of the Fizeau interferometer (Zygo) has been examined by Probst [10], Kruger [11], and Stone [12]. Validation of this method was provided by Kruger, who applied it in the intercomparisons of CCL.L-K3 [13] and APMP.L-K3 [14]. The uncertainty associated with this method for angle measurements was estimated by these authors to be within 0.05".

A similar approach to the previous interferometer application is discussed here, where two areas are selected, as shown in Figures 32 and 33. Following this selection, the angle between the two areas is measured following

the method described by Probst, Kruger, and Stone. This method, as described by Kruger [11], has been validated in the intercomparisons [13, 14].

As with previous applications, a baseline measurement is first taken, as shown in Figure 39, and subsequently, measurements are performed under vacuum conditions, as illustrated in Figure 40.

.

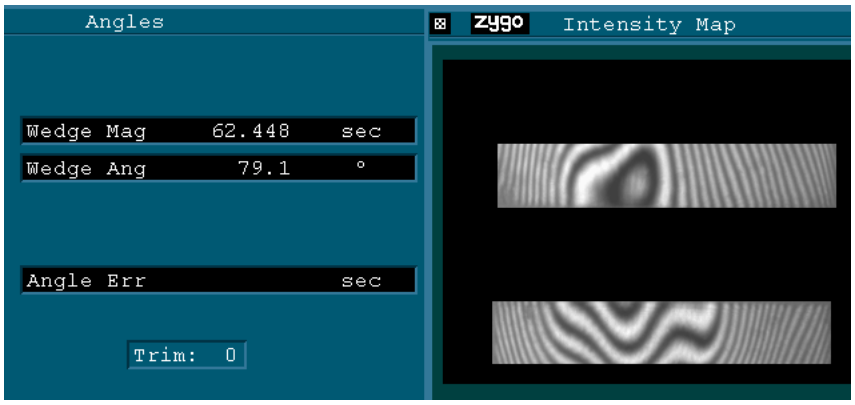

Figure 39 Two horizontal areas were selected to measure the differences between the vacuum and air.

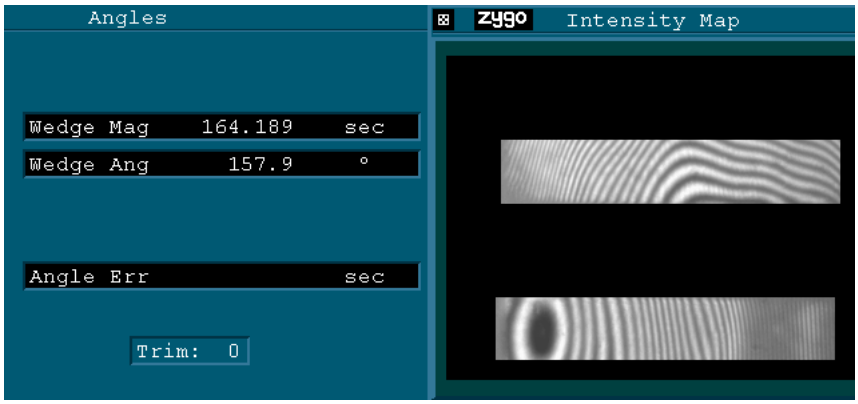

Figure 40 Two horizontal areas were selected to measure the differences between the vacuum and air.

The measured angle is utilised to calculate the optical displacement between the vacuum and air. Subsequently, Equation 4 is employed to determine the refractive index.

Table 9: Results for the angles of the prism as measured with the flatness interferometer.

Angle in air	11,3147408 °
Angle in vacuum	129,8198209 °
Combined angle	141,1345617 °
Combined optical displacement over 25 mm	0,017105 mm

Table 10: Results for the prism refractometer using the angle measuring method compared to the modified Edlén equation using weather station measurement calculations.

Horisontal distance (mm)		Air temp. (°C)	Air pres. (mbar)	Air humid. (%RH)	V.O.L. Edlén eq.	V.O.L. prism	Diff. in V.O.L. between Edlén eq. and prism refract.
		20,85	863,6	63	0,999769		
25	0,017105994					0,999769724	7,83E-08

The combined angle is used to calculate the optical displacement between air and vacuum, which for this measurement is 17,105 µm, as indicated in Table 9. Subsequently, Equation 4 is applied to calculate the refractive index.

Table 10 presents the refractive index calculated using this method and compares it to the Edlén method. The results show good agreement with the previous method and will be further discussed in the Future Work chapter.

As described in Section 5.3, the lateral accuracy of the Zygo interferometer serves as the limiting factor in this method for refractive index measurements. However, when utilising the angle measurement capability, the average is taken over the full profile reducing this limitation.

A significant advantage of this method over the previous approach is that the average is measured over the selected area to calculate the angle, rather than relying on just two or a few points, as was the case when the prism was traversed using the translation stage and the above method.

Chapter 5 Bibliography

1. Filmetrics. Refractive Index of Schott N-BK7. 2010 Oct. [cited 2021 Dec 11]. https://www.filmetrics.com/refractive-index-database/Schott+N-BK7#:~:text=For%20a%20typical%20sample%20of,nm%20are%201.51509%20and%200.
2. RefractiveIndexInfo. Refractive index database: Glass – glasses. [cited 2021 Dec 11]. https://refractiveindex.info/?shelf=glass&book=BK7&page=SCHOTT
3. Schott. P-BK7 516641.243. [cited 2021, Dec 11]. https://www.schott.com/shop/advanced-optics/en/Optical-Glass/P-BK7/c/optical-glass/glass-P-BK7
4. Hecht E, Zajac A. Optics. Addison-Wesley; 2002.
5. Brewster D. On the laws which regulate the polarisation of light by reflection from transparent bodies. Philosophical Transactions of the Royal Society of London. 1815;105:125–59. https://books.google.ca/books?id=U-U_AAAAYAAJ&pg=PA125&redir_esc=y#v=onepage&q&f=false
6. Zygo. Zygo GPI/HD flatness interferometer. [cited 2021, Dec 11]. https://www.zygo.com/products/metrology-systems/laser-interferometers
7. Chetty N, Kruger O. Robust air refractometer for accurate compensation of the refractive index of air in everyday use. OSA. 2016;55:9118–22.
8. Kruger O A. Robust air refractometer for accurate compensation of the refractive index of air in every day. Master Thesis. 2016.
9. Wedge and Prism Angle, https://www.zygo.com/applications/measurements/wedge-prism-angle
10. R. Probst and H. Kunzmann, Messung von Winkel- undFormabweichungen an Spiegelpolygonflächen mit einemPhaseninterferometer, PTB Mitteilungen 103, 43-50 (1993) Available from: https://www.researchgate.net/publication/277516913_Uncertainties_in_Small-Angle_Measurement_Systems_Used_to_Calibrate_Angle_Artifacts [accessed Jan 05 2022].https://www.ptb.de/cms/fileadmin/internet/fachabteilungen/abteilung_5/5.2_dimensionelle_nanometrologie/5.23/SP_PIV100_PTBMit93_KunzPr.pdf
11. Kruger O. Methods for determining the effect of flatness deviations, eccentricity and pyramidal errors on angle measurements, Metrologia 37 101, 2000. https://iopscience.iop.org/article/10.1088/0026-1394/37/2/1/pdf
12. Stone JA, Amer M, Faust B, Zimmerman B . Uncertainties in Small-Angle Measurement Systems Used to Calibrate Angle Artifacts Available from: https://www.researchgate.net/publication/277516913_Uncertainties_in_Small-Angle_Measurement_Systems_Used_to_Calibrate_Angle_Artifacts [accessed Jan 05

13. Kruger O. Final report on CCL-K3: Calibration of angle standards, Metrologia 46, 2009, https://iopscience.iop.org/article/10.1088/0026-1394/46/1A/04004
14. Kruger O, Kang C-S, Report on the APMP Key Comparison, Calibration of angle standards, 2016. https://www.bipm.org/documents/20126/45451433/APMP.L-K3.pdf/7bb543fd-13c5-592f-8bff-682818541439

Chapter 6: Equipment Used and Uncertainty Calculations

6.1 Equipment used.

This chapter focuses on the equipment used for traceability to the International System of Units (SI), the metre, along with the ancillary equipment. The uncertainties associated with each piece of equipment are analysed and documented in Sections 6.2 to 6.4 of this chapter, detailing the calculations of uncertainties for various components as required in this thesis. Although the chapter contains all aspects related to the uncertainty calculations, it is divided into two parts. The first part addresses the equipment used, including the traceability to the SI metre, while the second part discusses the combination of different uncertainties of the equipment to calculate a combined total uncertainty.

There are three different uncertainty budgets:

i) the weather station, and

ii) the two different refractometer designs

   a. prism with permanent vacuum and the use of the translation stage refractometer

   b. And lastly the same prism configuration but with the Fizeau interferometer layout.

Due to the differing approaches in these two parts, the references are also categorised accordingly.

When discussing the accuracy of measurements, two terms need consideration: traceability and calibration. The Dictionary of Measurements for VIM (DIMVIM) defines traceability as "the property of a result of a measurement where it can be related to appropriate standards, generally international or national standards, through an unbroken chain of comparisons" [1]. Where Calibration is defined as "the set of operations that establish, under specified conditions, the relationship between the values of quantities indicated by a measuring instrument or measuring system, or values represented by a material measure of a reference material, and the corresponding values by standards."

It is generally accepted that when equipment is calibrated to national or international standards, the measurements performed are correct with a small uncertainty. However, Tarnow [2] highlights the risks associated with these expectations, explaining that correct and accurate measurements are not guaranteed when calibrated equipment is used. He distinguishes between 'direct traceability' and 'indirect traceability' to clarify these risks. For example, direct traceability involves the calibration of gauge blocks, where the same

dimension (the length of the gauge block) is calibrated by interferometry and subsequently used in a secondary calibration that employs a mechanical comparator. In this case, the uncertainty of the gauge block, as calibrated by interferometry, can be directly applied to the calibration of the mechanical comparator. In the case of the calibration of electronic temperature devices, such as a platinum resistance thermometer, the uncertainty determined during calibration cannot necessarily be applied when these devices are used to measure temperature in experiments, as in this research, to measure air temperature.

Two main reasons explain this: using the accuracy of air temperature measurement as an example. The first reason, as described by Tarnow, is that calibration involves taking a series of readings at specified points, with an associated uncertainty calculated and assigned to only these points. However, the calibration uncertainty is only valid at these specified points, and when measurements are taken at different points—typically in the case of temperature measurements—this calibration uncertainty is no longer applicable. He recommends using the manufacturing specification (maximum permissible error) when measuring instruments used for measurements. The second reason is that calibration is typically performed under "ideal" conditions, which often differ from the actual measurement conditions. For example, in this case, the temperature sensors are calibrated in water using a typical calibration bath. However, the temperature is ultimately used to measure the air under varying conditions. Researchers such as Podestra and Boikovski have explained the challenges associated with calibrating air temperature sensors and the corresponding uncertainties. Considering these factors, the best uncertainty associated with measuring temperature cannot be better than 0,01 °C, which is the manufacturer's specification for the ASL F200. However, based on Podestra's research, a more realistic value is around 0,1 °C.

This approach was consistently applied to all measuring equipment. The equipment used for traceability differs between the different experimental setups. The laser displacement interferometer was used to measure the vacuum-air ratio, using two laser systems: the Zygo 2000 and the HP 5528 laser measuring system with the 5519A laser head. The HP brand was acquired from Keysight, and the model of the laser system is the 5529A Dynamic Calibration. According to the manufacturer's specifications, the Zygo system claims a lifetime accuracy of 0,1 parts per million (ppm) for the vacuum wavelength of the laser, with the HP laser also having a vacuum wavelength accuracy of 0,1 ppm. However, this accuracy applies to only the vacuum laser wavelength, which is critical for traceable calibrations against the Iodine HeNe laser. Both lasers were calibrated against Winters' iodine-stabilized HeNe lasers, model 200, which provides traceability to the SI metre, as defined in the mise en pratique for the definition of the metre in the SI. Nevertheless, both the uncertainty of the Zygo and Keysight laser systems heavily depend on the configuration of the laser with its optics setup. Since the measurement range is typically in the order of a few micrometers, the uncertainties for these systems are considered to be 2

nm for the Zygo and 500 nm for the HP laser system. The uncertainty of the HP laser was estimated conservatively and significantly less accurately, but in this research, it was primarily utilised for prism translation, where the accuracy required was less.

In the second setup, the Zygo flatness interferometer was used to measure the refractive index of air. This interferometer is specifically designed for assessing optical flatness and wavefronts of optical components, requiring high accuracy in its peak-to-valley measurements, although its lateral resolution is less critical. The manufacturer specifies a peak-to-valley measurement accuracy of 6 nm when using the three-flat absolute flatness method. Verification in two comparisons indicates that the system has an uncertainty of 15 nm over a 98 mm diameter when compared to the APMP LS-8, and 10 nm over a 100 mm diameter in a EURAMET comparison for flatness measurements. In the current setup for measuring the vacuum-air ratio, the uncertainty of the flatness interferometer was felt can be improved beyond the previously mentioned specifications, as this instrument was not originally designed for this type of measurement but needed to be validated to determine the specific uncertainty for these measurements. Therefore, it was decided to validate the setup by measuring a step height using the flatness interferometer and the Taylor Hobson profilometer. The results from the flatness interferometer and the profilometer demonstrated an agreement of less than 2 nm, as shown in Figures 41, 42, and 43, which show the gold coating step height and the measurement setups on both the flatness interferometer and the profilometer.

Figure 41 Gold coating setup in flatness interferometer.

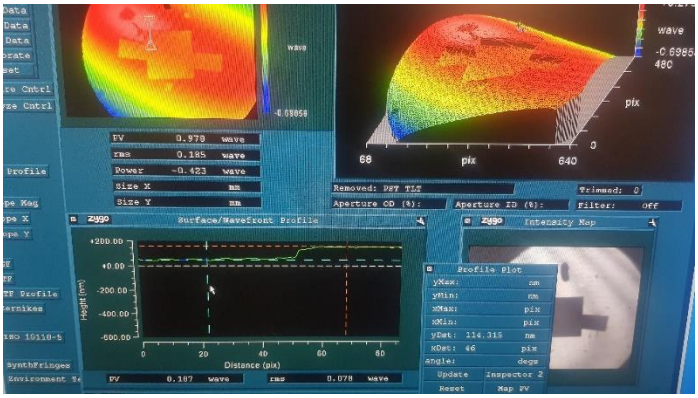

Figure 42 Measurement of gold coating using flatness interferometer.

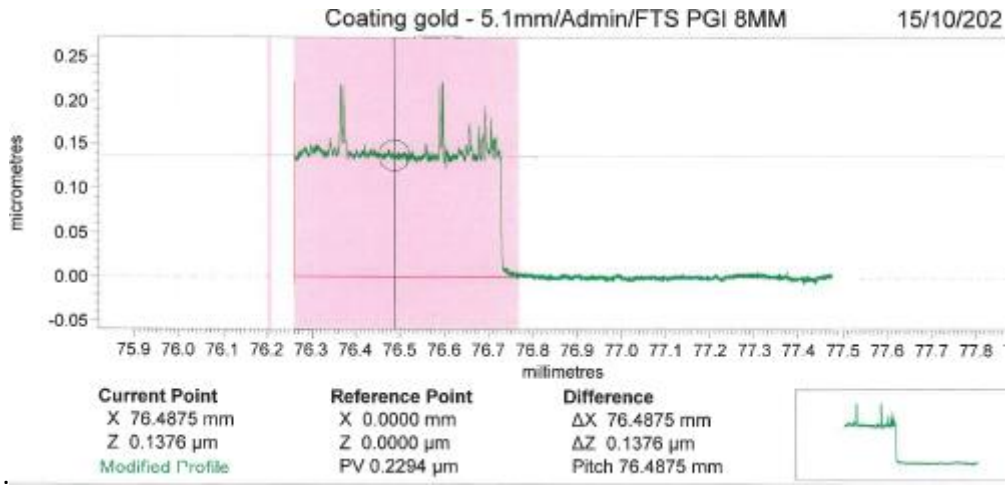

Figure 43 Measurement of gold coating using Taylor Hobson profilometer.

The following equipment was used in both experimental setups:

- **Coordinate Measuring Machine (CMM)**: The CMM used is a Zeiss Prismo, characterised by a manufacturer specification of (0,5+L/500) µm [17]. In this application, an estimated uncertainty of 0,5 µm is assumed, as the prism is relatively small, measuring only 25 mm across the measuring area. The CMM was also used to measure the deformation of the first prism. However, it was subsequently concluded that using the Taylor Hobson profilometer, known for its better uncertainty in such measurements, would be more suitable.
- **Taylor Hobson PGI Surface Texture Measuring Machine (Profilometer)**: This instrument was used to measure the deformation of the prism under vacuum conditions. The accuracy of the profilometer is specified to be less than 50nm [16].

- **Vacuum Pump and Vacuum Gauge**: An Agilent TwisTorr FS 84 Turbo Pump was used to create a vacuum within the prism [18]. This pump has a base pressure capability as low as 10^{-8} mbar, which is the recommended pressure achievable for turbo and roughing pumps. In the prism setup, a vacuum level of 10^{-5} mbar was achieved, significantly exceeding the vacuum requirements for a refractometer, which, as described by Kruger, only necessitates 10^{-3} mbar [19]. The vacuum gauge used was a 901 Plus (901P) Loadlock Transducer, which integrates both Piezo and Micro Pirani™ vacuum sensors [20,21]. The uncertainty of this gauge within the 10^{-3} mbar range is ±10% of the reading. This uncertainty was primarily used to validate that the vacuum was truly below the 10^{-3} mbar and was not incorporated into any uncertainty calculations.

In the weather station method, the following equipment was utilized:

- **ASL F200 Thermometer**: This thermometer was used to measure the air temperature, achieving an accuracy of 0,05 °C [6].
- **Druck Barometer, Model 140**: Used for measuring air pressure, this barometer has a specified accuracy of 0,15 mbar [22].
- **Humidity Measurement Systems**: Two systems were applied to measure humidity: a hygrometer and a dew point sensor. The impact of humidity on the refractive index is considerably less significant than that of air temperature and pressure. The systems employed include a Rotronic hygrometer and a General Electric dew chilled mirror hygrometer. The chilled mirror hygrometer offers superior uncertainty, with a manufacturer specification of 0,2 °C for the dew point measurements, whereas the Rotronic hygrometer claims an accuracy of better than 2%RH [23]. The chilled mirror's uncertainty estimated to be better than 0,2 °C [24], translates to a relative humidity uncertainty of better than 1% RH at 20 °C, as per the conversion guidelines on the NPL website [25].

  However, considering all contributing factors, a conservative overall accuracy of 2,5% RH was accepted and was used in the uncertainty calculations.

Chapter 6.1 Bibliography

1. BIPM. International vocabulary metrology—Basic and general concepts and associated terms. JCGM. 2012;200. https://www.bipm.org/en/publications/guides
2. Tarnow E. It can be a risky business assuming the calibration uncertainty applies to the points in between. NLA 2005 Test and Measurement Conference, https://researchspace.csir.co.za/dspace/bitstream/handle/10204/2813/Marais2_2006.pdf?sequence=1&isAllowed=y
3. ISO. ISO 3650 Geometrical Product Specifications (GPS)—Length standards—Gauge blocks. 1998 https://www.iso.org/standard/1241.html
4. Rusby R. Introduction into temperature measurement. Good Practice Guide 125. 2016. https://www.npl.co.uk/special-pages/guides/gpg125_intro2tempmeasure
5. Electronic Temperature Instruments. Calibration Water Bath. [citer 2021, Dec 12]. https://thermometer.co.uk/temperature-and-thermometer-calibration-equipment/1403-calibration-water-bath.html
6. Instrument. ASL F200 Precision Thermometer. [cited 2021, Dec 12]. https://www.instrumart.com/products/41396/asl-f200-precision-thermometer
7. De Podesta M, Underwood R, Bevilacqua L, Bell S. Air temperature measurement challenges in precision metrology. J. Phys.: Conf. Ser. 2018;1065:122027.
8. Boikovski, J. Uncertainty in the calibrations of air temperature sensors. XX IMEKO World Congress. Metrology for Green Growth. Busan, Republic of Korea. 2012 Sept 9−14. https://www.imeko.org/publications/wc-2012/IMEKO-WC-2012-TC12-O5.pdf
9. Zygo. Zygo laser system, ZMI-2000 system manual. 1997. [cited 2020 Sept] https://www.zygo.com/support/reference-library/product-manuals
10. Agilent (HP). 5528A Laser measurement system, user guide. 1988. [cited 202 Sept] https://www.pearl-hifi.com/06_Lit_Archive/15_Mfrs_Publications/20_HP_Agilent/HP_5528_Laser/HP_5528A_Measurement_System/HP_5528A_Users_Manual.pdf
11. Keysight Technologies. 5529A Dynamic Calibration System. [cited 2021, Dec 12]. https://www.keysight.com/zz/en/product/5529A/dynamic-calibration-system.html]
12. Winters. Model 200 Offset-Locked Iodine-Stabilized He-Ne Laser. 2004. [cited 2021, Dec 12]. http://www.winterseo.com/m200.html
13. BIMP. Practical realization of the definition of some important units. [cited 2021 Dec 8]. https://www.bipm.org/en/publications/mises-en-pratique

14. Buajarern J, Bitou Y, Zi X, Zhao L, Swift N, Agarwal A, Hungwe F. Report on APMP Supplementary Comparison. Measurement of flatness of optical flat by interferometry. Thailand: National Institute of Metrology. 2018 Feb. https://www.bipm.org/documents/20126/45452308/APMP.L-S8.pdf/eb0e50e6-2fa2-f893-411d-32eae2731008
15. Quabis S, Schulz M, Ehret G, Asar M, Balling P, Křen P. Intercomparison of flatness measurements of an optical flat at apertures of up to 150 mm in diameter. Metrologia. 2017;54:85–93. https://iopscience.iop.org/article/10.1088/1681-7575/aa535c/pdf
16. Taylor Hobson. Optic product solutions. 2018. https://www.taylor-hobson.com/-/media/ametektaylorhobson/files/product-downloads/pgi-optics/pgi-optics-range-3d-profilometers-en.pdf?la=en&revision=57e37552-b386-4dd8-8c03-8313f4f4d82b
17. Zeiss. ZEISS PRISMO family. [cited 2021, Dec 12]. https://www.zeiss.com/metrology/products/systems/coordinate-measuring-machines/bridge-type-cmms/prismo.html#technicaldata
18. Vacutec. Agilent Twistorr FS turbo pumps. South Africa. https://www.vacutec.co.za/Vacuum/Images/Products/pdf/Twistorr-FS-Turbo-Pumps-Brochure.pdf
19. Kruger OA. Robust air refractometer for accurate compensation of the refractive index of air in every day. Master Thesis. 2016.
20. MKS. 901P MicroPirani™ and Piezo Loadlock Vacuum Pressure Transducers. [cited 2021, Dec 12]. https://www.mksinst.com/f/901p-micro-pirani-vacuum-transducer
21. Vacuum Science World. The story behind the Pirani vacuum gauge. [2021, Dec 12]. https://www.vacuumscienceworld.com/vacuum-science-facts/marcello-pirani-vacuum-gauge
22. GE. Druck DPI 140/141. Precision pressure indicators. User manual K0023. http://www.met.reading.ac.uk/observatorymain/Druck_DPI140_manual.pdf
23. PST Rotronic. HC2A-S. Humidity Probe. [cited 2021, Dec 12]. https://www.rotronic.com/en-ch/humidity-measurement-feuchtemessung-temperaturmessungs/humidity-measurement-feuchte-messung/hc2a-s
24. Thunder Scientific Corporation. Chilled Mirror Hygrometer Calibration using the Model 2500 Two-Pressure Humidity Generator. [cited 2021, Dec 12]. https://www.thunderscientific.com/tech_support/support_docs/mirror-cal.html
25. NPL. Questions and answers. How do I convert between dew point and relative humidity? [cited 2021, Dec 12]. https://www.npl.co.uk/resources/q-a/how-do-i-convert-between-units-of-dew-point-and-re

6.2 Uncertainty of the Refractive index using the Edlén weather station method

In the calculation of the uncertainty for the different refractometer designs, the Guide to the Expression of Uncertainty in Measurement (GUM) [1] was used as the guiding document wherever practical.

The uncertainty associated with the Edlén weather station method was determined by estimating the measurement uncertainty for each sensor and then substituting these values into the Edlén equation to record the resultant differences in the refractive index. These estimates were generally made conservatively to ensure robustness in the calculations.

Most significant errors in determining the refractive index stem from inaccuracies in measuring atmospheric conditions, specifically air temperature and air pressure. Measurement errors that can lead to an error of 1×10^{-6} (1 part per million) in the refractive index, which corresponds to a length-proportional error of the same magnitude, include the following:

- an error of 1 °C in air temperature.
- an error of 0,4 kPa (3 mm Hg) in air pressure, and
- an error of 50% in relative humidity at sufficiently high air temperatures.

For this setup, the uncertainty of the air temperature measurement was estimated at 0,1°C, corresponding to an uncertainty of $5{,}1 \times 10^{-8}$ in the refractive index. The air humidity uncertainty was estimated to be 2,5 %RH, resulting in a $2{,}2 \times 10^{-8}$ refractive index. Finally, the air pressure uncertainty was estimated to be 0,15 mbar, resulting in an uncertainty of $4{,}05 \times 10^{-8}$ in the refractive index. By combining these uncertainties using root sum square, the overall uncertainties from the sensors are $6{,}87 \times 10^{-8}$ in the refractive index.

6.3 Uncertainty of Refractive Index using the Translation Stage Setup

The uncertainty of the translation stage using the first commercial prism was discussed in Chapter 4.4. The uncertainty calculations for the current setup are similar, with two key improvements that enhance accuracy:

i) an increased apex angle, which provides a larger vacuum-air ratio, and

ii) higher-quality optics. This section addresses the uncertainty of the translation stage and the second specially designed and manufactured prism.

The uncertainty calculations are as follows: the translation stage was moved over a maximum distance of 25 mm and measured with a laser displacement system from Keysight (HP) [2]. The uncertainty was conservatively estimated at 0,5 µm, resulting in an uncertainty of $0{,}47 \times 10^{-9}$ in the refractive index measurement.

The uncertainty in the prism's angle was calculated based on the Zeiss CMM manufacturing specification (MPE) [3], resulting in an uncertainty of 0,5 µm. Using the tangent function, this machine MPE translated to an uncertainty in the prism angle of 0,0007°, which contributed an uncertainty of 0,47 µm in the vacuum-air ratio and added $0{,}62\times10^{-9}$ to the refractive index of air.

The uncertainty due to deviation in the vacuum-air ratio by the Zygo laser was calculated as follows: the laser interferometer's uncertainty, according to the Zygo manual [4], is 2 nm, contributing an uncertainty of $2{,}7\times10^{-8}$ in the refractive index of air.

The imperfections in the prism faces were minimised by recording baseline readings in air, which were then subtracted from the vacuum measurements. This approach largely eliminated the impact of surface imperfections. However, the deformation of the prism under vacuum was included as an uncertainty component. Improved straightness measurements were achieved by using the Taylor Hobson Profilometer instead of the Zeiss CMM. The effect of this was discussed in Chapter 5.1 in Figures 24 and 25 the straightness measurements. The change in straightness between air and vacuum conditions was measured to be 1 µm over the tested area. Although the new prism was expected to reduce this deformation, the results showed a persistent deviation of 1 µm, contributing to an uncertainty of $0{,}7\times10^{-9}$ in the refractive index.

Using the root-sum-square method [1], the combined uncertainty in the refractive index measurement in the second prism and the translation stage was calculated to be $2{,}7 \times 10^{-8}$.

6.4 Uncertainty in the Refractive index using the Fizeau interferometer setup

This section discusses the uncertainty associated with using the Zygo flatness interferometer in a Fizeau interferometer setup.

The uncertainty in the prism's angle was previously calculated in this chapter, contributing $0{,}62\times10^{-9}$ to the refractive index of air.

In the Fizeau interferometer experiment, a lateral distance of 25 mm was used to measure the vacuum-air ratio. This distance was calibrated with a gauge block according to Zygo's manual [5]. The gauge block's uncertainty was 20 nm, which is small relative to the lateral scale calibration of the interferometer. Repeated lateral calibrations of the camera using different gauge blocks resulted in an uncertainty of 42 µm, which contributed to an uncertainty of $1{,}6 \times 10^{-8}$ in the refractive index reading.

The uncertainty in the measurement of the vacuum-air ratio, as estimated from the Zygo interferometer manual (Chapter 6, Equipment Used), was 2 nm, resulting in an uncertainty of $1{,}6\times10^{-8}$ in the refractive index.

To address the imperfections in the prism's side windows, baseline measurements were again taken with first air inside the vacuum etalon, as described in Chapter 5, and were then subtracted from the vacuum measurements. This process theoretically eliminated the influence of this uncertainty.

Table 11 presents the uncertainty budget for the Fizeau prism refractometer at the 25 mm position.

Table 11: Uncertainty budget for Fizeau prism refractometer at the 25 mm position only.

Symbol	Description	Value	Uncertainty	Sensitivity coefficient	Uncertainty contributor	Significance %
q	The angle of the prism (rad)	0,97825	0,000019	$-490*10^{-6}$	$-20*10^{-9}$	0,2
Lt	'Translation' distance (um)	25000	21	$-9,2*10^{-9}$	$-110*10^{-9}$	95,1
l	Difference in laser reading, (profile height difference) including repeatability (um)	17,15	0,002	$13*10^{-6}$	$16*10^{-9}$	1,9
Combined uncertainty					$120*10^{-9}$	
Expanded uncertainty					$240*10^{-9}$	

To combine the uncertainties, the root sum square method was used as described in the GUM [1]. The combined uncertainty was calculated to be 120×10^{-9} in the refractive index measurements.

The expanded uncertainty was calculated to be 240×10^{-9} in the measurements, which compared favourably with previous methods used in this research.

6.5 Conclusions and Recommendations from Uncertainty Calculations.

The uncertainty for the Edlén weather station method was calculated to be $6,87\times10^{-8}$, based solely on sensor contributions, excluding the theoretical uncertainty of the Edlén formula, which has an accuracy limit of 3×10^{-8}.

For the refractometer operating with the translation stage and the second prism, the uncertainty was calculated as $2,7\times10^{-8}$, representing an improvement by a factor of two over the theoretical uncertainty of the Edlén

weather station method. However, the optical windows of the second prism did not fully meet the design specifications, and further improvements will be necessary.

The uncertainty for the Fizeau interferometer method was calculated to be $8{,}4\times10^{-8}$. This value is marginally higher than that of the Edlén weather station method when the theoretical accuracy of the Edlén formula is excluded. The relatively higher uncertainty here is attributed to the lateral calibration of the interferometer, which from the table is clear to add 95% to the total uncertainty will be discussed in more detail in Chapter 7, Future Work.

.

Chapter 6.2 Bibliography

1. "*Evaluation of measurement data—Guide to the expression of uncertainty in measurement,"* JCGM **100** (2008).
2. Keysight Technologies. 5529A Dynamic Calibration System. [cited 2021, Dec 12]. https://www.keysight.com/zz/en/product/5529A/dynamic-calibration-system.html]
3. Zeiss, "Zeiss Prismo". https://www.zeiss.com/metrology/products/systems/coordinate-measuring-machines/bridge-type-cmms/prismo.html#technicaldata, Accessed on: July 2019.
4. Zygo, "Zygo operating manual of displacement measuring system". https://www.zygo.com/?/met/markets/stageposition/zmi/. Accessed on: July 2019.
5. Zygo GPI/HD flatness interferometer https://www.zygo.com/products/metrology-systems/laser-interferometers

Chapter 7: Concluding remarks and opportunities for future research and application

This study focused on the improvement in the permanent vacuum prism refractometer, using the two defined methods to measure the vacuum-to-air ratio needed to calculate the refractive index. The methods investigated were:

i) the translation stage method and

ii) the use of a Fizeau interferometer. Two prisms were employed for these methods, with the first being a commercial prism and the second a custom-designed prism built specifically for the study.

The initial objective of this research is to improve the use of the refractometer for practicality and uncertainty. During the development of the permanent vacuum, preliminary measurements were conducted using a commercial prism. Results indicated the potential for creating a permanently sealed vacuum prism. By translating this prism across a pair of laser displacement beams, it is possible to measure the vacuum-to-air ratio accurately, which can subsequently be used to determine the refractive index of air. Following these results, a second, custom-designed prism was developed with several improvements:

i) a larger apex angle to increase the vacuum-to-air ratio for greater resolution.

ii) two entry points into the vacuum etalon for better vacuum measurement

iii) high-quality optical windows with improved flatness and parallelism

iv) Thicker side windows that will not deform under vacuum, and

v) increased side window height, allowing both laser beams to pass through the same optical path. However, as described in Chapter 5, the second prism did not meet the expected improvements in optical flatness and parallelism due to insufficient control over the manufacturing process.

To address these issues, the decision was made to construct a third prism and perform measurements of the optical flatness and wavefront of the side windows prior to assembly. During the manufacturing of this third prism, further improvements were incorporated: the side windows were thickened to minimize distortion under vacuum conditions, and an additional chamber was created in the upper part of the prism for measuring gases other than air. This design change will expand the refractometer's applicability for standards measurements including the SI units of temperature (Kelvin), mass (kg), and derived SI unit the pressure (kPa).

Figures 44 and 45 show the optical flatness measurements of the side windows prior to assembly. Two horisontal profiles were selected at the locations where refractive index measurements would be taken, showing peak-to-valley height differences of only 115 nm and 50 nm, respectively.

.

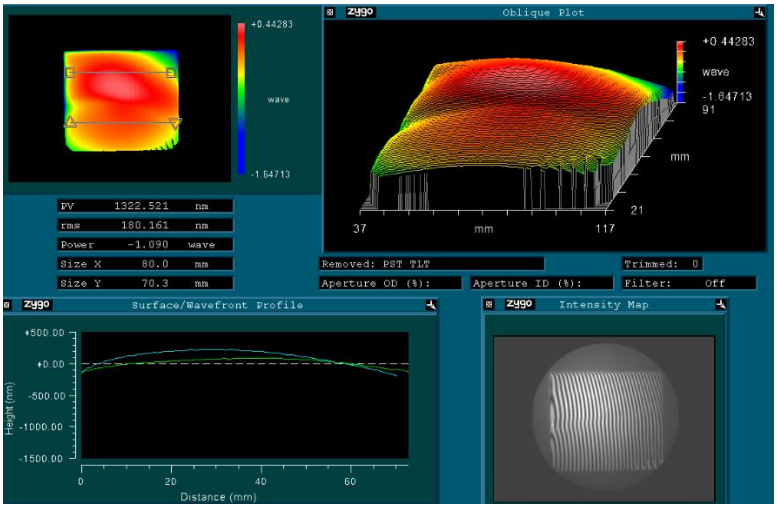

Figure 44 Side A, optical flatness.

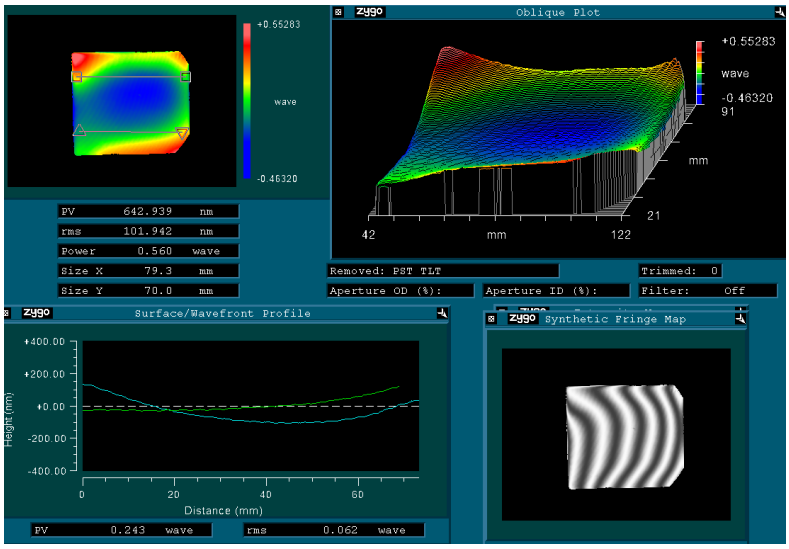

Figure 45 Side B, optical flatness.

Figure 46 presents the flatness measurements of the assembled third prism, highlighting the significant improvements in optical quality compared to the second prism. The horisontal profiles and fringe map demonstrate height (p-v) variations of less than 100 nm, indicating the improved optical flatness achieved in this assembly.

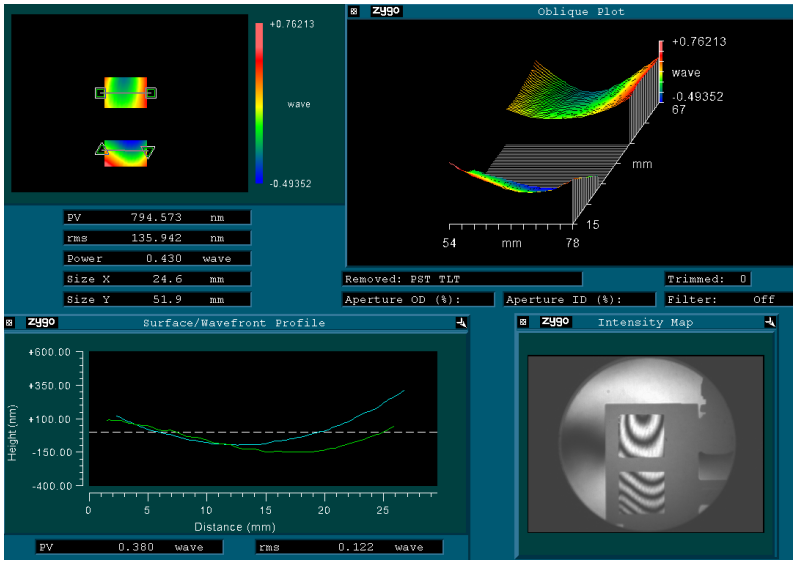

Figure 46 Third prism assembled; optical flatness measured.

Figure 47 is the completed third prism, incorporating the design improvements:

- Thicker side windows,
- High optical quality achieved through precise manufacturing and assembly, and
- A top chamber capable of being filled with gases other than air, supporting research in the new definitions of SI units, including Kelvin, Mass, and the optical pressure standard

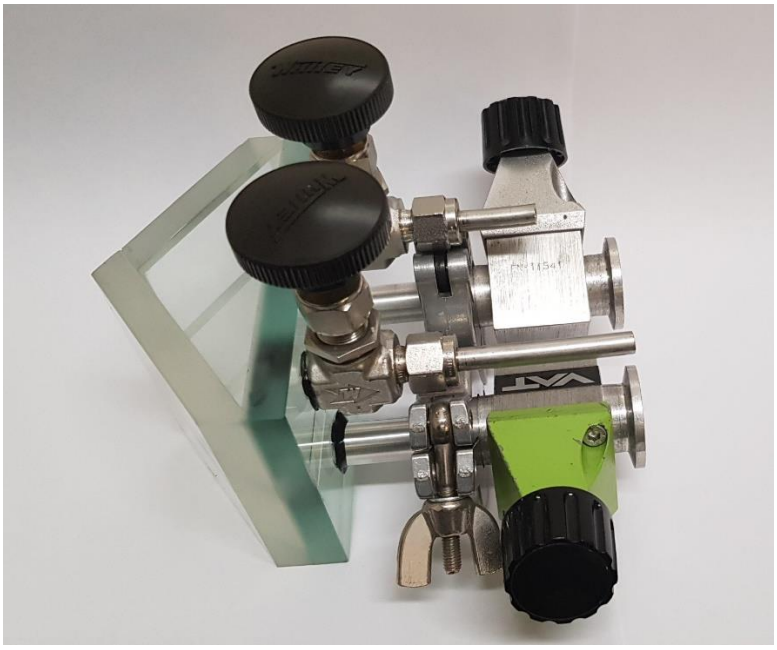

Figure 4710 Third prism assembly, underscoring the improvements in optical flatness.

The second focus area for future work is in advancing the Fizeau interferometer method for refractive index measurement. A Michelson interferometer setup was initially experimented with due to its simplicity. Future work will assess the optimum optical configuration—between the Michelson and Fizeau setups—most suitable for routine applications. This initial setup was a prompt investigation to evaluate the feasibility of a compact, cost-effective refractometer with potential applications across dimensional and other areas of metrology.

Figure 48 presents the Michelson interferometer setup, while Figure 49 displays the fringe map with a vacuum in the lower chamber and air in the upper chamber. The map observes the fringe patterns between the top and lower chambers, with the optical glass layer separating the two regions in the centre of the image.

The preliminary results suggest that, with further refinement, this setup holds promise for a practical, low-cost refractometer system suitable for broad metrological applications.

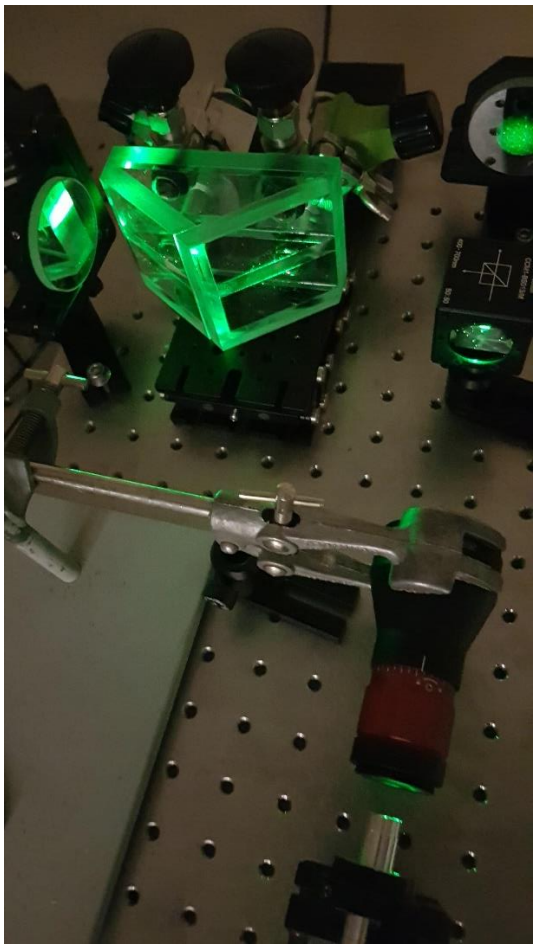

Figure 4811 A simple Michelson interferometer setup with the third prism.

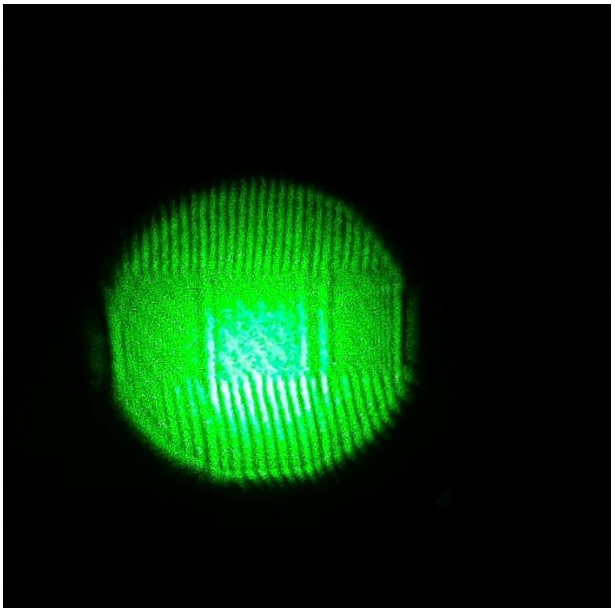

Figure 49 Fringes from the Michelson interferometer setup with the third prism.

Chapter 8: Journal Papers

8.1 A permanent vacuum refractometer for everyday use in dimensional metrology. Nature Scientific Reports. 2021; articles 11, 9290.

The following paper was published after stringent peer review in Nature Scientific Reports.

www.nature.com/scientificreports

scientific reports

Check for updates

OPEN

Development of a permanent vacuum hollow prism air refractometer for use in dimensional metrology

O. Kruger[1,2] & N. Chetty[1]✉

Refractive index measurements are required when light is used as the basis of a measurement system. In dimensional metrology, refractive index measurements are used to compensate for the change in the speed of light. This is crucial because the SI unit for the metre is defined as the speed of light in a vacuum. Air refractometers are the most accurate way to measure the speed of light in air. Many research works to date have been performed to measure the refractive index of air using refractometers. This research uses a commercial prism as the vacuum etalon instead of the tube that is used most often. This novelty and newness of our research were to focus on the design, fabrication and testing of a refractometer which uses a permanent vacuum for ease of use but that will still have the same accuracy of other refractometers currently in use. Modifications to existing designs improved the long-term stability compared to other prism refractometers and are also potentially more accurate than tube refractometers. The results achieved with this permanent vacuum refractometer are accurate to 8.4×10^{-8}, which compares favourably with other refractometers on accuracy. It also has the added advantage that it does not require a vacuum pump, and with added laser path improved long term stability but still portable and robust enough to use in everyday applications.

Refractive index measurements in the medical industry are used to measure, for example, the specific gravity of human urine to determine kidney function[1–3]. In veterinary medicine, it is used to measure the plasma protein and in-cell measurements in biological tissues[4–6]. It is also used in the design of optical systems, especially for the medical industry in eye difference design[7]. Refractive index measurements are also used to determine the sugar content in various beverages, including wine[8]. The application and impact of refractive index measurements are well captured by Singh[9].

This paper focuses on refractive index measurements in metrology and more especially dimensional metrology, an area that requires highly accurate measurements. Most measurements are performed at the highest sensitivity for accurate results by utilising laser light to perform the distance measurements. These measurements require the refractive index to be known to a high degree of accuracy.

Since 1983, the metre has been defined as the length of the path travelled by light in a vacuum in 1/299 792 458 of a second[10–16]. However, most dimensional and length measurements are performed in the air. The refractive index in air changes with environmental conditions (air pressure, air temperature, humidity and CO_2), and thus, the refractive index of air at the specific conditions must be calculated to make corrections compared to the definition of the metre. This is exacting work and sometimes difficult to achieve practically in the environment.

To calculate the refractive index, the speed (velocity) of light in a vacuum, c, is divided by v', the velocity of light in air at the time the measurements are taken.

The refractive index is thus:

$$n = \frac{c}{v'}, \tag{1}$$

where n is the refractive index, c is the velocity of light in a vacuum, and v' is the velocity of light in a particular medium, in this case, air.

[1]School of Chemistry and Physics, Discipline of Physics, University of KwaZulu-Natal (PMB), Private Bag X01, Scottsville 3209, South Africa. [2]National Metrology Institute of South Africa, CSIR Campus, Private Bag X34, Pretoria 0001, South Africa. ✉email: ChettyN3@ukzn.ac.za

Content courtesy of Springer Nature, terms of use apply. Rights reserved

Figure 1. Hollow prism from 3B Scientific.

Many research works to date have been performed to measure the refractive index of air using refractometers. This novelty and newness of our research were to focus on the design, fabrication and testing of a refractometer which uses a permanent vacuum for ease of use but that will still have the same accuracy of other refractometers currently in use. Our device would be suitable for use in everyday applications due to its simplicity of design and ease of use.

Refractive index measurements and refractometers in dimensional measurements. The most common method to determine the refractive index is to measure the environmental conditions (air temperature, air pressure, relative humidity and CO_2) and then calculate it by using equations from Edlin[17], Birch[18] or Ciddor[19]. Much research has been done on the differences between these equations by Bonsch and Potulski[20] and Kruger and Chetty[21]. The original calculations were updated specifically for the moisture content of the air. Metrologists in dimensional laboratories and commercial manufacturers of laser measurement systems, such as Rensihaw[22], Agilent[23] and Zygo[24], now mainly use the modified equation. Hence, it was decided to use the modified Edlin equation in this research.

Equation (2) is the modified Edlin equation used to calculate the refractive index of air[18].

$$(n-1)_{Tp} = \frac{p(n-1)_s}{93214.60} \cdot \frac{1 + 10^{-8}p(0.5953 - 0.009876T)}{(1 + 0.0036610T)}. \quad (2)$$

Here $(n - 1)$ is the refractivity of standard air, the temperature T is expressed in degrees Celsius, the air pressure p in torr, standard air at 1 atmosphere and 15 °C.

The more accurate method to determine the refractive index is to use a refractometer that measures the refractive index directly by comparing an optical path in the air to the same optical path in a vacuum, as described by Bonsch and Potulski[20] and Kruger and Chetty[21]. Research by Zhang et al.[25] and Wu and Takahashi[26] used frequency combs as the measuring system, and although these gave a very high resolution, the overall accuracy is similar to other designs due to the optical layout. The fact that the distance between the mirrors is not absolutely stable is also of concern.

The main reason the refractometer method is more accurate is that the weather station data have more technical difficulties[25–30]. Kruger and Chetty[21,31] studied these difficulties and decided to focus the research on refractometers that will be used for highly accurate refractive index measurements. Kruger and Chetty[21,31] developed a low-cost robust refractometer. Their research included the development of refractive index measurements and a robust refractometer that uses a commercial laser displacement interferometer together with a vacuum cylinder to measure the refractive index to parts in the 10^{-8}.

This refractometer is very accurate and can be used daily because of its simplistic design, however, it requires a vacuum pump to perform the refractive index measurements. The vacuum pump must be close to the refractometer to achieve a good vacuum, which leads to the heat from the pump affecting the air temperature of the laser measurements. Another limitation to this refractometer is that repeatedly drawing a vacuum can lead to dust particles entering the vacuum cylinder, and these can affect the measurements through diffraction of the laser beam.

A further challenge with the traditional tube refractometer is the change in the optical thickness of the side windows in the tube refractometer. Bonsch and Potulski[20] measured this to be 8 nm, and although it is very small, it adds to the inaccuracy of these tube refractometers.

These problems led to this research, the aim of which was to design, build and test a simple air refractometer that can be used in everyday laser-based measurements without the use of a vacuum pump and to eliminate the errors in tube refractometers as describe by Bonsch and Potulski[20].

Experimental details

Investigating a new refractometer led to using a hollow prism as the vacuum etalon. The concept was that the prism will have a permanent vacuum, consequently eliminating the use of a vacuum pump during measurements, thereby producing more reliable measurements.

The prism used is a commercial prism that is normally used for the refractive index measurements of liquids[32]. This specific prism is from 3B Scientific and shown in Fig. 1 [33]. Only basic specifications for the prism are

Content courtesy of Springer Nature, terms of use apply. Rights reserved

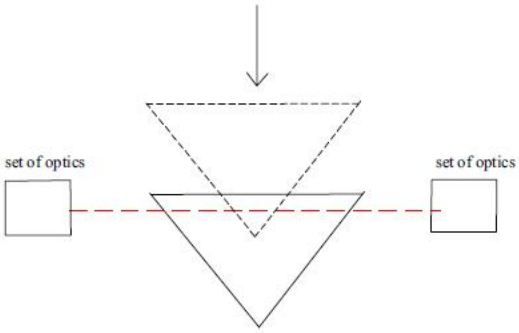

Figure 2. Schematic diagram of, with top view prism refractometer using laser displacement interferometer and translation stage.

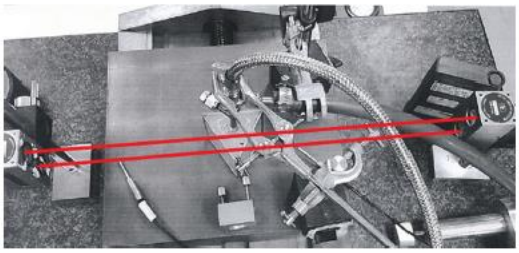

Figure 3. Prism refractometer with laser beams.

available, and there is no specification for the optical flatness and parallelism of the side windows, which is critical and will be discussed in more detail later. The prism was modified by attaching a vacuum pipeline to the opening of the prism so that a vacuum could be drawn inside the prism.

An optical layout similar to the design of the previous cylinder refractometer by Kruger and Chetty[21] was used. In this research, the vacuum cylinder was replaced with the above-mentioned prism. Instead of using a vacuum pump to generate the vacuum required to compare the air to vacuum ratio, the prism was moved across the laser beam to replace the optical path length from air to vacuum. This has the advantage of not requiring a vacuum pump during the measurements.

Figure 2 shows a schematic layout of the prism refractometer. Any laser system could theoretically be used, but in this design, a commercial heterodyne laser (Zygo ZMI 2000 laser interferometer) was used. The frequency difference of the two laser beams is about 20 MHz[24]. Agilent angle interferometer optics (10770A) was used to split the two laser beams in the polarising beam splitter. It separates the two beams, f1 and f2, and directs them parallel and 32.62 mm apart[23].

The vacuum prism was positioned in such a way that the one frequency of the laser, f2, passed through the prism, which is under vacuum and the other frequency, f1, passed above the prism in normal air. With the use of a translation stage, the prism was moved from position 1, the dotted prism, through laser beam f2 to position 2, the solid line prism, thereby replacing the air with a vacuum column.

Figure 3 shows the prism placed on the translation stage where a displacement laser (HP/Agilent Model 5519A) was used to measure the displacement accurately.

The distance the translation stage is moved, Lt, together with the half-angle θ are used to calculate the light path in the vacuum inside the prism, L. The light path in a vacuum, L, is a relative change as the zero position for L is already in a small part of the vacuum.

$$L = 2 \times (tan\theta \times Lt). \tag{3}$$

This method has also been researched by Renkens and Schellekens[34], and there was a US patent filed in 1995 by John Tsai[35].

Renkens and Schellekens[34], and John Tsai's[35] research was inconclusive because of doubt over whether it had a clear advantage over the tube refractometer. Therefore, the current research investigated whether this method creates an easier to use and more accurate refractometer than the tube refractometer.

Content courtesy of Springer Nature, terms of use apply. Rights reserved

Stage moved		Prism readings								
Transverse laser reading, *Lt* (mm)	Air length replaced, *L* (nm)	Laser reading in air (nm)	Laser reading in vacuum (nm)	Laser reading combined, *l* (nm)	Air temp (°C)	Air pres (mbar)	Air humid (%RH)	V.O.L. Edlin eq	V.O.L. prism	Diff. in V.O.L. between Edlin eq. and prism refract
Use only for Edlin calculation					20.14	866.53	45.3	0.999768124		
5	5,773,503	1305	33	1338	–	–	–	–	0.999768305	– 1.82E–07
10	11,547,006	2475	202	2677	–	–	–	–	0.999768219	– 9.50E–08
15	17,320,509	3248	770	4018	–	–	–	–	0.999768074	4.93E–08
20	23,094,012	3564	1791	5355	–	–	–	–	0.999768175	– 5.17E–08
25	28,867,514	3692	3003	6695	–	–	–	–	0.999768132	– 8.40E–09

Table 1. Results for the prism refractometer data compared to the modified Edlin equation using weather station measurement calculations.

Results of the hollow prism using a translation stage

The angle of the prism together with the distance of travel of the translation stage is needed to calculate the distance of air replaced within a vacuum. From this, the refractive index can be calculated in the same way as the tube refractometer[20,21].

$$n = \left(\frac{L+l}{L}\right). \tag{4}$$

By substituting Eq. (3) into (4), Eq. (5) is used to calculate the refractive index

$$n = \frac{2 \times (tan\theta \times Lt) + l}{2 \times (tan\theta \times Lt)}. \tag{5}$$

The angle of the prism was measured using a Zeiss Prismo Coordinate Measuring Machine (CMM). The accuracy of the CMM measurement is calculated from the CMM specification to be 0.5 µm[36].

The prism intended for liquid refractive index measurements was not ideal for air measurements, and while the angle could be measured accurately, the optical flatness and parallelism of the sides of the prism could not. These measurements are necessary to determine the wavefront of the optical path of the prism while the prism is traversed across the laser beam. To determine this, measurements were taken with air inside the prism. It was assumed that the air inside and outside the prism was at the same temperature, pressure and humidity. These readings were used as a baseline measurement and were added to the final measurements made when there was a vacuum inside the prism.

The results of the prism refractometer were compared to the weather station method, where the air temperature, pressure and humidity were measured and the refractive index calculated using the modified Edlin equation[17,18]. In Table 1, the velocity of light compensation (V.O.L.) was calculated as most manufacturers of laser displacement systems use the V.O.L. in their software calculations[22–24]. The relation between the V.O.L. and the refractive index is shown in Eq. (6) and is the inverse of the refractive index *n*.

$$\text{V.O.L.} = n^{-1}. \tag{6}$$

The readings were taken in 5 mm intervals over 25 mm transverse range. As discussed previously, the first set of readings was taken while the prism was filled with air to establish the baseline measurements (see column three, Table 1). The readings were not constant where one would have expected a smaller change in the laser reading. In a flawless prism, there should be no difference in the laser reading as the prism is traversed in front of the laser beam.

The combined laser reading is recorded in column five in Table 1. The combined laser readings were used to calculate the V.O.L. in the air (see column ten, Table 1). To validate the readings, it was compared to the weather station method, and the difference in the two readings are in the last column of Table 1. The worst difference between the two methods was 1.2×10^{-7}. The system became more accurate with a longer travel in the traverse direction. This is expected as the air/vacuum ratio is larger, and the laser readings become less sensitive to the overall accuracy.

Sets of readings were taken over a period of 2 weeks, and the standard deviation was calculated on the differences in the two methods. The worst standard deviation was 5.5×10^{-8} and will be discussed in detail in the next section.

The V.O.L was calculated using the Edlin equation for an Air temperature of 20.14, Air pressure of 866.53 mbar and Air humidity of 45.3%RH, to be 0.999768124.

Added laser to optical layout

The results of the prism refractometer with the translation showed an agreement of 1.82×10^{-7} with the Edlin weather station method for the short travel and better than 8.4×10^{-9} for the longer travel of the transverse stage. This proves that this method is accurate enough to be used in dimensional metrology.

Content courtesy of Springer Nature, terms of use apply. Rights reserved

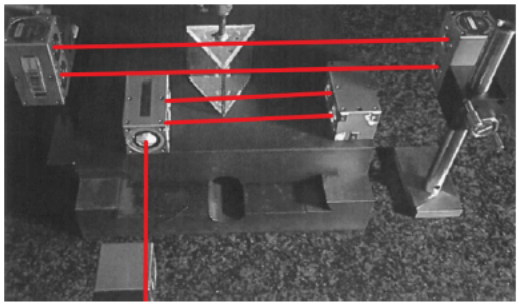

Figure 4. Setup with extra laser beams to continue measuring the zero position.

Sym	Description	Value	Uncertainty	Sensitivity coefficient	Uncertainty contributor	Significance %
q	Angle of prism (rad)	0.52359	0,000011	-530×10^{-6}	-6×10^{-9}	2
Lt	Translation distance (µm)	25,000	0,5	-9.3×10^{-9}	-3×10^{-9}	1
l	Difference in laser reading, including repeatability (um)	6677	0,002	35×10^{-6}	40×10^{-9}	97
Combined uncertainty					4×10^{-8}	
Expanded uncertainty					8.4×10^{-8}	

Table 2. Uncertainty budget for prism refractometer at the 25 mm position only.

The results over a short period was very promising, but when the system was used over a longer period (a few days), it did not agree with the weather station method to the same accuracy. The reason was the drift in the zero position. Although the laser beam for the zero position was through a very small amount of vacuum compared to the laser beam through the air, it was enough to drift over time compared with the laser through the air. The drift over a few days was as much as 50 nm between the two laser beams.

A new optical layout, Fig. 4, was used by adding an extra pair of laser beams to the system. This pair of laser beams was used to constantly measure the zero position. The optics of the second laser was in such a position that it will move with the translation stage and always measure the same position of the prism. This second laser reading will be used to correct the first laser reading for the zero-position drift and will substantially improve the long-term accuracy.

The new optical layout was tested with both laser beams at the zero position over a few days. The difference between the two laser readings was less than the uncertainty in the laser readings.

Uncertainty calculations

The uncertainty for the Edlin weather station method was calculated by approximating the uncertainty in the measurement for each of the sensors. The uncertainty of the measurements was taken not only from the uncertainty of the calibration but also the accuracy of each sensor during the measurements. This was necessitated by the fact that the sensors are calibrated under near-ideal conditions but the measurements were performed in lesser conditions in the laboratory.

The uncertainty of the air temperature measurements was estimated to be 0.05 °C, which resulted in an uncertainty of 5.1×10^{-8} in the refractive index; the air humidity uncertainty was estimated to be 2% RH, resulting in an uncertainty of 1.7×10^{-8} in the refractive index; and lastly, the air pressure uncertainty was estimated to be 0.1 mbar, and this resulted in an uncertainty of 2.7×10^{-8} in the refractive index. When combining these uncertainties using the root sum square method, the overall uncertainties from the weather station method were 5.9×10^{-8} in the refractive index[21,37].

The uncertainty for the prism refractometer was calculated using Eq. (5), where the sensitivity coefficients were calculated for each contributor. The Laser system was calibrated directly against the National Standard in South Africa, an Iodine stabilised HeNe laser. The CMM was calibrated but for the uncertainty calculations the manufacturing specification was used[36]. In Table 2, the uncertainty budget for the refractive index was only calculated for the 25 mm position, as this is the most accurate.

Apart from the contributors in the table, the imperfections of the prism faces were calculated by measuring the baseline readings. These measurements were taken in air and added to the readings under vacuum. This eliminated this uncertainty, and only the repeatability in the readings was added to the total uncertainty.

However, the deformation of the prism under vacuum had to be included as an uncertainty component. Straightness measurements using the Zeiss CMM were performed under normal environmental conditions with air in the prism at atmospheric conditions. The straightness of the left side of the prism is shown in Fig. 5. Thereafter, a vacuum was drawn, and the straightness of the same side was measured again and shown in Fig. 6.

Content courtesy of Springer Nature, terms of use apply. Rights reserved

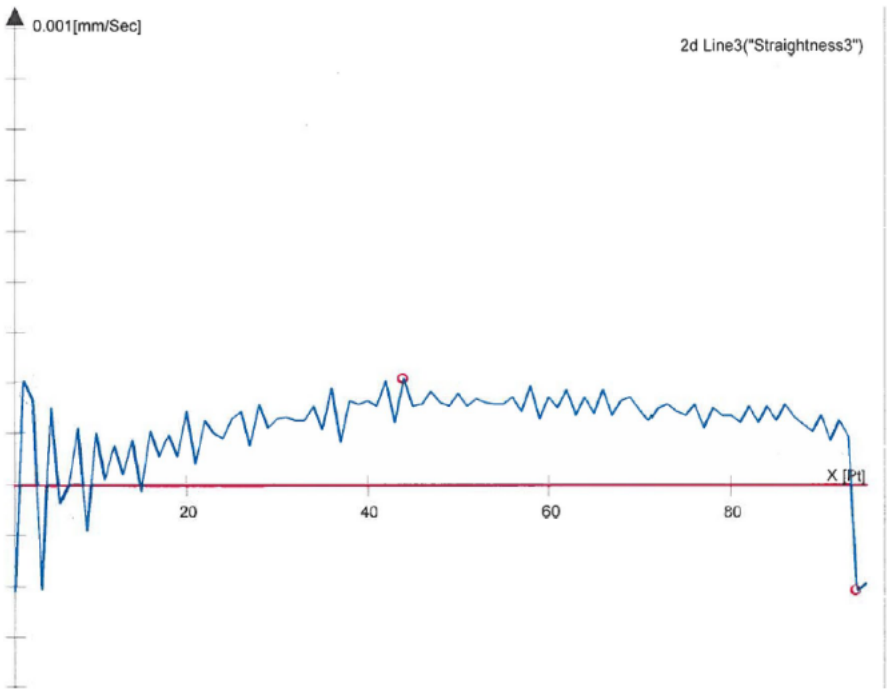

Figure 5. Profile of prism side under atmospheric conditions.

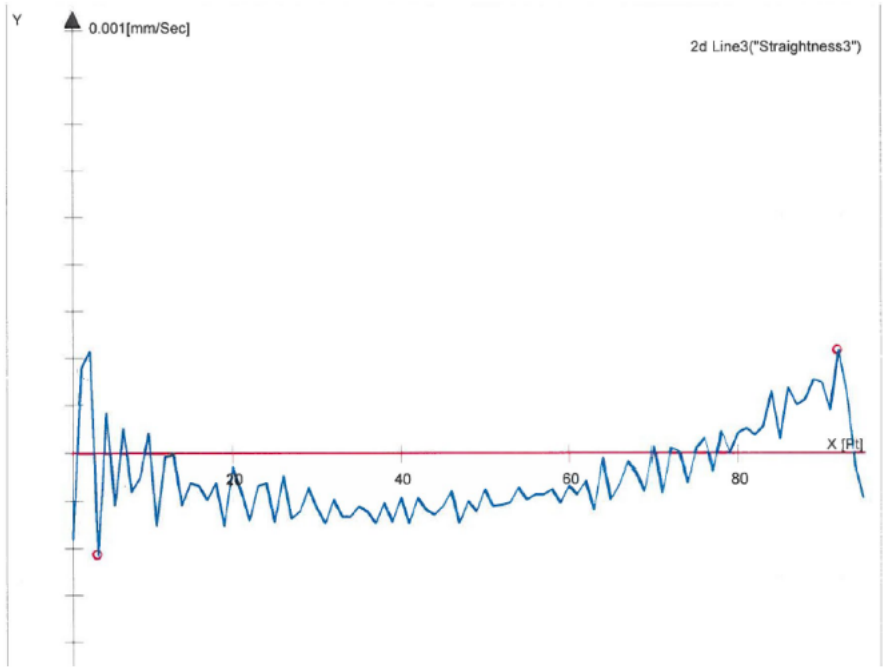

Figure 6. Profile of prism side under vacuum.

Content courtesy of Springer Nature, terms of use apply. Rights reserved

The straightness value between air and vacuum changed by 1 µm over the area used during the measurements, and taking the uncertainty for the deformation in the sides to be less than 0.5 µm over the area that was used during the measurements, resulted in less than 1×10^{-9} in the velocity of light compensation and was not included in this uncertainty budget.

The combined uncertainties using the root sum square method[37] is 8.4×10^{-8} in the measurement of the refractive index.

Conclusion

The aim of this research was to investigate the use of a permanent vacuum hollow prism as the vacuum etalon in an air refractometer in order to eliminate the use of a vacuum pump during refractive index measurements. The results of the translation showed an agreement of 1.82×10^{-7} with the Edlin weather station method for the short travel and better than 8.4×10^{-9} for the longer travel of the transverse stage.

The use of a prism as the vacuum etalon further eliminated the difficulties due to the change of the optical length of the side windows of a tube refractometer as describe by Bonsch and Potulski[20]. This is due to the optics being under the same conditions during the entire measurement. This is a great improvement in the potential accuracy of prism refractometers over tube refractometers.

Adding an extra set of laser beams to the prism refractometer improved the long-term accuracy of the refractometer, compared to other prism refractometers as describe by Renkens and Schellekens[34], and John Tsai's[35]. This design can now be used for a prolonged period after the prism had been translated and kept at the 25 mm position, which is a big improvement over previous designs. With these improvements, the refractometer proved advantageous not only for refractive index air measurements in dimensional metrology on a daily basis but also for high accurate research.

Future improvements to the system will focus on the commercial prism. The side windows of the prism should be manufactured of better-quality optical material and to a higher accuracy in flatness and parallelism to increase the overall accuracy of the system.

The results, both in everyday use for long-term measurements and highly accurate research, prove the original objective of this research.

Received: 28 November 2020; Accepted: 15 April 2021
Published online: 29 April 2021

References

1. Joo, H.-Y. & Kim, S. J. Spectrophotometric analysis of aluminium nitride thin films. *J. Vac. Sci. Technol. A.* **17**, 862–870. https://doi.org/10.1116/1.582035 (2016).
2. Putnam, D. F. Composition and concentration properties of human urine. *NASA*. Accessed Sept 2020. https://ntrs.nasa.gov/archive/nasa/casi.ntrs.nasa.gov/19710023044.pdf (1971).
3. Anton Paar. Refractometric analysis of urine. https://www.anton-paar.com/corp-en/products/applications/refractometric-analysis-of-urine. Accessed 2020.
4. Osborne C. A. & Nwaokorie, E. Urine specific gravity measurement and interpretation in veterinary medicine. *Veterinary News*. Accessed Sept 2020. https://www.dvm360.com/view/urine-specific-gravity-measurement-and-interpretation-veterinary-medicine (2013).
5. Carpignano, F., Rigamonti, G., Mazzini, G. & Merlo, S. Low coherence reflectometry for refractive index measurements of cells in micro capillaries. *Sensors* **16**, 1670 (2016).
6. Zhou, Y., Chan, K. K. H., Lai, T. & Tang, S. Characterizing refractive index and thickness of biological tissues using combined multiphoton microscopy and optical coherence tomography. *Biomed. Opt. Express* **4**, 38–50 (2013).
7. Pierscionek, B. K. The refractive index in the eye lens—implications for clinical practice and optical design. *Eyenews*. Accessed Sept 2020. https://www.eyenews.uk.com/features/ophthalmology/post/the-refractive-index-in-the-eye-lens-implications-for-clinical-practice-and-optical-design (2016).
8. Robinson, J. *The Oxford Companion to Wine* Vol. 3 (Oxford University Press, 2006).
9. Singh, S. Refractive index measurements and its applications. *Phys. Scr.* **65**(2), 167 (2006).
10. BIPM. Resolution. *Metrologia* **20**(1), 25 (1984).
11. Quin, T.J. Mise en practique of the definition of the metre. *Metrologia*. https://iopscience.iop.org/article/10.1088/0026-1394/30/5/011 (1992).
12. Quinn, T. J. Practical realization of the definition of the metre. *Metrologia* **36**, 211. https://doi.org/10.1088/0026-1394/36/3/7 (1997).
13. BIPM. Strategy 2018–2028 Consultative Committee for Length. Accessed Sept 2020. https://www.bipm.org/documents/20126/41414762/CCL+Strategy/0f4af537-1729-b44a-e39ef0023e439435 (2013).
14. BIPM. *17e Conference Generale Des Poids at Mesures*. Accessed Sept 2020. https://www.bipm.org/utils/common/pdf/CGPM/CGPM17.pdf (1983).
15. Giacomo, P. News from the BIPM. *Metrologia* **20**(1), 25–30 (1984).
16. BIPM. Documents concerning the new definition of the metre. *Metrologia* **19**, 163–177. https://iopscience.iop.org/article/10.1088/0026-1394/19/4/004/pdf. Accessed Sept 2020 (1984).
17. Edlén, B. The refractive index of air. *Metrologia* **2**, 71–80 (1965).
18. Birch, K. P. & Downs, M. J. An updated Edlén equation for the refractive index of air. *Metrologia* **30**, 155–162 (1993).
19. Ciddor, P. E. Refractive index of air: New equations for the visible and near infrared. *Appl. Opt.* **35**, 1566–1573 (1996).
20. Bonsch, G. & Potulski, E. Measurement of the refractive index of air and comparison with the modified Edlin formulae. *Metrologia* **35**, 133–139 (1998).
21. Chetty, N. & Kruger, O. A. Robust air refractometer for accurate compensation of the refractive index of air in everyday use. *Appl. Opt.* **55**(32), 9118–9122 (2016).
22. Chapman, M. A. V. Environmental compensation of linear laser interferometer readings. Renishaw Technical White Paper: TE329. Accessed Sept 2020. https://resources.renishaw.com/en/details/white-paper-environmental-compensation-oflinear-laser-interferometer-readings—94445 (2013).
23. Agilent(HP). 5528A Laser Measurement System, User Guide. Accessed Sept 2020. https://www.pearl-hifi.com/06_Lit_Archive/15_Mfrs_Publications/20_HP_Agilent/HP_5528_Laser/HP_5528A_Measurement_System/HP_5528A_Users_Manual.pdf (1988).

Content courtesy of Springer Nature, terms of use apply. Rights reserved

24. Zygo laser system, ZMI-2000, System Manual. Accessed Sept 2020. https://www.zygo.com/support/reference-library/product-manuals (1997).
25. Zhang, J., Lu, H. & Wang, L. J. Precision measurement of the refractive index of air with frequency combs. *Opt. Lett.* **30**(24), 3314 (2005).
26. Wu, G., Takahashi, M., Arai, K., Inaba, H. & Minoshima, K. Extremely high-accurate correction of air refractive index using two-colour optical frequency combs. *Sci. Rep.* **3**, 1894 (2013).
27. Muijilwijk, R. Update of the Edlén formulae for the refractive index of air. *Metrologia* **25**, 189 (1988).
28. Lazar, J., Číp, O., Čížek, M., Hrabina, J. & Buchta, Z. Suppression of air refractive index variations in high-resolution interferometry. *Sensors* **11**, 7644–7655 (2011).
29. Lazar, J. *et al.* Refractive index compensation in over determined interferometric systems". *Sensors* **12**, 14084–14094 (2012).
30. Ishige, M., Aketagawa, M., Quoc, T. B. & Hoshino, Y. Measurement of air refractive index fluctuation from frequency change using a phase modulation homodyne interferometer and an external cavity laser diode. *Meas. Sci. Technol.* **20**(8), 084019 (2009).
31. Kruger, O. A. Robust air refractometer for accurate compensation of the refractive index of air in everyday use. Master Thesis: University of KwaZulu-Natal. Accessed Sept 2020. https://researchspace.ukzn.ac.za/handle/10413/14501 (2016).
32. Daimon, M. & Masumura, A. Measurement of the refractive index of distilled water from the near-infrared region to the ultraviolet region. *Appl. Opt.* **46**, 3811–3820 (2007).
33. 3B Scientific. Accessed Sept 2020. https://www.3bscientific.com/hollow-prism-equal-sided-1014618-u11922,p_639_23222.html.
34. Renkens, M. J. M. & Schellekens, P. H. J. An accurate interference refractometer based on a permanent vacuum chamber: Development and results. *CIRP Ann. Manuf. Technol.* **42**(1), 581–583. https://doi.org/10.1016/S0007-8506(07)62514-1 (1993).
35. Tsai, J. C. Ambient air refracture index measuring device. US 5394244 A (1995).
36. Zeiss Prismo. Accessed Sept 2019. https://www.zeiss.com/metrology/products/systems/coordinate-measuring-machines/bridge-type-cmms/prismo.html#technicaldata.
37. BIPM. Evaluation of measurement data—Guide to the expression of uncertainty in measurement. JCGM 100:2008. Accessed Sept 2020. https://ww.ipm.org/documents/20126/2071204/JCGM_100_2008_E.pdf/cb0ef43f-baa5-11cf-3f85-4dcd86f77bd6 (2008).

Author contributions

Both authors had equal input in the research work and writing of the paper.

Competing interests

The authors declare no competing interests.

Additional information

Correspondence and requests for materials should be addressed to N.C.

Reprints and permissions information is available at www.nature.com/reprints.

Publisher's note Springer Nature remains neutral with regard to jurisdictional claims in published maps and institutional affiliations.

Open Access This article is licensed under a Creative Commons Attribution 4.0 International License, which permits use, sharing, adaptation, distribution and reproduction in any medium or format, as long as you give appropriate credit to the original author(s) and the source, provide a link to the Creative Commons licence, and indicate if changes were made. The images or other third party material in this article are included in the article's Creative Commons licence, unless indicated otherwise in a credit line to the material. If material is not included in the article's Creative Commons licence and your intended use is not permitted by statutory regulation or exceeds the permitted use, you will need to obtain permission directly from the copyright holder. To view a copy of this licence, visit http://creativecommons.org/licenses/by/4.0/.

© The Author(s) 2021

8.2 Fizeau interferometer to measure the refractive index of air with permanent vacuum prism etalon.

Comparison between a permanent vacuum Fizeau refractometer, a cylinder refractometer, and the weather station method to measure the refractive index of air

O A KRUGER, N CHETTY***

**School of Chemistry, Discipline of Physics, University of KwaZulu-Natal (PMB), Private Bag X01, Scottsville, 3209, South Africa*
***National Metrology Institute of South Africa, CSIR Campus, Private Bag X34, Pretoria, 0001, South Africa*

Abstract: This paper examines the critical impact of refractive index measurement within dimensional metrology. With a focus on air, the primary medium for most dimensional measurements, accurate determination of the refractive index becomes paramount. While the widely adopted weather station method is prevalent, this research underscores the superior precision achievable through refractometry. Specifically, the study investigates an innovative approach involving a permanent vacuum prism as the vacuum cell, a departure from conventional vacuum cylinders. The key advantage lies in commencing measurements from a vacuum zero position, eliminating complications associated with transitioning from air to vacuum. Introducing a new method employing an optical flatness interferometer with a Fizeau interferometer layout, the research not only contributes original insights but also presents results displaying an accuracy of $8{,}38 \times 10^{-8}$ in refractive index measurements of air. The results verify a robust setup for improving high dimensional methods for refractive index measurements, with potential applications and implications across various scientific and industrial domains.

1. Introduction

The General Conference on Weights and Measures (CGPM) fixed the speed of light at exactly 299 792 458 metre per second (m/s) [1, 2]. Since the definition for the speed of light was fixed in a vacuum, the refractive index is required to make the correction when measuring the speed of light in any other medium. The refractive index is shown in Equation 1.

$$n = \frac{c}{v'}$$

[Eq. (1)]

Where *n* is the refractive index, *c* is the velocity of light (V.O.L.) in a vacuum, and v' Is the V.O.L. in a particular medium, in this case air.

Much research has been done to measure the refractive index of air using refractometers [2–10]. This research proves the accuracy of the refractometers but has limitations, as described by Bonsch and Potulski and Kruger and Chetty [2,3,8].

In previous research by the authors [9], a hollow prism with a permanent vacuum was used to compare the refractive index of air to that of a vacuum, comparable to Renkens and Schellekens [10]. The results showed that it is possible to measure the refractive index of air using a prism refractometer, but the prism was a

commercial design and not ideal for highly accurate refractive index measurements. The current study aimed to design, build, and test a new prism refractometer using the specially designed prism. During the research a new method using a Fizeau interferometer to measure the vacuum/air ratio was investigated, and a comparison between this method and the previous method using a cylinder as the vacuum etalon as researched by Kruger and Chetty is presented here.

2. Refractive index measurements and refractometers

The most common method to determine the refractive index is to measure the environmental conditions, namely air temperature, air pressure, relative humidity, and CO_2. The refractive index is then calculated using equations from Edlén [11,12] or Ciddor [13].

The more accurate method to determine the refractive index is using a refractometer, which measures the refractive index directly by comparing an optical path in the air to the same length optical path in a vacuum. Much research has been published on this [2–10], and the conclusions of these are well captured by Bonsch and Potulski [2].

Kruger and Chetty's [3,8] investigation into these focused on refractometers that could be used for both their highly accurate refractive index measurements and their simplistic design for everyday applications. They researched the development of refractometers and developed a robust refractometer that uses a commercial laser displacement interferometer together with a vacuum cylinder accurate to parts in the 10^{-8} [8]. They continued the research into the use of a permanent vacuum prism refractometer but with similar accuracy [9].

3. Design of a new prism for use in the refractometer

Previous research by Kruger and Chetty into an advanced refractometer used a hollow prism as the vacuum etalon instead of a vacuum cylinder and proved the use of the prism successfully [9]. This was a big improvement in the simplicity of the system and because it uses a permanent vacuum, the amount of heat generated by the vacuum pump that negatively impacts the length measurements is for all purposes eliminated.

The prism used previously was made for refractive index measurements of liquids, as described by Daimon and Masumura [17], and is manufactured by 3B Scientific [18] (Figure 1). Because these prisms are designed to measure the refractive index of liquids with less accuracy than is required for the refractive index of air, it is not designed and built to the accuracy required for the measurement of the refractive index of air.

Fig. 1. Hollow prism from 3B Scientific.

The new prism (Figure 2) was designed with two entries, one where the vacuum pump connects and the second for the gauge as described by Kruger [9]. The second design modification is that the two side windows were made to be flat and parallel. This is to ensure the least beam deflection of the laser light passing through the prism. The windows were manufactured using quartz, but although improved not perfectly flat and parallel,

and corrections for it had to be made, which is discussed in the results section. The sides were also made higher, allowing both laser beams to pass through the same quantity of optics, similar to the design of the vacuum cylinder described by Chetty and Kruger [3].

The last design change incorporated into the new prism is the angle of the top corner of the prism. To achieve the maximum vacuum/air ratio, this angle must be as large as possible. However, a too-large angle will lead to total reflection of the laser on the side windows of the prism. Therefore, it was decided to use the Brewster angle for the windows [19]. For quartz medium, *n* approximating 1,5, and vacuum *n* approximating 1, the Brewster angle is near 56 degrees for each window, resulting in a 112-degree angle at the apex of the prism. Equation 2 was used to determine the Brewster angle.

$$Tan\theta = \frac{n1}{n2}$$

[Eq. (2)]

Figure 2 shows the new prism with the improvements, namely the larger apex angle, two vacuum ports, and higher, better-quality side windows.

Fig. 2. Newly designed prism.

4. Method using Fizeau interferometer to measure air refractive index together with prism vacuum etalon

The optical wavefront of the side windows of the prims was measured using a Zygo GPI XP/D phase-shifting interferometer [23]. During these measurements, the use of the shift in the fringes of the interferometer was investigated to measure the change in the optical path length of the air/vacuum ratio.

The Zygo interferometer is designed to measure the optical quality, such as flatness, parallelism, and wavefront, of optical components and is based on a Fizeau interferometer setup. The spacing and the angle of the fringes are used to measure the optical quality of the optics under investigation [23].

The orientation of the fringes in the interferometer was measured simultaneously in the vacuum chamber and the surrounding air. Subsequently, the same principle as in the previous method was used to calculate the air/vacuum ratio, but instead of using a laser displacement interferometer and a translation stage, the Zygo flatness interferometer was used to measure this change in vacuum/air ratio. Figure 3 shows the prism placed between the reference and test flats of the Zygo interferometer.

Fig. 3. Prism refractometer setup in Zygo flatness interferometer

An interferometer map, as shown in Figure 4, was generated. The vacuum chamber is at the bottom of the figure and air is at the top. In Figure 7 the same air was inside and outside the vacuum chamber of the prism.

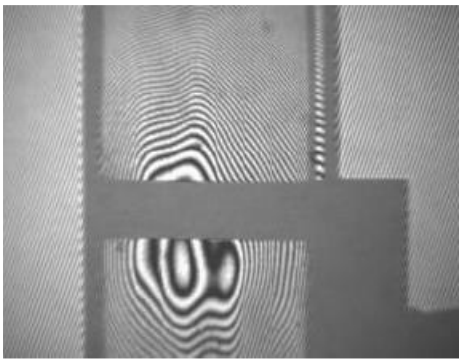

Fig. 4. Fringes generated with similar air inside and outside of the prism

The standard Zygo interferometer software [23] was used to select two areas for the measurement. Figures 5 and 7 show the prism with the areas selected with the same air inside and outside the vacuum chamber. Figure 5 is the fringe map and Figure 7 is the oblique plot. This was used to calibrate the baseline, as described in Kruger and Chetty [9]. Thereafter a vacuum was drawn in the bottom chamber, and this fringe map is shown in Figures 6 and 8. The difference in the oblique plot from the air to the vacuum is visible between Figures 7 and 8.

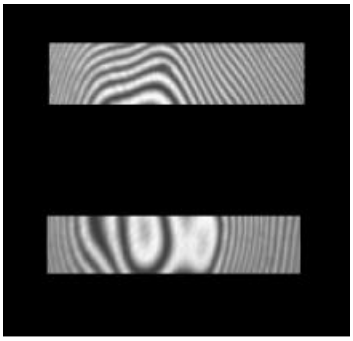

Fig. 5. Fringe map with air in the vacuum chamber of the prism

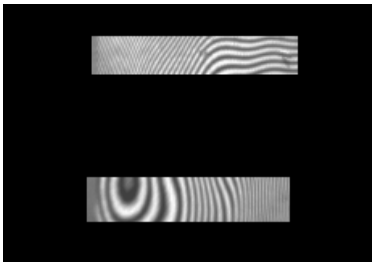

Fig. 6. Fringe map with a vacuum in the vacuum chamber of the prism

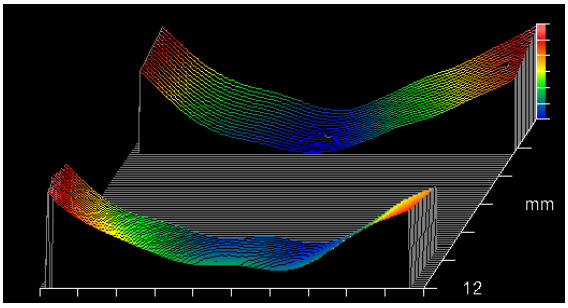

Fig. 7: Oblique plot with air in the vacuum chamber

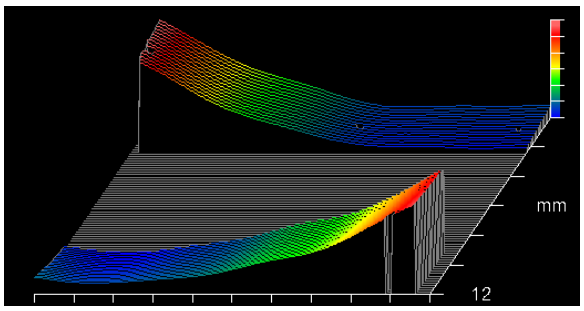

Fig. 8. Oblique plot under vacuum measuring the air/vacuum ratio

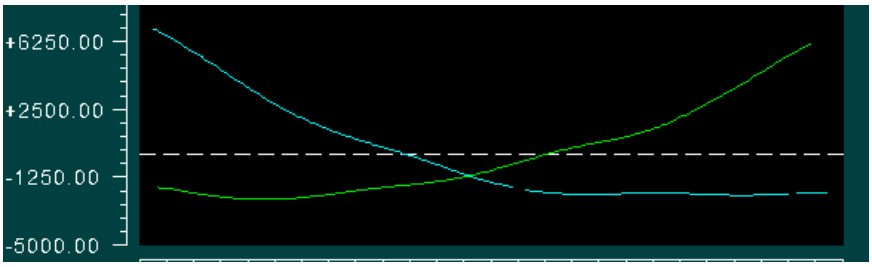

Fig. 9. Profile of two lines selected, one through air (blue line) and the second through vacuum (green line)

The Zygo interferometer software was used to select two horizontal profiles from the oblique plot as in Figure 9, one profile through the vacuum chamber and one profile through the surrounding air, to measure the differences in the vacuum/air ratio. A total distance of 25 mm was used to calculate the vacuum/air ratio.

5. Results from Zygo flatness interferometer

The results of the prism refractometer were compared both to the weather station and to a tube refractometer as was used in previous research by Chetty and Kruger [4,9].

In Table 10 readings over a period of 3 days were taken and the refractive index was calculated using the Edlin equation, tube refractometer, and Fizeau interferometer.

The differences between these three were also calculated and displayed in the table.

The worst difference between the Fizeau refractometer and using the Edlin Equation is $3{,}5 \times 10^{-7}$ with an average difference of $1{,}95\times 10^{-8}$.

The worst difference between the Fizeau refractometer and the Tube refractometer is $8{,}38 \times 10^{-8}$ with an average difference of $7{,}62\times 10^{-9}$.

It is expected that the difference between the Fizeau and the tube refractometer will be better compared to the Edlin weather station. This is as Bonsch G and Potulski E describe that the Edlin equation is at its best accurate to 1×10^{-7}[3].

Table 1: Results for the prism refractometer data compared to the modified Edlén equation using weather station measurement calculations

Reading Number	Air temperature (°C)	Pressure (mbar)	Humidity (%RH)	Refractive index from refractometer, Tube	Refractive index (Edlin)	Difference between Refractometer and Edlin	Zygo/Fizeau Refractive interferometer	Difference between Refractometer Tube and Fizeau
1	20.354	870.185	50.3	1.00023271	1.000232693	-2.1525E-08	1.00023269	-2.4525E-08
2	20.187	870.081	51.3	1.00023275	1.000232794	4.20475E-08	1.00023272	-3.1952E-08
3	20.451	869.964	55.4	1.00023245	1.00023251	5.74711E-08	1.000232474	2.1471E-08
4	20.014	868.923	52.4	1.00023255	1.000232616	6.36632E-08	1.000232515	-3.7337E-08
5	20.289	871.043	52.5	1.00023261	1.000232957	3.50601E-07	1.000232609	2.6007E-09
6	20.932	871.49	53.2	1.00023288	1.000232542	-3.3887E-07	1.000232797	-8.3871E-08
7	20.224	867.712	50.1	1.00023213	1.000232138	5.68803E-09	1.000232191	5.8688E-08
8	20.365	871.814	56.3	1.00023298	1.000233068	8.73211E-08	1.000232919	-6.1679E-08
9	20.105	870.174	52.6	1.00023289	1.000232875	-1.8347E-08	1.000232919	2.5653E-08
10	20.517	869.751	50.5	1.00023247	1.000232441	-3.2322E-08	1.000232528	5.4678E-08

6. Uncertainty calculation for the Fizeau (Zygo) flatness interferometer

The uncertainty for the cylinder refractometer is discussed in detail in previous research by Chetty and Kruger [4,9]. The uncertainty for this method in this setup was previously calculated to be $1{,}8 \times 10^{-8}$ in the refractive index [9]. The uncertainty calculation of the Zygo flatness interferometer method is discussed here.

The uncertainty in the angle of the prism was measured using a Zeiss Prismo Coordinate Measuring Machine and the uncertainty in length measurements is 0,5 µm. The tan function of this uncertainty was used to first calculate the uncertainty of the angle of the prism to be 0,004°, and then to calculate the length of the air

replaced, resulting in a 0,47 µm uncertainty in the vacuum/air ratio. This resulted in an uncertainty of 20 × 10^{-9} in the refractive index.

A lateral distance of 25 mm was used to measure the vacuum/air ratio in the interferometer. This distance was calibrated using a gauge block, as per the Zygo manual [23]. The uncertainty in the size of the gauge block was 20 nm, which is relatively small compared to the calibration of the interferometer lateral scale. Repeatable calibrations using various gauge blocks resulted in a relatively large uncertainty of 21 µm. This value resulted in an uncertainty of 110 ×10^{-9} in the refractive index reading.

The uncertainty in the measurement of the change in the vacuum/air ratio was calculated from the Zygo interferometer manual [24], and the repeatability of the readings in this setup was 2 nm, resulting in an uncertainty of 7,2 × 10^{-8} in the refractive index.

The baseline measurements for the imperfection in the side windows of the prism described earlier were taken with air inside the vacuum etalon and added to the readings under vacuum. This theoretically eliminated this uncertainty of the side windows and only the repeatability in the readings were added to the total uncertainty. The repeatability was included in the uncertainty of the laser reading uncertainty.

Table 2: Uncertainty budget for prism refractometer at the 25 mm position only

Sym.	Description	Value	Uncertainty	Sensitivity Coefficient	Uncertainty Contributor	Significance %
q	The angle of the prism (rad)	0,97825	0,000019	-500*10^{-6}	-20*10^{-9}	3
Lt	Horizontal distance (um)	25000	21	-9.2*10^{-9}	-110*10^{-9}	87
l	Difference in laser reading, (profile height difference) including repeatability (um)	17.15	0,002	13*10^{-6}	39*10^{-9}	10
Combined uncertainty					120*10^{-9}	
Expanded uncertainty					240*10^{-9}	

In Table 2 the uncertainties are presented in an uncertainty budget with the significance of each contributor in column 7.

To combine the uncertainties, the root sum square method was used as described in the GUM [24]. The combined uncertainty was calculated to be 120 × 10^{-9} in the refractive index measurements and 240 × 10^{-9} in an expanded form.

7. Conclusion

The research investigated a permanent vacuum prism refractometer using a new method to measure the air/vacuum ratio required to calculate the refractive index. The results of the interferometer show an agreement of worst 3,5 × 10^{-7} with the Edlén weather station method and a worst value of 8,38 × 10^{-8} to the previously developed cylinder refractometer. The results demonstrate that the accuracy is sufficient to be used for

refractive index measurements of air in high accurate dimensional metrology without the use of a vacuum pump.

In the method that uses a flatness interferometer with a Fizeau interferometer layout, to measure the refractive index, the largest contributor to the uncertainty is the horizontal distance due to the lateral calibration of the camera, with an 87% significance to the total uncertainty. This interferometer is not designed for this type of measurement and a high-resolution camera will vastly improve this uncertainty contributor. It does however show that this method can perform these measurements with the advantage that it takes the readings between the vacuum and air instantly and does not require moving a translation stage. Future research will be performed into a purpose-built system with higher resolution cameras that will result in better lateral resolution and more points over the horizontal distance.

The research demonstrated a new method to measure the air/vacuum ratio in refractometers. It can lead to systems that are faster and cheaper, and with improved camera resolution, it will have an improved accuracy, which was the original objective of this research.

Disclosures

The authors declare no conflicts of interest.

References

1. "News from the BIPM" 1975 *Metrologia* **11** 179–183
2. Quinn TJ 2003, "Practical realization of the definition of the metre, including recommended radiations of other optical frequency standards, *Metrologia* **40 103-133**
3. Bonsch G and Potulski E 1998 "Measurement of the refractive index of air and comparison with the modified Edlin formulae" *Metrologia* **35** 133–139
4. Chetty N and Kruger O A 2016 "Robust air refractometer for accurate compensation of the refractive index of air in everyday use" *Appl. Opt.* **55**(32) 9118–9122
5. Muijilwijk R 1988 "Update of the Edlén formulae for the refractive index of air" *Metrologia* **25** 189
6. Lazar J 2011 "Suppression of air refractive index variations in high-resolution interferometry" *Sensors* **11**
7. Lazar J 2012 "Refractive index compensation in over determined interferometric systems" *Sensors* **12**
8. Ishige M 2009 "Measurement of air refractive index fluctuation from frequency change using a phase modulation homodyne interferometer and an external cavity laser diode" *Meas. Sci. Technol.* **20**
9. Kruger O A 2016 "Robust air refractometer for accurate compensation of the refractive index of air in every day" *Master's Thesis* University of KwaZulu-Natal
10. Kruger O A and Chetty N 2021 "A permanent vacuum refractometer for everyday use in dimensional metrology" *Nature/articles* **11** 9290
11. Renkens M J M and Schellekens, P H J 1993 "An accurate interference refractometer based on a permanent vacuum chamber: development and results" *CIRP Ann.-Manuf. Techn.* **42**(1) 581–583
12. Edlén B 1965 "The refractive index of air" *Metrologia* **2** 71–80
13. Birch K P and Downs M J 1993 "An updated Edlén equation for the refractive index of air" *Metrologia* **30** 155–162
14. Ciddor P E 1996 "Refractive index of air: new equations for the visible and near-infrared" *Appl. Optics* **35** 1566–1573
15. Chapman M A V 2013 "Environmental compensation of linear laser interferometer readings" Renishaw Technical White Paper **TE329**
16. Agilent "Agilent (HP) operating manual of laser interferometer" (ver. 2.003) http://cp.literature.agilent.com/litweb/pdf/05517-90101.pdf Accessed on: July 2015
17. Zygo "Zygo operating manual of displacement measuring system" https://www.zygo.com/?/met/markets/stageposition/zmi/. Accessed on: July 2019
18. Daimon M and Masumura A 2007 "Measurement of the refractive index of distilled water from the near-infrared region to the ultraviolet region" *Appl. Opt.* **46** 3811–3820
19. 3B Scientific. https://www.3bscientific.com/hollow-prism-equal-sided-1014618-u11922,p_639_23222.html

20. Brewster D 1815 "On the laws which regulate the polarisation of light by reflection from transparent bodies" *Philosophical Transactions of the Royal Society of London* **105** 125–159
21. Zygo "Compact Optical Wavelength Compensator" http://www.zygo.com/?sup=/resource/manuals.cgi?type=zmi Accessed June 2019
22. Zeiss "Zeiss Prismo" https://www.zeiss.com/metrology/products/systems/coordinate-measuring-machines/bridge-type-cmms/prismo.html#technicaldata Accessed on: July 2019
23. Tsai J C 1995 *Ambient air refracture index measuring device* US 5394244 A
24. Zygo GPI/HD flatness interferometer https://www.zygo.com/products/metrology-systems/laser-interferometers
25. "*Evaluation of measurement data—Guide to the expression of uncertainty in measurement"* 2008 *JCGM* **100**

Chapter 9: Conclusion

The original aim of this research was to investigate, design, develop, build, and validate a permanent vacuum refractometer that can be used in everyday uses in dimensional metrology. The research was built on the refractometer that was designed by Kruger and Chetty [1,2]. This previous research showed that using a refractometer has numerous advantages over the weather station method. The one area that stands out is the simplicity of the setup from measuring the vacuum-air ratio to the calculation of the refractive index. Such a simple setup means very few uncertainty contributions, which has the benefit of having a small uncertainty in the measurements of the refractive index.

However, one main area of concern with the previous research was the use of a vacuum pump for each time a refractive index measurement is recorded. The vacuum pump added two extra uncertainties and difficulties to the refractometer system. The first is the temperature generation from the pump as the vacuum pump needs to be close to the refractometer to draw a low enough vacuum, leading to an increase in temperature around the refractometer and subsequently the laser interferometer measuring system used in the dimensional measurements. The second uncertainty contribution is dust entering into the vacuum etalon every time a vacuum must be drawn. This dust leads to the diffraction of the laser beams and evidently the vacuum-air ratio. Both these uncertainty contributions are difficult to quantify and it was decided to focus this research on developing a refractometer that does not require a vacuum pump.

Other research showed the use of a permanent vacuum prism as the vacuum etalon, as described by Tsai and Renkens and Schellekens [3,4] and was a good initial knowledge for this research. A comparable refractometer was constructed and tested. However, one area of concern was the long-term stability. The measurements when taken were very accurate but the drift of the zero position needed to be addressed. An optical layout was added where the zero position is constantly monitored and the corrections applied to the readings were constructed and tested and showed a good improvement in the long-term stability. The results from this setup were very promising and a paper was published. The prism used as the vacuum etalon was a commercial prism and its optical quality needed to be improved. The second prism was designed and manufactured with:

i) improvements to the optical windows,
ii) adding an extra entry for more accurate vacuum measurements, and
iii) with a larger apex angle for a larger vacuum-air ratio that resulted in a better resolution of the refractive index measurements, and

iv) higher side windows to have both laser beams travel through the same amount of optical path.

The research into improving the optical quality of the vacuum prism led to research on a new method to measure the vacuum-air ratio. A Fizeau interferometer, which is generally used to measure the optical flatness and wavefront of optics, was researched to measure the vacuum-air ratio. The results were satisfactory but not an improvement in uncertainty over the translation stage method. The results of the translation stage showed an agreement of $6{,}13 \times 10^{-8}$ with the Edlén weather station method and the results of the Fizeau interferometer show an agreement of $9{,}28 \times 10^{-8}$ with the Edlén weather station method. The results of both methods presented the uncertainty is adequate to be used for refractive index measurements of air in high-accurate dimensional metrology without the use of a vacuum pump.

In the method using a flatness/Fizeau interferometer to measure the refractive index, the largest contributor to the uncertainty is the lateral calibration of the camera, with a 95% significance. This interferometer is not designed for measurements where a high lateral accuracy is required, and the use of a high-resolution camera will greatly improve this uncertainty contributor. It does however show that this method can perform these refractive index measurements with the advantage that it takes the readings directly, without the required moving of a translation stage, meaning the results are instantaneous and more points along the windows can be taken, giving a better average reading over the full side window. Future research will be performed into a purpose-built system with a higher resolution camera.

A third prism was designed and built to improve the side windows for improved optical quality, wavefront and thicker for less deformation under vacuum.

The two methods with the use of the improved designed and manufactured prisms will be further developed and used in high-accurate refractive index measurements for use in

i) the new SI unit of temperature,
ii) buoyancy correction in SI unit of mass metrology and
iii) optical pressure standards.
iv) use in everyday dimensional metrology

Over and above this research, it will be a cost-effective stand-alone system which can be used in everyday dimensional metrology.

The research demonstrated two permanent vacuum prism methods to measure the refractive index, an improved translation stage method and a new method using a Fizeau interferometer, to measure the air-vacuum ratio in refractometers, which was the original objective of this research.

Chapter 9 Bibliography

1. Chetty N, Kruger OA. Robust air refractometer for accurate compensation of the refractive index of air in everyday use. OSA. 2016;55:9118–22.
2. Kruger OA. Robust air refractometer for accurate compensation of the refractive index of air in every day. Master Thesis. 2016.
3. Tsai JC. Ambient air refracture index device. US Patent: US5394244A. 1992.
4. Renkens M, Schellekens P. An accurate interference refractometer based on a permanent vacuum chamber. CIRP Annals: Manufacturing Technology. 1993;42:581–3. https://doi.org/10.1016/S0007-8506(07)62514-1

Appendix I

The following is the Edlén calculation of the index of refraction as described by J Stone and J Zimmerman [https://emtoolbox.nist.gov/Wavelength/Documentation.asp]:

(a) Preliminaries:

- Convert all temperatures to Celsius.
- Convert all pressures to Pascal.
- Calculate partial pressure p_v as described previously.

(b) Define constants:

$$A = 8342.54 \quad B = 2406147$$

$$C = 15998 \quad D = 96095.43$$

$$E = 0.601 \quad F = 0.00972 \quad G = 0.003661$$

(c) Convert the laser vacuum wavelength λ to micrometres and then find

$$S = 1/\lambda^2$$

(d) Calculate intermediate results at air pressure p, water vapour partial pressure p_v, and temperature t:

$$n_s = 1 + 10^{-8}\left[A + B/(130 - S) + C/(38.9 - S)\right]$$

$$X = [1 + 10^{-8}(E - Ft)p]/(1 + Gt)$$

$$n_{tp} = 1 + p(n_s - 1)X/D$$

(e) Calculate the final result for the index of refraction n, using our variation of the water vapour term:

$$n = n_{tp} - 10^{-10}\left[(292.75)/(t + 273.15)\right] \times \left[3.7345 - 0.0401S\right] \times p_v$$